To the Graduate Council:

I am submitting herewith a dissertation written by Susan Kay Raths entitled "Characterization of the Primary Interaction Between the Mating Pheromone, Alpha-Factor, and Its Receptor in Saccharomyces cerevisiae." I have examined the final copy of this dissertation for form and content and recommend that it be accepted in partial fulfillment of the requirements for the degree of Doctor of Philosophy, with a major in Microbiology.

Jeffrey M. Becker, Major Professor

We have read this dissertation
and recommend its acceptance:

W. S. Riggs

John W. Koontz

Accepted for the Council:

Vice Provost
and Dean of The Graduate School

CHARACTERIZATION OF THE PRIMARY INTERACTION BETWEEN THE MATING PHEROMONE, ALPHA-FACTOR, AND ITS RECEPTOR IN *SACCHAROMYCES CEREVISIAE*

A Dissertation

Presented for the

Doctor of Philosophy

Degree

The University of Tennessee, Knoxville

Susan Kay Raths

December 1987

DEDICATION

I dedicate this dissertation to my parents for the countless sacrifices they've made to insure that I received a good education. Their love, guidance, advice and encouragement have been a cherished driving force for me throughout my life. Many thanks Mom and Dad!

ACKNOWLEDGMENTS

This work would have never been possible without the generous support and contributions of many people who merit special thanks. Perhaps those who deserve to be commended most for their guidance, patience and trust throughout the development of this project are the members of my committee: Dr. Stuart Riggsby, Dr. John Koontz and Dr. Tom Chen. A special thanks to Dr. Riggsby and Dr. Koontz for the individual concern they have shown in my development as a critical scientist. Thanks also goes to Dr. Chen and Dr. Koontz for their valuable suggestions during the difficulties experienced in this work.

Of particular value, however, has been the constant friendship and encouragement of my major professor, Dr. Jeff Becker. To he and his wife, Nancy, I owe much gratitude for their interest in me both professionally and personally. A listing of Dr. Becker's contributions to my graduate education would be too long to include here so instead let me just say thanks a million!

To the many friends I have made, most of whom are or have been members of Dr. Becker's research effort, thank you for making this experience much more enjoyable. You will all be missed.

Finally, a very special thanks goes to my husband, Scott, who has certainly made this endeavor easier. His love, understanding, patience and support have been of inestimable worth in this accomplishment. I thank him for this and the many other ways he has enriched my life in graduate school.

ABSTRACT

Alpha-factor is a peptide of thirteen amino acids which is required for mating between the haploid mating types, a and α, in Saccharomyces cerevisiae. An analogue of alpha-factor, DHP^{8} DHP^{11} Nle^{12} tridecapeptide, was catalytically reduced in the presence of ^{3}H gas for production of a radiolabelled pheromone suitable for use in binding studies. Incorporation of tritium resulted in ^{3}H-alpha-factor with high specific activity, purity, biological activity and long shelf-life. Binding studies revealed that alpha-factor interacts with its receptor via a simple, reversible process which obeys the law of mass action. Association and dissociation kinetics indicate values of 2.92×10^{6} M^{-1} min^{-1} for k_1 and between 4 and 7×10^{-2} min^{-1} for k_{-1}. Saturation binding studies reveal an equilibrium dissociation constant equal to 2.32×10^{-8} M which approximates the kinetically-derived K_D of 2.12×10^{-8} M. Scatchard and Hill analyses as well as dissociation behavior in the presence of excess unlabelled ligand indicate alpha-factor interacts with a homogeneous population of binding sites (13000 sites/cell) which do not interact and exhibit one affinity for the alpha-factor pheromone. Studies using unlabelled competitors confirm the specificity expected for a receptor-mediated process, i.e., binding affinities of alpha-factor analogues parallel their efficiency at inducing biological activities. Preliminary evidence obtained from the thermodynamic analysis of the temperature dependance of binding of alpha-factor (an agonist) and $desTrp^{1}$ Ala^{3} dodecapeptide (an antagonist) suggests that agonist binding is entropy-driven and antagonist binding

is enthalpy-driven. This may reflect differences observed when binding of the ligand involves interaction with, or traversing of, the cell wall.

TABLE OF CONTENTS

LIST OF TABLES

LIST OF FIGURES

FIGURE PAGE

I. INTRODUCTION

Commonly found in soil and on fruits and leaves in vineyards and orchards, the yeast Saccharomyces cerevisiae, although regularly exploited for its talent for leavening bread and bubbling champagne, has become a popular subject for experimental research today. Evolutionarily, Saccharomyces is seen as a simple eukaryote in which model studies with applicability to higher organisms can be easily accomplished. Saccharomyces contains <1% of the genetic material that humans do (66, 2) yet it is still a eukaryote containing basically all the cell constituents of its more complex relatives. Saccharomyces is easy to grow in the laboratory. Because the generation time is only approximately 120 minutes, many cells can be obtained in a short time without difficulty. The genetics of Saccharomyces have been studied extensively. Due to the progress made in the last ten years and the ease with which Saccharomyces can be manipulated genetically, yeast may soon become the premier organism for industrial production of many recombinant proteins (102). Although much applied research is being done with Saccharomyces, its use as a model system for the study of more general cellular processes such as hormone receptor interactions is sure to be just as fruitful. It is hoped that basic research efforts like the one presented here will help uncover the details necessary to decipher similar interactions found in more complex eukaryotes.

S. cerevisiae can exist stably in either a haploid or diploid state and can propagate both sexually and asexually (for reviews see 113, 114, 126, 103, 72). Haploid and diploid cells can reproduce through a

process of assymetric cell division called budding or haploids of opposite mating type (termed MATa and MATα) can mate to form diploids (MATa/α) which in turn under the appropriate conditions (nutrient and nitrogen starvation) can sporulate to form four new haploids (see figure 1).

Cell type in Saccharomyces is determined by the allele MATa or MATα that is resident at a master regulatory locus termed MAT (mating type locus) on chromosome III (49). Each allele produces transcripts for proteins which regulate the expression of a number of unlinked genes required for mating and sporulation. One of the proteins termed matα1 is a positive regulator for the genes required for alpha cells to mate, whereas matα2 blocks the expression of those genes required by a cells to mate. Therefore in accordance with the α1α2 model for mating type control, both α1 and α2 are transcribed in alpha cells. MATa1, a positive regulator for a-specific genes, is transcribed in a cells and both MATa1 and MATα2 are transcribed in a/α diploids (see figure 2). Simultaneous expression of MATa1 and MATα2 in diploids consequently prevents expression of MATα1 which in turn prevents expression of haploid specific genes and a-specific genes thus allowing sporulation functions to be expressed.

Preparation for mating in Saccharomyces is mediated by the reciprocal action of two diffusable peptide pheromones, a- and alpha-factor (114). A variety of a- and alpha-cell responses have been associated with exposure to the appropriate pheromone, most notably cell surface agglutinin synthesis, cell cycle arrest in G1 as unbudded cells

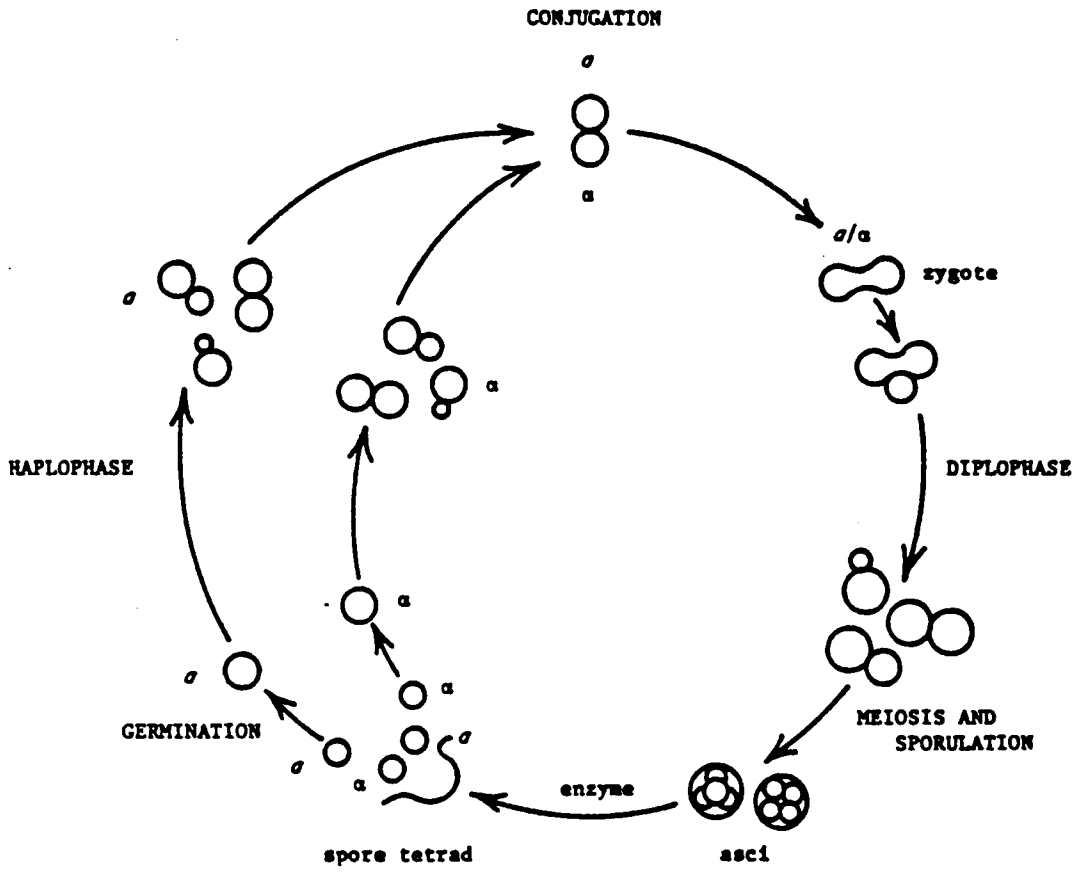

Figure 1. Life cycle of Saccharomyces cerevisiae. Shown here in schematic form are the developmental options open to haploid cells (vegetative growth or conjugation) and diploid cells (vegetative growth or sporulation) of a heterothallic strain of baker's yeast (113).

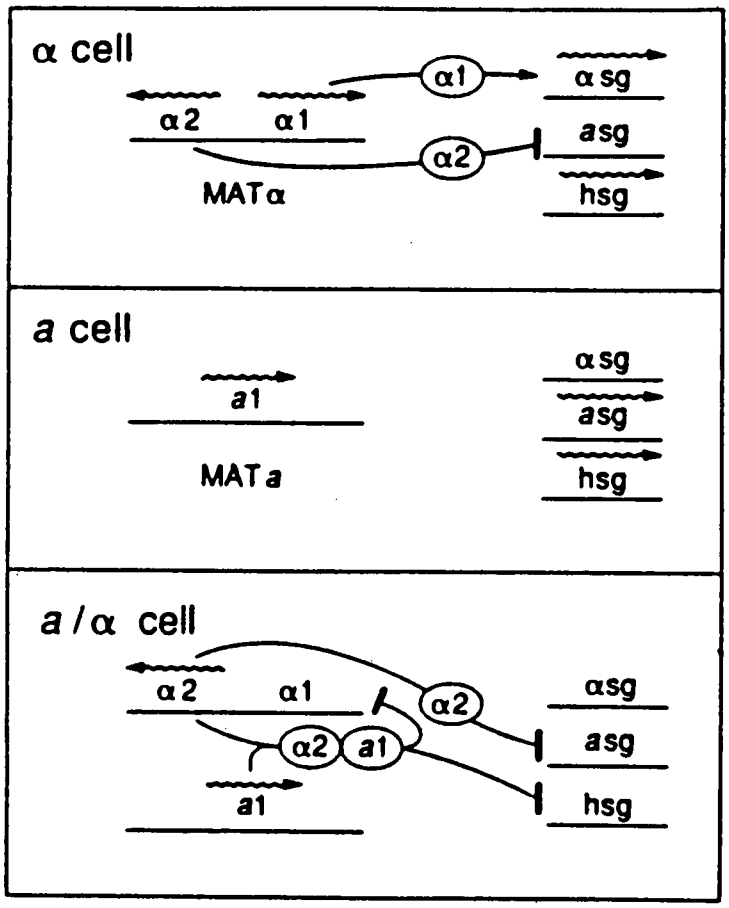

Figure 2. Control of expression of cell-type-specific gene sets by the mating type locus. The mating type locus is drawn to the left and the cell-type-specific gene sets (αsg, α-specific genes; asg, a-specific genes; hsg, haploid specific genes) are drawn to the right. The mating type locus codes for 3 regulatory activities--α1, α2, and a1-α2, that govern expression of the indicated gene sets. Wavy arrows indicate transcription. Pointed arrowheads indicate stimulation of gene expression; lines with blunt ends indicate inhibition of gene expression (49).

prior to DNA synthesis and nuclear spindle pole body duplication, and pronounced morphological alteration termed the "shmoo" (114).

Alpha-factor is synthesized constituitively by alpha-cells and secreted into the culture medium as a family of peptides having the basic sequence

$$H_2N\text{-}(Trp)\text{-}His\text{-}Trp\text{-}Leu\text{-}\underset{(Asn)}{(Gln)}\text{-}Leu\text{-}\underset{(Arg)}{(Lys)}\text{-}Pro\text{-}Gly\text{-}Gln\text{-}Pro\text{-}\underset{(MetSO)}{(Met)}\text{-}Tyr\text{-}COOH$$

(30, 31, 106)

Two genes, MFα1 and MFα2, which code for the alpha mating factor have been identified and cloned (see figure 3 and 17, 85). MFα1 contains the coding information for four identical peptides of the sequence, H_2N-Trp-His-Trp-Leu-Gln-Leu-Lys-Pro-Gly-Gln-Pro-Met-Tyr-COOH, within a putative 165 amino acid precursor. This precursor contains a hydrophobic segment which acts as a signal sequence for secretion, followed by 60 amino acids which contain three N-glycosylation sites important for alpha-factor maturation. Four copies of the mature pheromone separated by spacer peptides (Lys-Arg-Glu-Ala-[Glu/Asp]-Ala-Glu-Ala) are found in the carboxy-terminal portion of the prepro-alpha-factor.

The organization of MFα2 is similar but not identical to MFα1. MFα2 contains two copies of the alpha-factor coding sequence within a 120 amino acid precursor: one copy identical to the four encoded by MFα1 and the other differing by Gln→Asn and Lys→Arg substitutions. Like the peptide hormones made by many higher eukaryotes, alpha-factor is generated through proteolytic processing of the larger precursor

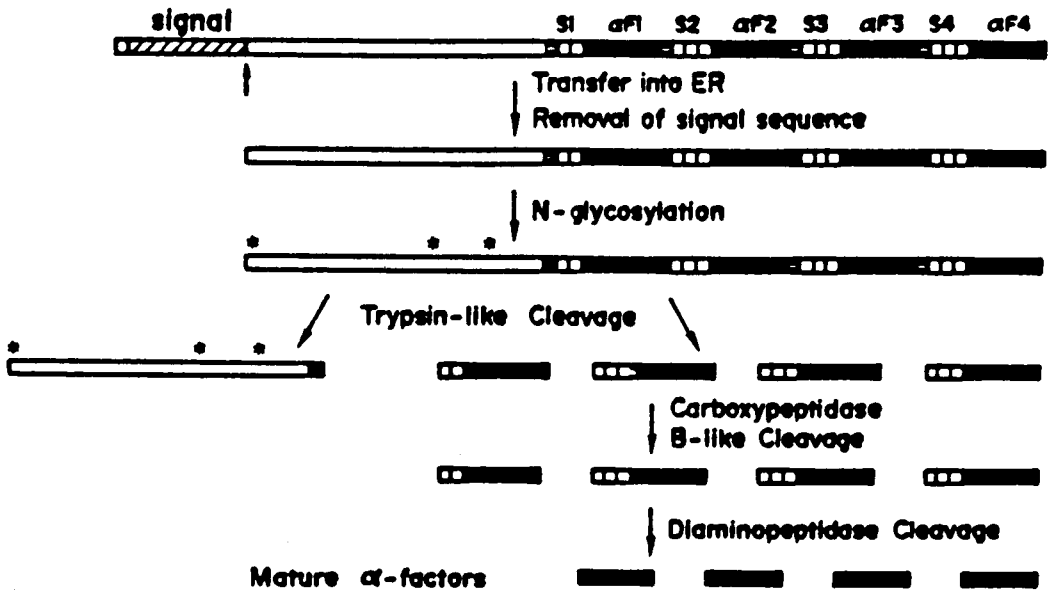

Figure 3. MFα1, scheme for processing of the α-factor precursor. α-factor oligopeptides are indicated by solid rectangles; the signal sequence by a diagonally crosshatched rectangle; spacer peptides consist of Lys-Arg (horizontally crosshatched box) followed by two or three Glu-Ala or Asp-Ala pairs (open boxes). The order of some of the steps (for example, involving cleavages by carboxypeptidase and dipeptidylaminopeptidase activities) is arbitrary (65).

polypeptide (32). Processing of prepro-alpha-factor into the mature pheromone peptides requires the endopeptilytic role of KEX2 and the dipeptidyl aminopeptidase A activity of STE13 (1, 57, 58).

The structural genes for a-factor, MFa1 and MFa2, have also been cloned and sequenced (see figure 4 and 14). MFa1 produces a transcript of 340 bases and MFa2 produces a transcript of 420 bases. Both genes are expressed in a cell-type specific manner and when subcloned into a high-copy number yeast plasmid vector, both produce greater amounts of biologically active a-factor than vector-containing control MATa transformants (14).

The precursors encoded by MFa1 and MFa2 contain no signal sequence and no sites for Asn-linked glycosylation (14). Furthermore, processing and posttranslational modification appear to require the products of STE6, STE14 and STE16 (RAM,SUPH) (91, 124). Because of the above characteristics, the small size of the a-factor precursors and the fact that a-factor is secreted at the restrictive temperature in temperature-sensitive secretion (SEC) mutants, a-factor, unlike alpha-factor, is thought to be exported by a route independent of the secretory pathway (105).

The biologically active structure of a-factor remains unclear. A collection of four a-factor undecapeptides were originally isolated from a-culture supernates by Betz et al. (10, 8, 11) having the general sequence

$$H_2N\text{-Tyr-Ile-Ile-Lys-Gly-}\begin{matrix}(\text{Val})\\(\text{Leu})\end{matrix}\text{-Phe-Trp-Ala-Asx-Pro-COOH}$$

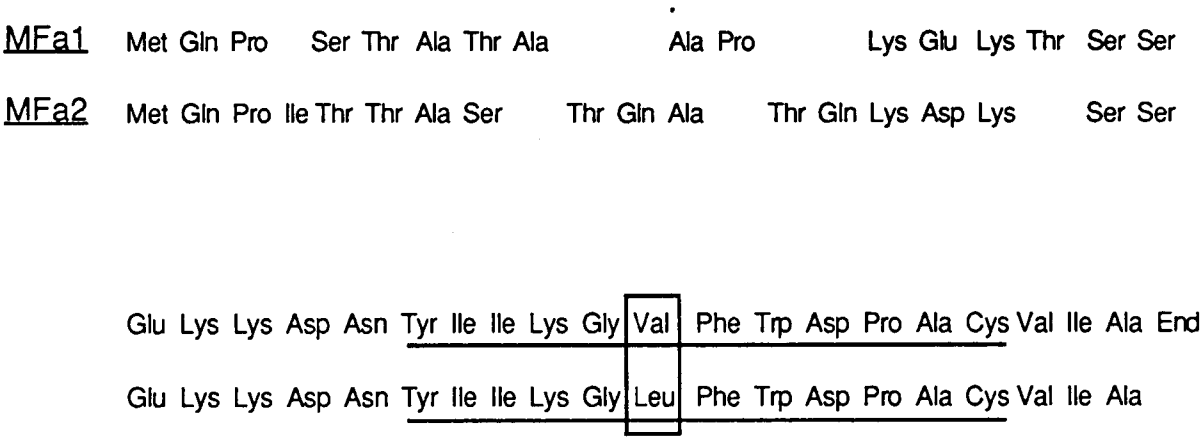

Figure 4. Predicted precursor from the a-factor structural genes, MFa1 and MFa2.

However, when the nucleotide sequences of MFa1 and MFa2 were published by Brake et al., the a-factor carboxy-terminal Ala-Asx-Pro sequence found by Duntze et al. did not agree with that predicted from the two genes. MFa1 and MFa2 predict similar pheromones of the following sequence

$$H_2N\text{-Tyr-Ile-Ile-Lys-Gly-}\underset{(Leu)}{(Val)}\text{-Phe-Trp-Asp-Pro-Ala-Cys-Val-Ile-Ala-COOH}$$

When a-factor peptides corresponding to

$$H_2N\text{-Tyr-Ile-Ile-Lys-Gly-}\underset{(Leu)}{(Val)}\text{-Phe-Trp-Ala-}\underset{(Asp)}{(Asn)}\text{-Pro-COOH} \quad (14)$$

were synthesized and tested by Becker et al. (6), no biological activity was found. However, these peptides in addition to chemically synthesized biologically inactive derivatives of the sequence predicted from the DNA

$$H_2N\text{-Tyr-Ile-Ile-Lys-Gly-Val-Phe-Trp-Asp-Pro-Ala-Cys-Val-Ile-Ala-COOH} \quad (14)$$

did antagonize the activity of a crude a-factor preparation suggesting the sequences, while not complete, were similar to the natural biologically active peptide.

Many observations support the idea that native a-factor is a lipopeptidyl pheromone as has been found in the peptide sex hormones of several Basidiomycetes species (59, 96). First of all, it is difficult to isolate in reproducibly sufficient yields mainly due to its apparent hydrophobic nature. Secondly, a functional RAM gene (RAS protein and

a-factor maturation function) is necessary for the acylation and membrane localization of RAS proteins as well as a-factor production. Both RAS and a-factor share the common carboxy-terminal sequence Cys-A-A-X, where A is an aliphatic amino acid and X is the C-terminal amino acid. The cysteine residue in this conserved sequence of the RAS protein is palmitoylated (91). Thirdly, of the a-factor peptides synthesized by Becker et al. (6), the most potent antagonist of biologically produced a-factor activity was the palmitoylated cysteine-containing pentadecapeptide. Recently, using NMR spectroscopy Betz and Duntze have shown that biologically produced a-factor contains both a carboxymethyl group and a farnesyl cysteine (9). Verification of this as the correct structure for a-factor awaits chemical synthesis and subsequent biological testing.

Both a- and alpha-factor elicit their observed responses through interactions with the products of two genes, STE2 (alpha-factor receptor) and STE3 (alleged a-factor receptor). Chemical and genetic evidence for an alpha-factor receptor was first provided by Jenness and coworkers by showing that ^{35}S-labeled alpha-factor bound specifically to a-cells and not to alpha-cells or a/α diploids (53). Jenness also examined the thermostability of binding for a number of mutants temperature sensitive for response to alpha-factor. His analyses revealed only one alpha-factor receptor candidate, ste2, whose binding activity was stable at permissive temperature and unstable when heated. Based on this evidence, two groups cloned the STE2 gene by

complementation (see figure 5 and 17, 85). Recently, the locus has been mapped to chromosome VI (54).

The primary sequence encoded by STE2 shows no homology to other peptide hormone receptors responsible for regulating growth in higher eukaryotes. In fact, the general organization of the predicted translated precursor suggests that the alpha-factor receptor is structurally and functionally different in some ways from previously characterized hormone-receptor systems (17): there is no amino terminal signal sequence in the STE2 protein and no sequence homology to protein kinases can be found in the carboxyterminal cytoplasmic domain. Deletion studies indicate mutants lacking up to 105 of the carboxyterminal amino acids still function to mediate the response to the pheromone in a-cells (63). Therefore, the functional significance of the carboxyterminal portion of the alpha-factor receptor remains unknown.

The predicted structure of the alpha-factor receptor does, however, resemble that of rhodopsin, the β-adrenergic and acetylcholine receptors in that the hydropathic profile of the STE2 gene product predicts seven membrane spanning regions (17, 85). This raises the possibility that it may function as a ligand-activated channel (17). In any case, exactly how this integral membrane protein mediates the diverse cellular events which occur upon pheromone binding is currently under investigation.

There is no extensive sequence homology between the gene products of STE2 and STE3, the putative a-factor receptor (85, 44). However, their predicted structural organization seems strikingly similar (see

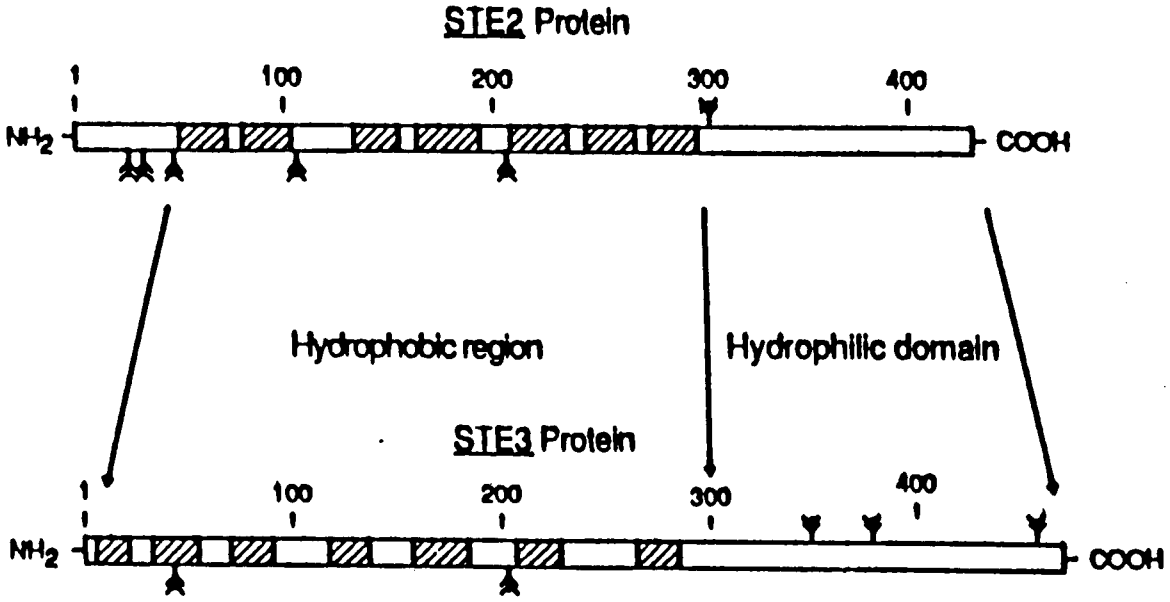

Figure 5. Predicted protein structure for STE2 and STE3. Slashed regions indicate hydrophobic domains. The double Y indicates possible N-glycosylation sites [Asn-x-Ser (Thr)] (85).

figure 5). Both contain seven hydrophobic segments in the amino-terminal portion with a long carboxyterminal hydrophilic domain (85). Subclones of the STE3 gene lacking the coding information for the COOH-terminal 106 amino acids complement the mating defect observed in ste3-1 mutants, suggesting that a large portion of the carboxyterminal domain of the a-factor receptor, like the alpha-factor receptor, is also dispensable (85).

Experiments by Bender and Sprague indicate these structural similarities have functional significance (7). When either a- or alpha-factor receptor structural genes were expressed in cell types in which they are normally silent, the capacity to respond to the appropriate pheromone was acquired. These experiments show that the cell-type specificity of pheromone response is determined solely by the species of receptor which the cells synthesize. Consequently, both a- and alpha-factor activate a common response mechanism in their target cells.

Studies of STE2 and STE3 gene expression have revealed that they are regulated on at least three levels: (1) by the alpha- and a-pheromones (44, 45), (2) by products of the mating type locus (45, 104) and (3) by products of non cell-type specific sterile genes (45). Northern analyses show that the steady-state levels of STE2 and STE3 mRNA increase with subsequent exposure of a-cells to alpha-factor and alpha-cells to a-factor. This phenomenon has also been noted for the epidermal growth factor receptor (27), the prolactin receptor (74) and the human interleukin 2 receptor (93, 120) and furthermore is consistent

with the increase of alpha-factor binding seen during incubation of a-cells with radioactive alpha-factor (52).

Transcriptional regulation of STE2(an a-specific gene) in alpha-cells is also mediated by the α2 protein expressed from the mating type locus (45). The consensus sequence for the putative binding site of the α2 protein has been reported and is found in the upstream noncoding region of STE2 as well as other cloned a-cell specific sterile genes(MFa1, MFa2, STE6 and BAR1) (56, 78). The expression of STE3 and other alpha-specific genes such as MFα1 and MFα2, on the other hand, require the MATα1 product for positive regulation (104, 107). Comparison of the 5' noncoding regions of MFα1, MFα2 and STE3 show no extensive homology to indicate a consensus sequence for binding of the α1 protein, the positive regulator of transcription produced by the MATα1 gene of the mating type locus (101).

The products of some of the nonspecific STE genes are also involved in the regulation of STE2 and STE3 transcription. STE4 mutants show a tenfold reduction in STE2 transcript levels (45). Temperature sensitive alleles of this same locus lose the ability to bind alpha-factor when grown at the restrictive temperature (54). Another nonspecific STE gene, STE12, is also required for normal levels of STE2 RNA (35). Similarly, STE7 and STE11 gene disruptions cause decreased levels of STE3 RNA in alpha-cells (45). Therefore, like the S. cerevisiae HO gene, which codes for an endonuclease and participates in mating-type switching of homothallic cells (87, 64), multiple levels of

transcriptional regulation exist for the a-factor receptor and the alpha-factor receptor structural genes.

Despite the progress that has been made towards correlating pheromone production and response with cell type and the mating process, little is currently known about the mode of action of alpha-factor at the molecular level. Throm and Duntze (115) were the first to realize that a-cells eventually recover from the effects of alpha-factor, that is, alpha-factor induced growth arrest is reversible. Subsequent studies by Ciejek and Thorner (25) showed that similar to other hormone effector systems, the a-mating type has a cell-associated hydrolase which cleaves alpha-factor at the Leu^{6}-Lys^{7} peptide bond into two inactive component peptides. Although similar activities in other systems act to relieve the target from stimulation, the precise role for this activity in Saccharomyces is obscure. Originally thought to be a mechanism by which a-cells could recover from the effects of alpha-factor, recent data suggests that proteolysis is not required for the resumption of normal budding after alpha-factor induced G1 arrest. In fact, a-cells become desensitized and resume the normal cell division cycle in the presence of residual intact peptide (81).

Hoping to implicate proteolysis in recovery, Chan et al. (21) identified several mutants supersensitive to the effects of alpha-factor, which defined two genes, SST1 and SST2. sst1 is cell-type specific conferring the supersensitive phenotype to MATa cells only. sst2, on the other hand, is nonspecific, allowing both MATa cells and

MATα cells to respond to their corresponding pheromones at lower concentrations than normal (21).

Physiological studies have shown the SST1 or BAR1 gene controls the "barrier" function first defined by Hicks and Herskowitz (50) as responsible for the ability of MATa cells to impede the diffusion of alpha-factor. Evidence from experiments by Manney et al. (72) suggest that this barrier activity is secreted as a soluble, heat stable protein with a sharp pH optimum for activity at pH 6.5. Additional results confirm that this activity is stimulated upon exposure to alpha-factor and under the control of the MATa2 and BAR1 genes. The product of the BAR1 gene is probably not an alpha-factor protease, however, for the following reasons: (1) most proteases are not heat stable, (2) the kinetics of biologically active alpha-factor disappearance in BAR1 strains are not consistent with that expected for a catalytic function (72) and (3) BAR1 has also been shown to control other a-type specific proteolytic functions (40).

Also under BAR1 control are two alpha-factor inactivating glycoproteins with the molecular weights of 200,000 and 400,000 (40). These proteins, which were purified from heat shock extracts of MATa cells, are likely responsible for the a-type specific cell wall-bound proteolytic activities reported by Ciejek and Thorner (25), Finklestein and Strausberg (37), and Manness and Edelmann (71). Furthermore, results from experiments using bar1-1 and sst1-1 mutants indicate that these cell wall glycoproteins are synthesized under the control of BAR1 (40). Clearly, evidence exists for a number of a-cell specific

alpha-factor proteolytic activities under the regulation of one locus, BAR1. However, the relevance of alpha-factor hydrolysis to biological activity and a-cell recovery remains uncertain.

The major way by which a-cells recover from alpha-factor induced division arrest is via a process called desensitization or adaptation (81). Moore found that after initial desensitization to 1 nM alpha-factor at low cell density (10^2 cells/ml), a-cells could remain completely insensitive to 1 nM concentrations for greater than three generations (81). Furthermore, transmission of the desensitized state occurs assymetrically. Desensitized parents remain insensitive to the effects of alpha-factor while their daughters display normal alpha-factor induced arrest (81).

Desensitization to biologically active ligands is common among a number of eukaryotic organisms (19). In many cases, desensitization occurs by receptor modification. In other cases, adaptation has been correlated with receptor internalization. A common way in which many mammalian polypeptide hormone-receptor complexes are internalized is through a process termed endocytosis. Endocytic pathways have been described in detail for a number of mammalian ligands and their receptors and recently described in Saccharomyces cerevisiae by Riezman et al. (94).

To investigate the possibility that endocytosis might play a role in pheromone response, Riezman used ^{35}S-alpha-factor to show that alpha-factor is internalized by a-cells in a time, temperature and energy-dependent manner (24). Two mutants, end1 and end2 both defective

in endocytosis were also shown to be defective in pheromone response (24). Consistent with these findings Jenness and Spatrick (55) found that down regulation of alpha-factor receptors on yeast a-cells was accompanied by internalization of alpha-factor. Furthermore, a-cells bearing a STE2 disruption were unable to internalize alpha-factor. From these studies it appears that alpha-factor receptor complexes enter the cell by receptor-mediated endocytosis and this entry is required for pheromone response, however, the details of the molecular mechanisms involved in endocytosis and response have not been uncovered.

The most studied mechanism by which receptors translate external stimuli into internal control of cellular processes involves the second messenger cyclic AMP. cAMP levels in turn control the activity of cAMP-dependent protein kinase which regulates a variety of susceptible proteins by affecting their state of phosphorylation. In this manner, one signal, cAMP, can cause a diverse set of effects on the physiology of the cell (42).

Evidence for the involvement of a cAMP-based regulatory cascade in cell cycle progression has been found in Saccharomyces cerevisiae but the role for cAMP in pheromone response remains uncertain. Liao and Thorner (67), initially found that the membrane bound adenylate cyclase of Saccharomyces is inhibited in a dose dependent manner by alpha-factor in vitro. Furthermore, addition of cAMP or cyclic nucleotide phosphodiesterase inhibitors to an alpha-factor treated a-cell culture decreases the length of time the cells remain arrested in G1. This lead them to postulate that decreased levels of cAMP are in part responsible

for the physiological consequences of alpha-factor exposure. This work, however, could not be repeated by Casperson et al. (18), who showed that S. cerevisiae contains a guanine nucleotide sensitive adenylate cyclase. Under the conditions previously published by Liao and Thorner, alpha-factor was not an effector of the guanine nucleotide sensitive adenylate cyclase (18). That adenylate cyclase was affected by alpha-factor was later retracted by Thorner, an author of the original observation.

Adenylate-cyclase deficient mutants termed cyr1 of Saccharomyces have been isolated by Matsumoto et al. (77) which in the absence of an exogenous supply of cyclic AMP, arrest growth at G1 as single unbudded cells like alpha-factor or a-factor treated cells. Therefore it appears that yeast cells do require a sufficient intracellular pool of cyclic AMP in order to initiate a new round of cell division. That this effect is mediated by cAMP-dependent protein kinase is concluded from studies using second site suppressor mutations (bcy1) of cyr1 (77). cyr1 bcy1 double mutants appear to lack a functional cAMP-binding regulatory subunit for cAMP-dependent protein kinase as judged by (a) reduced radiolabelling of cell extracts with a photoactivatable affinity label 8-azido-^{32}P-cAMP and (b) failure to stimulate total protein kinase activity in cell extracts upon addition of cAMP. These results demonstrate that cAMP-dependent protein phosphorylation plays a major regulatory role in the progression of yeast through the cell cycle (77).

On the basis of these studies one group attempted to correlate the levels of phosphorylation of specific a-cell proteins with the

physiological effects of exposure to alpha-factor. Although one phosphorylated protein, P17 (M_r = 17000) was found to undergo alpha-factor mediated modification to a form having an apparent M_r of 17500, no alterations in specific protein phosphorylation were observed (36). These data are difficult to reconcile with recent results published by Tripp et al. (117). Using cyr1-2(ts) and bcy1 mutants, these authors revealed the existence of several proteins whose phosphorylation is controlled either positively or negatively by the cAMP pathway in yeast. Conclusions from their data indicate cAMP-dependent protein kinase must be inactivated before cell cycle arrest can occur. Inactivation of cAMP protein dependent kinase for cell cycle arrest is consistent with decreased levels of cAMP seen in alpha-factor arrested cells. This discrepancy between these two labs addressing differential protein phosphorylation is not resolved.

The divalent ion calcium, like the cyclic nucleotides, is also a major second messenger for the regulation of numerous cellular processes in higher eukaryotes inclusive of energy metabolism, endocytosis and exocytosis, microtubule polymerization and cyclic nucleotide metabolism (118). Yeast cells possess all these processes and therefore by analogy may be expected to contain calcium-responsive regulatory circuits similar to those found in higher eukaryotes.

Several studies suggest that both calcium and calmodulin at least are involved in the response to alpha-factor. Ohsumi and Anraku found that alpha-factor induced a dose-dependent specific accumulation of calcium after a lag of 30-40 minutes in MATa but not in MATα or MATa/α

cells (89). Similar experiments using a-factor and alpha-cells produced the same pheromone-induced calcium accumulation. Further evidence (108) has indicated that although long-term calcium accumulation is seen, a very rapid transient pheromone-specific increase in cellular calcium concentration can be noted first. By analogy to similar results using Rhodosporidium toruloides and its lipopeptidyl mating factor, rhodotorucine A, this calcium flux in Saccharomyces is thought to manifest its intracellular effect through modification of calcium/calmodulin-dependent protein kinase activity (108, 79).

The gene for calmodulin in Saccharomyces has been cloned and found through disruption and deletion to be essential for vegetative growth (28). Recent evidence involving calmodulin as a mediator in the action of alpha-factor has been published also. In the presence of trifluoperazine or chlorpromazine, two phenotizine-derived drugs known to inhibit calmodulin dependent processes, alpha-factor induced arrest of cell growth is reduced and even undetectable in some cases (95). These results are not unexpected in light of the previously discussed findings by Liao et al. (67) and Matsumoto et al. (77); calmodulin has been shown to modulate the activity of enzymes involved in cAMP metabolism in higher eukaryotes.

Efforts are being made to dissect the pathway(s) responsible for hormonal control of development in Saccharomyces. The approaches currently underway rely on the prerequisite proof that STE2 and STE3 encode the alpha-factor and a-factor receptors respectively. Since this accomplishment, a number of avenues have been opened for identifying

genes and proteins involved in the response pathway for hormone action. One approach has already been successful: the identification of second site suppressor mutations which allow restoration of conjugational competence to ste2 mutants.

The SST2 mutant, as previously stated, exhibits supersensitivity of a-cells to alpha-factor and alpha-cells to a-factor. This nonspecificity suggests that SST2 codes for a component of the response pathway common to both mating types (21). sst2-1 was found to suppress the sterility of a temperature sensitive ste2-3 mutant whose mating seems to be limited by its sensitivity to alpha-factor (54). Because sst2 does not block down-regulation of alpha-factor receptors, it is suspected that sst2 is involved in blocking the receptor modification process which results in response inactivation or adaptation (54).

Recently, Nakafuku et al. have cloned a gene tentatively designated GPA1 from S. cerevisiae which predicts a protein strikingly homologous to the amino acid sequence of rat brain Gi_{α}, a guanine nucleotide binding protein involved in inhibition of adenylate cyclase activity (86). J. Kurjan has cloned the SST2 gene and found the nucleotide sequence to be identical to that published for GPA1 suggesting these two genes are one in the same(personal communication, J. Kurjan). Given the phenotype observed for SST2 mutants and the sequence homology observed with the guanine nucleotide binding protein, Gi_{α}, it is tempting to postulate that once alpha-factor binds to its receptor, the receptor modulates the activity of adenylate cyclase through a number of GTP

binding proteins. In fact, the gene for the counterpart of mammalian Gs has already been isolated from S. cerevisiae and termed RAS2 (116).

Another complementation group has been found which will suppress the mating defect of several temperature sensitive alleles of ste2 (ste2-3, ste2-4 and ste2-6). This mutation designated stp21-1 (sterile pseudoreversion; the first digit of the gene number indicates the ste mutation suppressed) suppresses ste2-3, ste2-4 and ste2-6 but does not suppress a null allele of STE2 (60). This indicates that the stp21-1 allele does not suppress by simply bypassing the requirement for pheromone-receptor interaction, but confers suppression by interacting with and compensating for the temperature sensitive receptor defects of ste2-3, ste2-4 and ste2-6.

Another approach towards identifying proteins which interact with the alpha-factor receptor is underway in at least one laboratory. A method for obtaining membrane fractions and spheroplasts which quantitatively retain alpha-factor binding activity has been reported as a preface to biological isolation of active alpha-factor receptors (12). Furthermore, a number of labs have reported the successful production of anti-alpha-factor receptor antibodies (12, 48). Presumably, these tools are currently being used to identify other membrane proteins to which the STE2 protein may be coupled.

While the efforts outlined above seek to define interacting components of the alpha-factor response pathway by genetic characterization and biochemical isolation of the proteins involved, an understanding of the primary interaction of alpha-factor and its

receptor is incomplete. The activity of a given peptide or protein in nature must obviously be coded in its primary sequence; otherwise, the specificity and regulation of cellular processes and response by these participants would be impossible. To what extent the linear sequence contributes to a conformational pattern stabilized by intermolecular interactions among individual amino acids is unknown. However, this is likely different in each recognition system to be examined. Still, within a particular system, many studies involving the synthesis and testing of peptide analogues have been successful in outlining the properties specific to the effector molecule which allow or determine biological response.

Two laboratories have been largely responsible for structure-function studies of the alpha-factor peptide. Most of the analogues of the tridecapeptide pheromone have been synthesized and evaluated in the laboratory of Masui. In contrast, all the structure-function relationships determined using analogues of the dodecapeptide sequence have been published by Becker, Naider et al. The combined efforts of these two laboratories have allowed an evaluation of the sequence and structural requirements for biologically active alpha-factor.

From the testing of a number of synthetic analogues, the following important conclusions can be made:

1. There is a correlation between pheromone length and activity. Shenbagamurthi et al. found that the alpha-factor tridecapeptide is sixteen times more potent than the homologous dodecapeptide (99). The $desTyr^{13}$ dodecapeptide shows a

thousand-fold reduction in activity and desTrp^1, His^2 dodecapeptide as well as most fragments containing partial sequences of the alpha-factor have less than one-millionth of the activity associated with tridecapeptide (75). Fragments comprising the amino-terminal six-amino-acids (Trp^1-Leu^6) and the carboxyl terminal seven amino acids (Lys^7-Tyr^{13}) have virtually no activity (25). Furthermore, a tetradecapeptide (NH_2-Ala-tridecapeptide) had activity equal to the tridecapeptide but analogues containing from 2-7 amino acids amino-terminal to the first Trp of the natural sequence showed 5-10 fold less activity than the tridecapeptide (103). An alpha-factor peptide with Lys-Arg residues at the C-terminus (expected as an unprocessed form in biosynthesis) also shows no activity (109). These results support the idea that the receptor can accomodate a maximum of 14 amino acids and still retain biological activity equivalent to the natural sequence.

2. A free alpha-amine is not required for the biological activity of either the dodecapeptide or tridecapeptide. desTrp^1(α-Dns)His^2, CHA^3 dodecapeptide and amino-terminally extended alpha-factors mimicing the unprocessed precursors of naturally synthesized alpha-factor show significant activity (99, 109).

3. Although some amino acid residues are not well tolerated at position 1, the amino-terminal tryptophan is not essential for activity. Substitution of hydrophobic residues at position 1

lead to a 10-100 fold decrease in biological activity. Furthermore, phenylalanine and tyrosine replacements at position 1 reduce biological potency to one tenth and 1/2500 of the parent compound, respectively (76). Most conclusively, the dodecapeptide pheromone in which the tryptophan is absent retains biological activity (99).

4. The histidine at position 2 is very important for biological activity. All substitutions made at position two by Masui resulted in a corresponding 100,000-fold loss in biological activity (76).
5. A minimum hydrophobicity at position 3 is necessary for activity. While replacement of Trp^3 with Ala, Leu, Phe or Tyr only resulted in 50-fold reductions in potency, insertion of basic, neutral or acidic residues at position 3 resulted in activity reductions of at least 10,000-fold (76).
6. Neutral changes at position 5 are tolerated. The product of MFα2, Asn^5, Arg^7 tridecapeptide, has biological activity equivalent to the native sequence (92).
7. A minimum hydrophobicity or steric bulkiness in the position 6 side chain is required for pheromone activity. Substitutions of leucine for alanine at position 6 result in an inactive pheromone (76, 3). Furthermore, an increase in biological activity can be correlated with a corresponding increase in the position 6 side chain from a methyl to an isopropyl group (3).

8. The ε-amine of lysine at position 7 is not required for activity. Arg^7-alpha-factor has identical activity to the Lys^7-natural sequence (97). Similarly, $desTrp^1,CHA^3,NLe^7$ dodecapeptide is one-tenth as active as the parent $desTrp^1,CHA^3$ dodecapeptide (4). Furthermore, analogues containing Lys^7 with the ε-amine blocked by dansyl, FITC or biotin are all active (99, 84).
9. A type IIβ turn existing at positions 8 and 9 in the pheromone may define an important feature of the biologically active conformation. $desTrp^1$ CHA^3 $D\text{-}Ala^9$ dodecapeptide is active where as the corresponding $L\text{-}Ala^9$ homolog is inactive (84). Evidence exists that type IIβ turns will tolerate D-residues but not L-residues (119).
10. A nucleophilic sulfur atom is not required at position 12. A replacement of norleucine for the methionine at position 12 in both the $desTrp^1$ dodecapeptide and tridecapeptide results in no loss of pheromone activity (84).
11. Modification or loss of the tyrosine in position 13 lead to reduced activity. A $desTyr^{13}$ dodecapeptide synthesized by Masui et al., showed a 1000-fold reduction in activity (75). Esterification (113), ^{125}I-labelling (37), or conversion of the carboxyl terminus to a carboximide (76) reduces biological activity to between a thousand- and ten-thousand-fold.

All of the studies to date using analogues of alpha-factor have assessed the importance of individual amino acid residues to biological

consequences far removed from the primary interaction of the pheromone with its receptor. This study is an extension of these analyses and attempts to answer additional questions relative to this initial ligand receptor interaction. It is hoped that the experiments presented here will aid in directing future efforts to understand the interaction between alpha-factor and its receptor in Saccharomyces cerevisiae.

II. MATERIALS AND METHODS

Organisms, Media and Growth Conditions

The Saccharomyces cerevisiae strains, 4202-15-3 (MATa cry1 bar1-1 ade2-1 his4-580 lys2 trp1 tyr1 SUP4-3) and 4202-1-2 (MATα cry1 bar1-1 ade2-1 his4-580 lys2 trp1 tyr1 SUP4-3), used in this study were obtained from Duane Jenness, Department of Molecular Genetics and Microbiology, University of Massachusetts Medical School, Worchester. Strains were maintained on YM-1 agar containing (grams per liter): yeast extract, 5; peptone, 10; yeast nitrogen base without amino acids (filter sterilized),6.7; adenine, 0.01; uracil, 0.01; succinic acid, 10; sodium hydroxide, 6; glucose, 10; agar, 20; final pH, 5.8 (46). Cells used in the binding assays were grown in liquid YM-1 medium at 30°C and 200 rpm overnight in a rotary water bath (New Brunswick Scientific, Edison, New Jersey) to a density no greater than 1 X 10^7 cells per ml (A550=0.4). Inhibitor medium (YM-1+i) was YM-1 with the addition of 10 mM NaN_3, 10 mM KF and 10 mM p-tosyl-L-arginine methyl ester (TAME). Inhibitor medium was routinely prepared and filtered through Millipore filters (Millipore Corp., Bedford, MA; type HA, 0.45 micron) immediately before use.

Alpha-Factor Peptides

Alpha-factor is a tridecapeptide of the following structure: H_2N-Trp-His-Trp-Leu-Gln-Leu-Lys-Pro-Gly-Gln-Pro-Met-Tyr-COOH. Analogues of this peptide are designated according to IUPAC convention (121). Thus, if norleucine is substituted for methionine at position 12, the

analogue is designated NLe^{12} tridecapeptide or NLe^{12}-alpha-factor. The removal of tryptophan at residue one gives $desTrp^{1}$-alpha-factor. Other residues used for substitution were: CHA, cyclohexylalanine; AIB, aminoisobutyric acid; Dns, dansyl; DHP, dehydroproline.

The following alpha-factor peptides used in this study were synthesized by Drs. Fred Naider and Ponniah Shenbagamurthi at The College of Staten Island, CUNY, Staten Island, New York: alpha-factor; NLe^{12} tridecapeptide; Asn^{5}, Arg^{7} tridecapeptide; Phe^{3} tridecapeptide; DHP^{8}, DHP^{11}, NLe^{12} tridecapeptide; $desTrp^{1}$ dodecapeptide; $desTrp^{1}$, Ala^{3} dodecapeptide; $desTrp^{1}$, Phe^{3} dodecapeptide; $desTrp^{1}$, CHA^{3} dodecapeptide; $desTrp^{1}$, CHA^{3}, D-Leu^{6} dodecapeptide; $desTrp^{1}$, CHA^{3}, Lys^{7}(Acetyl) dodecapeptide; $desTrp^{1}$, CHA^{3}, Lys^{7}(Octanoyl) dodecapeptide; $desTrp^{1}$, CHA^{3}, AIB^{8} dodecapeptide; $desTrp^{1}$, CHA^{3}, L-Ala^{9} dodecapeptide; $desTrp^{1}$, CHA^{3}, D-Ala^{9} dodecapeptide; $desTrp^{1}$, αDns-His^{2}, CHA^{3} dodecapeptide.

Tritium-labelled alpha-factor was prepared by the Amersham tritium labelling service (Amersham, Arlington Heights, IL) by subjecting the unlabelled precursor DHP^{8}, DHP^{11}, NLe^{12} tridecapeptide to catalytic reduction in the presence of tritium gas (TR3 method). Removal of catalyst and labile tritium was performed by Amersham. Further purification and characterization was performed as outlined in this methods section.

Thin Layer Chromatography

The radiolabelled alpha-factor was analyzed by thin layer chromatography (TLC) on precoated F254 silica gel plates (Merck, Darmstadt, Germany) in a chamber saturated with butanol:propionic

acid:water (50:25:35, V/V/V) (24). Unlabelled NLe^{12} tridecapeptide (10ug) was located using a handheld UVSL-25 ultraviolet lamp (Ultra-violet Products Inc., San Gabriel, CA). ^{3}H-alpha-factor was visualized by autoradiography using either XOMAT XAR-5 (Eastman Kodak, Rochester, NY) or Curix RP2-100AFW Xray film (Agfa-Gevaert, Belgium) and EN^{3}HANCE spray (New England Nuclear Research Products, Boston, MA) as instructed by the manufacturers.

When TLC was used to assess label degradation during the course of binding assay incubation, 10 ul aliquots from a binding association reaction (1×10^{9} cells/ml; 4×10^{-8} M ^{3}H-alpha-factor) were spotted on precoated F254 silica gel plates over the course of 30 minutes. After drying, plates were developed in the butanol:propionic acid:water solvent system indicated above. Radiolabelled species were visualized by autoradiography and unlabelled controls with UV flourescence.

High Performance Liquid Chromatography (HPLC)

Purification of tritium-labelled alpha-factor was carried out on a Waters Chromatograph (Waters Associates, Milford, MA) equipped with two Model 510 solvent delivery systems, a U6K injector, Model 481 variable wavelength detector, Model 680 automated gradient controller and a Model 730 data module. Separations were performed on a Waters uBondapak reversed-phase C_{18} column (30 cm X 3.9 mm I.D., 10 u particle size) employing a linear gradient of 25-40% acetonitrile, 0.025% trifluoroacetic acid as the mobile phase. Flow rates were typically 1.4 or 1.5 ml/min as indicated. The absorbance of the column eluant was recorded at 220nm. When necessary 0.26 min fractions (360 ul or 390 ul

depending on the flow rate) were collected over the duration of the run (30 minutes) using a Pharmacia Frac-100 fraction collector (Pharmacia Inc., Piscataway, NJ) equipped with silicanized borosilicate tubes. Fractions containing tritium-labelled species were identified by taking 10 ul aliquots from the fractions and counting them in Brays Solution (Research Products International, Mt. Prospect, IL) on program 5 of a Beckman LS7000 scintillation counter (Beckman Instruments, Palo Alto, CA). Efficiency of counting for tritium on this machine was 26%. Specific activities were defined according to the number of counts associated with the A220 peak area. Peak areas were compared against two external unlabelled NLe^{12} tridecapeptide alpha-factor standard injections for quantitation.

Peptide Sequence Determination

Unlabelled tridecapeptide and HPLC purified tritium-labelled alpha-factor were subjected to automated sequence analysis by sequential Edman degradation on a Beckman System 890M Series sequenator. The dried HPLC purified peptides were reconstituted in 100 ul 50% acetic acid and applied to the polybrene primed glass cup of the sequenator. Phenylisothiocynate (PITC) coupling and heptafluorobutyric acid cleavage of the sequential amino-terminal amino acids occurred in the cup. Thiazolinone amino acid derivatives were collected in the fraction collector and converted into their corresponding phenylthiohydantoin (PTH) derivatives by treatment with aqueous acid. After drying, each sequence cycle fraction was reconstituted in 50 ul of 100% methanol. 10 ul of this were analyzed by HPLC on a Waters Liquid Chromatograph

Amino Acid Analysis System equipped with a Wisp 710B injector, two Model 510 pumps, a Model 440 absorbance detector, a Model 730 data module and a Waters programmable system controller. Separations were achieved using a 3.9 mm X 15 cm (particle size, 4u) Waters Pico-Tag C_{18} column and gradient conditions as described previously for PTH amino acids (15). The derivatives produced in each cycle were quantitated by comparison to a set of external standards injected immediately before and after each sequence cycle sample was run. An amino acid was placed in sequence if the amount of the corresponding derivative increased in a certain sequencing cycle and decreased in subsequent cycles.

Extinction Coefficient Determination for Unlabelled Alpha-Factor Analogues

In order to faithfully reproduce assays, standardized stocks of unlabelled alpha-factor analogues were made and kept frozen. To establish criteria for standardization, extinction coefficients were determined for a number of unlabelled compounds having at least one representative from three major categories: (1) tridecapeptides containing two tryptophans, (2) $desTrp^1$ dodecapeptide and Phe^3 tridecapeptide, which contain one tryptophan residue and (3) peptides lacking tryptophan such as $desTrp^1$, X^3 dodecapeptide where X ≠ tryptophan. 1 mg/ml solutions as weighed on a Mettler AE163 analytical balance (Mettler Instrumente AG, Greifensee, Switzerland) were made in sterile milli-Q water. 1:40 dilutions were read at absorbances of 280 and 220 nm on a Shimadzu UV-Vis Recording Spectrophotometer UV160 (Kyoto, Japan). Duplicate aliquots of these dilutions were lyophilized

on a Labconco freeze dryer (Kansas City, MO) in sealable reaction vials for quantitative amino acid analysis. Hydrolysis of the lyophilized peptides in constant boiling 6N HCl at 105°C for 24 hours for quantitative amino acid analyses was performed on a duplicate 1:40 dilution of the 1 mg/ml solutions described above. Once lyophilized, these solutions were derivatized using PITC for subsequent injection of 4 ul onto the Pico-Tag column of the Waters Liquid Chromatograph Amino Acid Analysis System. The phenylthiocarbamyl (PTC) amino acids were separated as recommended by the column manufacturer. Extinction coefficients (ε) in nm were calculated according to the following equation:

$$\frac{\text{Actual Concentration (M)}}{\text{Absorbance at 220 nm or 280 nm}} = \frac{\text{1Molar}}{\varepsilon}$$

Enzyme Linked Immunoadsorbant Assay (ELISA)

The ELISA technique was performed based on preliminary experiments which determined the optimum alpha-factor antibody and peroxidase-labelled goat anti-rabbit immunoglobin dilutions to be used. The anti-alpha-factor antibody was made against the synthetic tridecapeptide in rabbits. Tests revealed this antibody to be primarily directed against the carboxyl terminus of the peptide. All dilutions for the ELISA were done manually in duplicate. Horseradish peroxidase activity was determined by reading optical density at 490 nm using the Model EL310 automated microplate ELISA reader (Bio-Tek Instruments Inc., Burlington, VT). As a positive control, tridecapeptide was diluted

sequentially two-fold from 5ug/ml (well 1) to 0.298 pg/ml (well 24) into sodium carbonate buffer, pH 9.6. 10 ul (4 ng) of the HPLC purified tritiated alpha-factor were diluted sequentially as described above into 96-well Immulon 2 plates (Dynatech Laboratories Inc., Alexandria, VA). These plates were incubated overnight at 4°C to allow the peptide to bind to the plate. This solution was removed and the wells were washed three times with wash buffer (10 mM Tris; 0.9% NaCl; 0.05% Tween 20; pH 7.4) allowing the second wash to remain at room temperature for 30 minutes. 100 ul of serum (1:100 dilution of either preimmune or immune-anti-alpha-factor in wash buffer) were added to each well. Following a 1 hour, 37°C incubation with agitation to allow the antibody-antigen complex to form, the plate was washed three times with wash buffer. 100 ul of peroxidase-labelled goat anti-rabbit IgG (1:1000 dilution in wash buffer; Cappel, Cooper Biochemical, Malvern PA) were added to each well and incubated at 37°C for one hour with frequent agitation. The plates were washed three times with wash buffer after which 100 ul of the substrate solution (ortho-phenylenediamine dissolved in pH 6 citrate-phosphate buffer, 0.3% hydrogen peroxide) were dispensed to each well. The optical density (490nm) of the solution in the wells was read at 10 and 15 minutes. A background blank consisted of 100 ul of the substrate solution alone.

Radioimmunoprecipitation of ^{3}H-Alpha-Factor

Radioimmunoprecipitation (RIP) of tritium-labelled alpha-factor was accomplished using procedures similar to those previously published (126). Basically, 5 ul of labelled alpha-factor (approximately 2 ng)

were added to 50 ul undiluted anti-alpha-factor antiserum or preimmune serum and 245 ul TNE buffer (0.05 M Tris, 150 mM NaCl, 5 mM EDTA, 0.025% Triton, pH 7.4) in a sterile microfuge tube. Quadruplicate tubes were incubated at 37°C one hour on a rotating platform. To four of the tubes (two immune and two preimmune) 6.25 units of goat anti-rabbit gamma globulin (Calbiochem-Behring, La Jolla CA) were added. Following incubation at 4°C overnight for all tubes, Pansorbin (Calbiochem-Behring, 10% W/Vol) was added in a ratio of 1:1 (vol:vol; reaction:Pansorbin) for precipitation of the antibody-antigen complexes. After incubation at 4°C for 5 hours, precipitates were pelleted in a Model 5414 Eppendorf microfuge (Brinkmann Instruments, Westbury, NY; 15,600 X g) for two minutes and washed five times with TNE buffer. 100 ul aliquots of the supernatants were taken for counting in 5 mls of Brays scintillation fluid. A second round of RIP was carried out on the supernatant from the initial centrifugation. Percent precipitable counts were those total counts precipitated by immune sera and not by preimmune sera after three successive rounds of RIP divided by the total counts available for precipitation.

Alpha-Factor Biological Activity Assays

Halo Assay for Growth Arrest. S. cerevisiae 4202-15-3 or 4202-1-2 cells (1×10^6) were plated using 4 ml of 0.8% top agar for each minimal medium plate (2% noble agar, 2% glucose, 0.67% yeast nitrogen base without amino acids, 20ug/ml adenine, histidine and tryptophan and 30ug/ml lysine and tyrosine). Whatman no. 1 filter paper disks containing the specified amounts of the indicated peptides were placed

on each plate. After incubation for 36 hours at 30°C, halos of growth arrest were measured and described.

Shmoo Assay. S. cerevisiae 4202-15-3 or 4202-1-2 cells were grown to slightly less than 1 X 10^7 cells/ml in YM-1 medium overnight in a rotary water bath at 30°C. Cells were harvested by centrifugation in a Beckman Model TJ-6 tabletop centrifuge (1500xg, 5 minutes), washed one time with fresh medium and resuspended for a final assay concentration of 2 X 10^6 cells/ml. 96-well microtiter plates (Costar, Cambridge, MA) were used to make 24 two-fold dilutions of each peptide in YM-1 medium. The final concentration range tested for each alpha-factor peptide was 25ug/ml to 2.98 pg/ml. Once 100 ul of the cell stock (4 X 10^6 cells/ml) were added to the 100 ul of peptide solution in each well the plates were incubated at 30°C on a rotary agitator. At 4.5 hrs samples were removed from each well for microscopic examination. Affected cells were identified by comparison to control wells containing cells without alpha-factor peptide. The activity endpoint was defined as the last well showing morphologically aberrant cells at 4.5 hrs.

Time Course for Alpha-Factor Binding

To determine the time course of association and dissociation for a kinetically derived K_D, 500 ml of YM-1 in 1L erlenmeyer flasks were prewarmed for three hours to 30°C. These flasks were inoculated with 4202-15-3 and 4202-1-2 (final cell concentration = 1.5 X 10^5) from YM-1 plates for growth overnight at 30°C in a rotary water bath. A_{550} readings and hemocytometer counts of the culture indicated when harvest was appropriate. Under these conditions, the generation time is 120

minutes. Cells were harvested at 1 X 10^7 cells/ml by centrifugation at 6370 xg, 4°C in a JA-10 rotor on a Beckman Model J-21C centrifuge. The resultant pellets were washed two times with ice cold fresh, filtered YM-1+i media and eventually resuspended to 1.11 X 10^9 cells/ml for a cell stock solution (final reaction cell concentration = 1 X 10^9 cells/ml). This concentration was checked before use by diluting and counting an aliquot microscopically. The reaction was initiated by the addition of 200 ul of labelled alpha-factor working dilution (7.5 X 10^{-7} M) to 1.8 ml of the cell stock solution. At 1, 2, 3, 4, 5, 8, 10, 15, and 20 minutes, 50 ul of the reaction mixture were diluted into 1.5 ml of ice cold YM-1+i medium and filtered over 1% bovine serum albumin presoaked GN-6 Metricel filters (Gelman Sciences Inc., Ann Arbor, MI). The dilution tube was then rinsed two times with 1.5 mls of ice cold YM-1+i, each rinse being put over the same filter. Finally 1.5 ml ice cold YM-1+i medium was used to wash the filter directly one time. Over the course of the reaction, the temperature of incubation was kept constant at 22°C using a Thermomix 1442D (B. Braun Instruments, Burlingame, CA). On the average, tubes were vortexed one time every 5 minutes. At 20 minutes, four 10 ul aliquots of the reaction mixture were taken to determine total ligand concentration (total amount bound plus total amount free). To determine the amount of nonspecific binding, alpha cells were incubated identically to a-cells. At 20 minutes, triplicate aliquots were withdrawn, diluted into 1.5 mls ice cold YM-1+i and processed as described above for the a-cells. Specific binding was defined as those counts bound to a-cells minus those counts

bound to alpha cells. At 23 minutes, the dissociation phase was initiated by diluting separate aliquots of the reaction mixture 200-fold into (a) temperature equilibrated YM-1+i medium only or (b) temperature equilibrated YM-1+i medium containing a 10-fold molar excess of unlabelled alpha-factor. Parafilm was used to invert tubes for mixing. At 2.5, 5, 7.5, 10, 15, 20, 30, 45, 60, 90, 120, and 135 minutes aliquots were filtered and washed as described previously to determine the amount of alpha-factor remaining bound. Filters were counted in 5mls Bray scintillant. All assays and manipulations were done in silicanized borosilicate tubes or vials.

Steady State Saturation Binding

To obtain steady state saturation binding for Scatchard and Hill analysis, cells were grown and harvested as described above with the following changes. The cell stock solution was made 3.75×10^8 cells/ml for a final assay cell concentration of 3×10^8 cells/ml. More specifically, working dilutions of tritium-labelled alpha-factor at 5×10^{-6}, 5×10^{-7}, and 5×10^{-8} M were made in order to achieve target assay concentrations of 3×10^{-7} M, 1×10^{-7} M, 7×10^{-8} M, 5×10^{-8} M, 3×10^{-8} M, 1×10^{-8} M, 7×10^{-9} M, 5×10^{-9} M and 1×10^{-9} M tritiated alpha-factor. Initiation of binding by the addition of label was staggered by 5 minutes such that each concentration could be processed at 35 minutes with ample time for the manipulations involved. At 5 minutes post binding initiation, two 50 ul aliquots were taken to determine total alpha-factor concentration (bound + free) for each experimental point. Incubation was at 22°C with intermittant vortexing

on the average of one time every five minutes. At 35 minutes, two 150 ul aliquots were taken, diluted, filtered on BSA presoaked GN6 Metricell filters and washed as described previously. To determine the level of nonspecific binding, alpha cells were tested at the same concentrations using the same method.

Competition for Tritium-labelled Alpha-Factor Binding by Unlabelled Alpha-Factor Analogues

Competitive displacement of bound radiolabelled alpha-factor by unlabelled alpha-factor analogues was measured in assays with the following protocol. In general, a- and alpha cells were grown and harvested as described above for the time course of alpha-factor binding. Changes include resuspending the cells in YM-1+i medium to 1.25×10^9 cells/ml with a final assay concentration of 1×10^9 cells/ml. Final assay concentrations of the unlabelled competitors were 3×10^{-9} M, 6×10^{-9} M, 1×10^{-8} M, 3×10^{-8} M, 6×10^{-8} M, 1×10^{-7} M, 3×10^{-7} M, 6×10^{-7} M, 1×10^{-6} M, 3×10^{-6} M, 6×10^{-6} M, and 1×10^{-5} M. Typically, the reaction was started by the addition of 50 ul of the working ^{3}H-alpha-factor dilution (6×10^{-7} M) to 400 ul of the cell stock (1.25×10^9 cells/ml) and either 25 or 50 ul of the appropriate unlabelled alpha-factor analogue stock. When necessary prior to the addition of the label, volumes were adjusted to total 450 ul by the addition of YM-1+i. Positive control reactions consisted of either a or alpha cells and labelled alpha-factor but no unlabelled competitor. Alpha cells were tested at competitor concentrations of 1×10^{-8} M, 1×10^{-7} M, 1×10^{-6} M and 1×10^{-5} M to determine the level

of nonspecific binding. All incubations were done at 22°C. Starting of the reactions was staggered five minutes to allow time for the needed manipulations at 35 minutes. To determine total ligand concentration, two 20 ul aliquots were taken at five minutes for counting. Duplicate 150 ul aliquots were taken at 35 minutes, diluted, filtered and treated as previously described to determine the amount of alpha-factor bound.

Equilibrium Thermodynamic Parameters of Alpha-Factor Binding

To determine the effect of temperature on the kinetic and equilibrium constants of binding for the tridecapeptide and the desTrp^{1}, Ala^{3} dodecapeptide, competition assays as described above were carried out at 10, 20, 30 and 40°C. See appendix C for details.

III. RESULTS

^{3}H-Alpha-Factor Purification

Tritiated alpha-factor was prepared from the parent pheromone DHP^{8}, DHP^{11}, NLe^{12} alpha-factor as outlined in the methods section and illustrated in figure 6. Purity of the crude, labeled preparation was initially assessed by thin layer chromatography. As seen in plate B lane 2 of figure 7, at least nine different species are contained in the crude preparation, however the most abundant species (plate A, lane 2) comigrates with the unlabelled NLe^{12} tridecapeptide visualized by flourescence and indicated by the circles in the same figure.

Because label purity is important in binding data interpretation, the labelled alpha-factor was purified from the crude preparation using reverse phase HPLC. Figure 8, panel A shows the profile of counts obtained in fractions taken from the HPLC run illustrated in panel B of the same figure. As seen in panel A the majority of the counts elute with the void volume at the polar end of the gradient. This is probably attributable to ^{3}H-incorporation into the aqueous diluent of the preparation during the commercial labelling process. Smaller peaks with retention times less than 16.5 min may be fragments of the labelled 13-mer either generated during the process of catalytic reduction or through radioactive decay in storage. None of these smaller peaks were biologically active in the halo assay (data not shown). The major A_{220} peak (R_t = 16.5 mins, panel B) corresponds to the major peak of radioactivity retained (fractions 57-59, panel A) by the C_{18} column.

NH_2 -Trp-His-Trp-Leu-Gln-Leu-Lys-DHP-Gly-Gln-DHP-NLe-Tyr-COOH

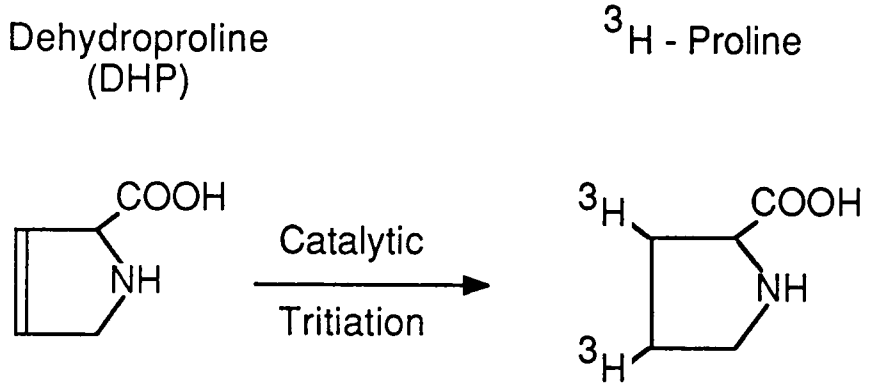

Figure 6. The synthesis of tritiated α-factor by catalytic reduction in the presence of tritium gas.

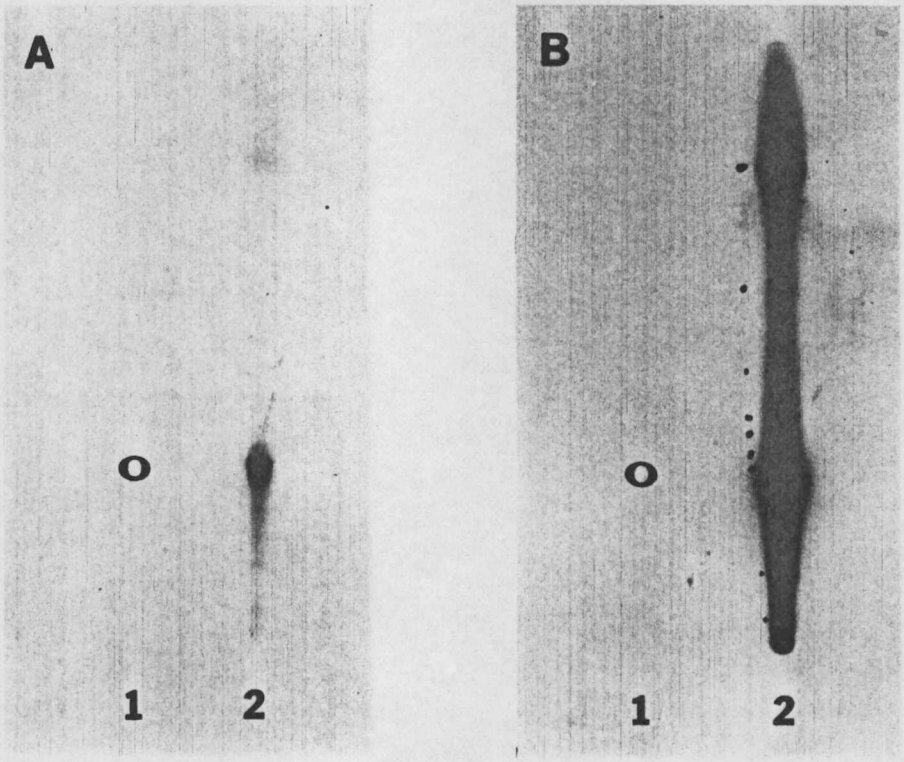

Figure 7. Assessment of crude ^{3}H-α-factor purity by thin layer chromatography.

Panel A. Lane 1: Unlabelled Nle^{12} Tridecapeptide
Lane 2: ^{3}H-α-factor
One hour exposure.

Panel B. Lane 1: Unlabelled Nle^{12} Tridecapeptide
Lane 2: ^{3}H-α-factor
Four hour exposure.

Circles indicate spots located using a handheld UV light. 4.25×10^{6} dpm of ^{3}H-α-factor were applied.

Figure 8. High performance liquid chromatography (HPLC) of Crude ^{3}H-α-factor.

Panel A. Radioactivity associated with 0.29 minute fractions taken over the 30 minute HPLC run in Panel B.

Panel B. Profile of the absorbance (220 nm) for HPLC separation of crude ^{3}H-α-factor.

Mobile phase A: Acetonitrile containing 0.025% trifluoroacetic acid

Mobile phase B: H_2O containing 0.025% trifluoroacetic acid

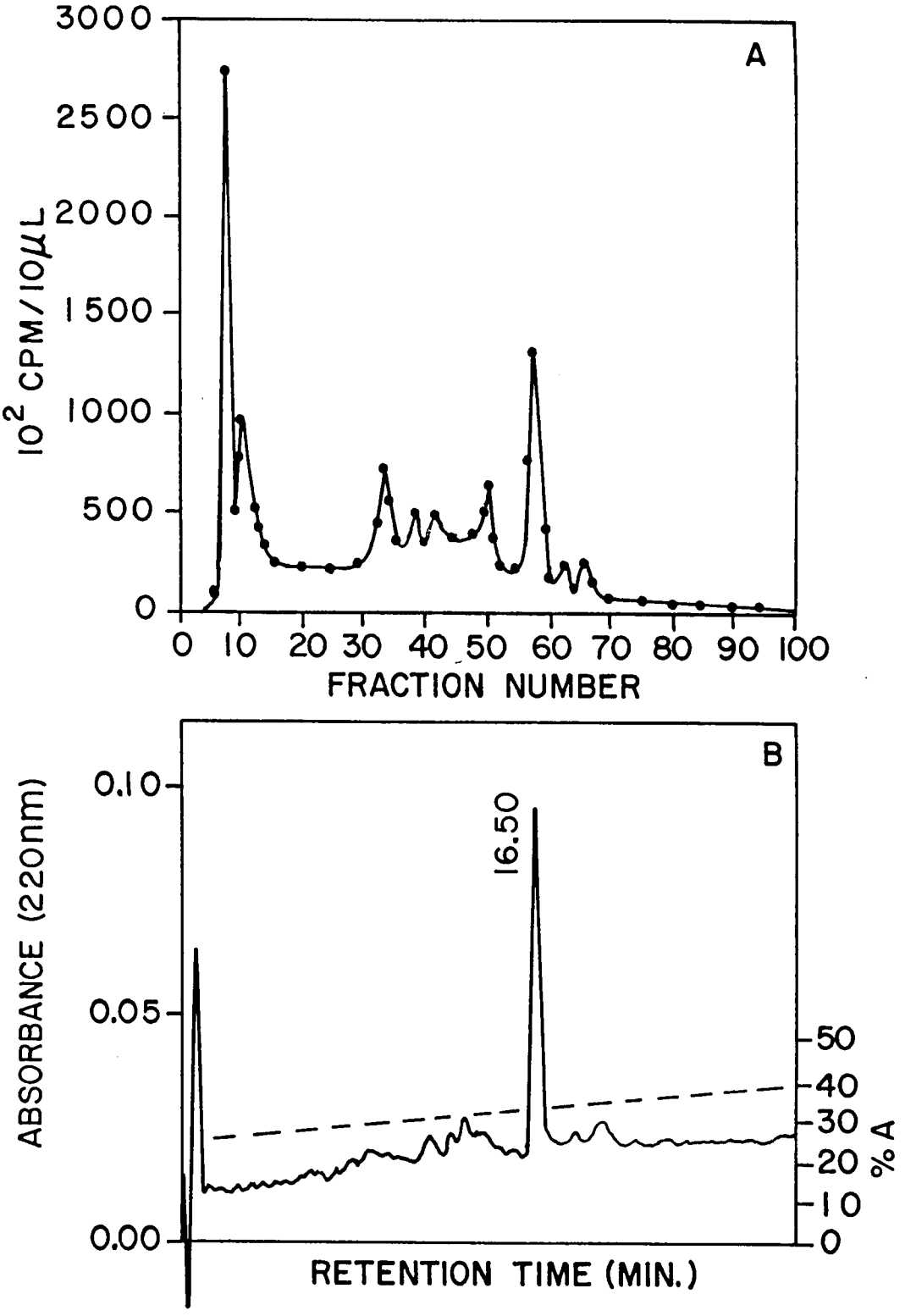
A
3000
2500
2000
1500
1000
500
0
10^2 CPM/10μL
0 10 20 30 40 50 60 70 80 90 100
FRACTION NUMBER
B
0.10
0.05
0.00
ABSORBANCE (220nm)
16.50
50
40
30
20
10
0
%A
RETENTION TIME (MIN.)

Figure 8.

These peaks also co-elute with the unlabelled parent compound, DHP^{8}, DHP^{11}, NLe^{12} alpha-factor(data not shown).

As a check for purity, those fractions corresponding to the 16.5 minute peak were pooled, concentrated as described in the methods section and reinjected using the same system for HPLC separation. The profiles for elution of radioactivity and 220 nm absorbing material are shown in panels A and B, respectively of figure 9. Once again the peak of radioactivity in panel A corresponds to the 14.88 minute peak of absorbance in panel B. Therefore, panel A indicates the material is radiochemically pure and panel B indicates the material is free from other peptide impurities. These results along with the fact that the unlabelled parent compound, DHP^{8}, DHP^{11}, NLe^{12} tridecapeptide co-elutes with both peaks indicates the purified species is tritiated alpha-factor.

Further evidence indicating successful isolation of tritiated alpha-factor resulted from the use of an anti-alpha-factor antibody in an ELISA. When 0.1 ug tritiated alpha-factor was sequentially diluted 2-fold in parallel with 1 ug of the native pheromone, endpoints were observed in wells containing the same amount of peptide (0.2 ng ^{3}H-alpha-factor and 0.2 ng native pheromone). As expected, tritiation of the alpha-factor pheromone does not effect its ability to be recognized by an antibody made to the carboxyl terminus of the unlabelled tridecapeptide.

To determine if the ^{3}H-alpha-factor was radiolabelled at the amino acid positions expected, the HPLC-purified pheromone was sequenced. In

Figure 9. High performance liquid chromatography (HPLC) of purified ^{3}H-α-factor.

Panel A. Radioactivity associated with 0.29 minute fractions taken over the 30 minute HPLC run in Panel B.

Panel B. Profile of the absorbance (220 nm) for HPLC separation of purified ^{3}H-α-factor.
Mobile phase A: Acetonitrile containing 0.025% trifluoroacetic acid
Mobile phase B: H_2O containing 0.025% trifluoroacetic acid

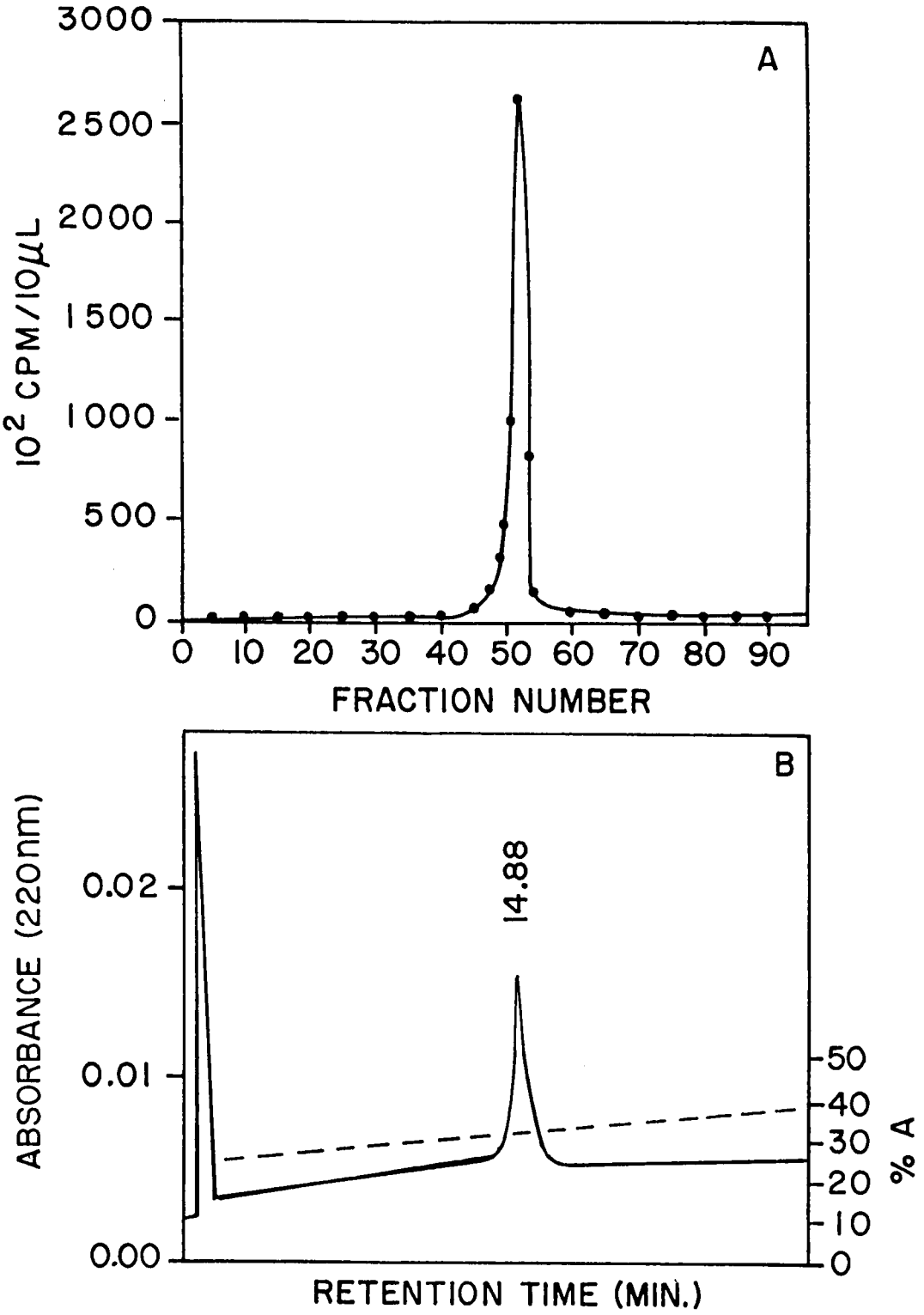
A
3000
2500
2000
1500
1000
500
0
10^2 CPM/10μL
0 10 20 30 40 50 60 70 80 90
FRACTION NUMBER
B
14.88
0.02
0.01
0.00
ABSORBANCE (220nm)
50
40
30
20
10
0
% A
RETENTION TIME (MIN.)

Figure 9.

order to facilitate sequencing and conserve label, the specific activity of the ^{3}H-alpha-factor was diluted with unlabelled NLe^{12} alpha-factor before sequencing. The sequencing results are illustrated in figure 10. Subsequent amino acid analysis of the fractions produced the correct alpha-factor sequence in the molar ratios expected for the NLe^{12} tridecapeptide (data not shown). Scintillation counting of aliquots from the sequencing fractions indicated radioactivity in the position 2 amino acid (30% of total), and in the position 8 (43% of total) and 11 (27% of total) amino acids. Although the radioactivity associated with residues 8 and 11 was expected since catalytic reduction of dehydroproline should have favored labelling at these positions, the incorporation of tritium into residue 2 was unexpected.

In order to determine whether the counts associated with residue 2 were present in histidine, fractions were collected over the duration of the amino acid analyses for residues 2, 8 and 11. These results are found in figure 11. All the radioactivity contained in cycle 2 co-eluted with unlabelled histidine. Likewise, the radioactivity in cycles 8 and 11 co-eluted with unlabelled proline (data for cycle 11 not shown). Therefore the catalytic reduction of DHP^{8},DHP^{11},NLe^{12} tridecapeptide resulted in the insertion of tritium at histidine 2, dehydroproline 8 and dehydroproline 11 of the alpha-factor pheromone. Furthermore, judging from the HPLC profiles and the sequencing data, the tritiated alpha-factor isolated is greater than 98% pure.

The specific activity of ^{3}H-alpha-factor was calculated based on the total counts associated with the corresponding A_{220} peak areas. Two

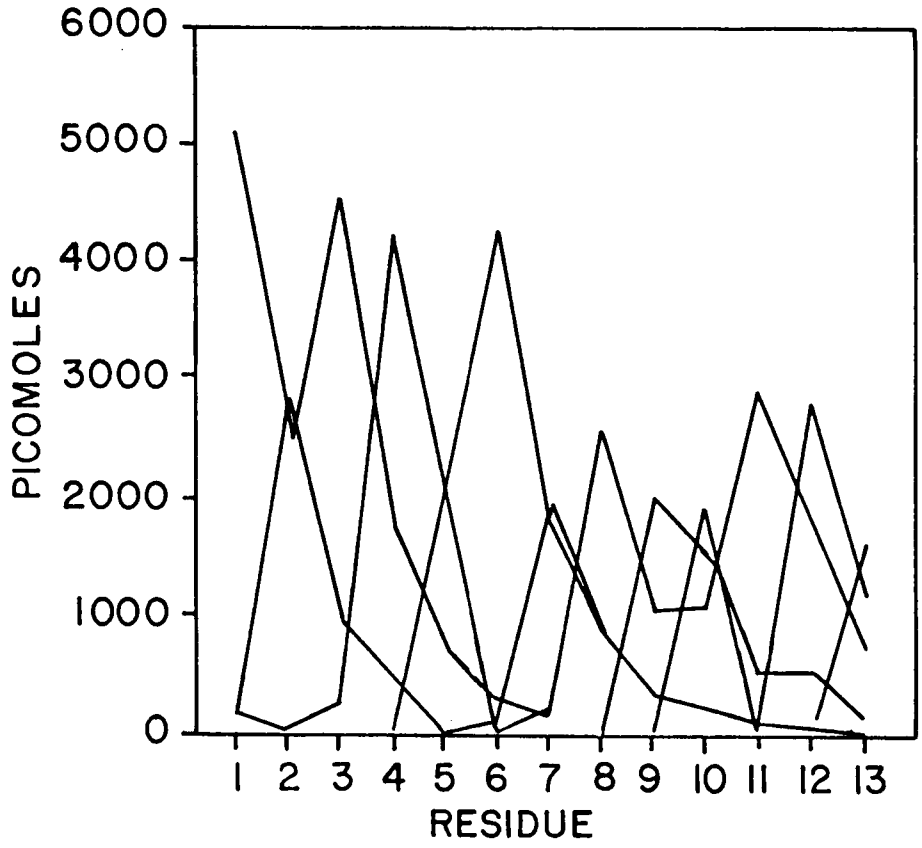

Amino Acid	NH_2-Trp	Trp	Gln	Lys	Gly	Pro	Tyr-COOH
	His	Leu	Leu	Pro	Gln	Nle	
% of Total Radioactivity	30			43		27	

Figure 10. Sequencing of the purified ^{3}H-α-factor. The amino acids identified by amino acid analysis for each residue are listed below the figure. The percent of total cpm associated with residues 2, 8 and 11 are noted.

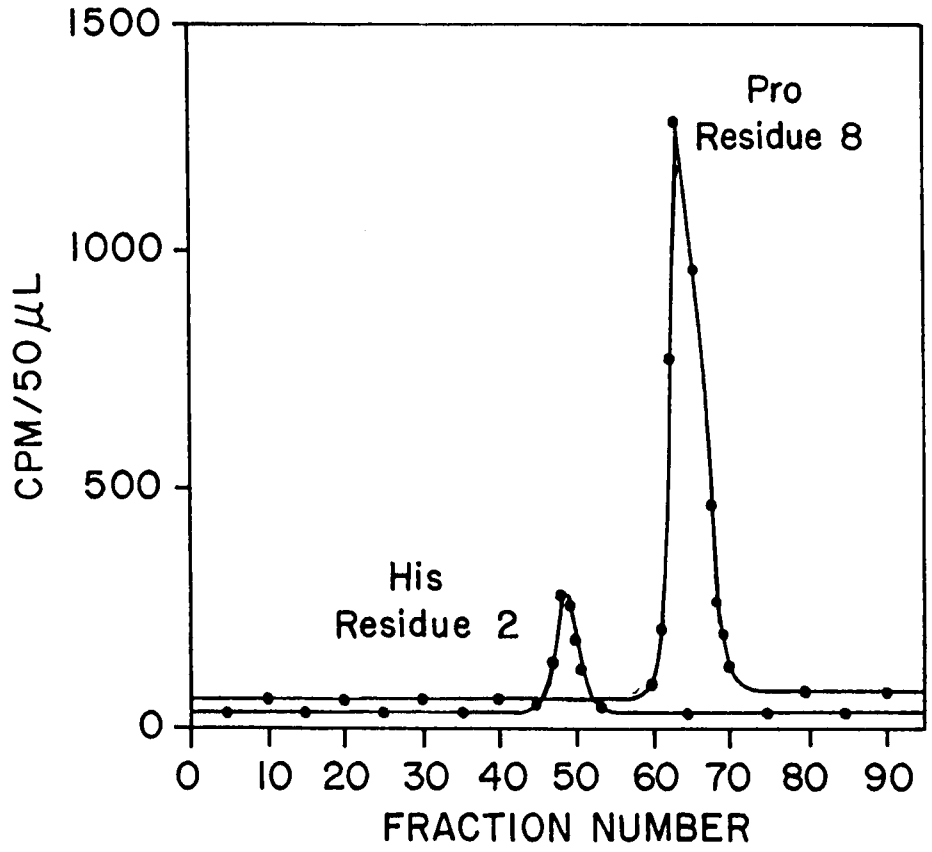

Figure 11. Radioactivity associated with fractions from amino acid analyses of residues 2 and 8. Baselines are equal but offset in this figure for clarity.

10 ug standards of unlabelled DHP^{8},DHP^{11},NLe^{12} tridecapeptide were injected separately for peak area comparisons and subsequent quantitation. The specific activities varied slightly between batch purifications but always equaled between 8 and 10 Ci/mmol.

Characterization of ^{3}H-Alpha-Factor

Because previous efforts to radiolabel alpha-factor to high specific activities had rendered the pheromone inactive, the biological activity of the purified ^{3}H-alpha-factor was tested using the halo assay for growth arrest. In figure 12 disks 1, 2, 3 and 4 contain 0.1 ug, 0.25 ug, 0.5 ug and 1 ug of the parent DHP^{8},DHP^{11},NLe^{12} tridecapeptide, respectively. Disks 5 and 6 contain the native tridecapeptide sequence at 1 ug and 0.1 ug amounts. The center disk contains approximately 0.1 ug of the purified ^{3}H-alpha-factor. As indicated by the clearing of growth around the center disk, the tritiated alpha-factor is equivalent in biological activity to the NLe^{12} tridecapeptide. Plating of the tridecapeptide, DHP^{8},DHP^{11},NLe^{12} tridecapeptide and ^{3}H-alpha-factor on a lawn of congenic alpha cells (4202-1-2) showed no inhibition of growth(data not shown). These results indicate that the incorporation of tritium into the histidine and two prolines of the alpha-factor pheromone does not alter biological activity.

An experiment was done to determine whether the tritium-labelled alpha-factor interacts with a-cells in a way identical to its unlabelled homolog. Using 1×10^{9} 4202-15-3 cells/ml, the amount of labelled alpha-factor was varied with the amount of unlabelled alpha-factor to always give the same total peptide concentration. Binding was

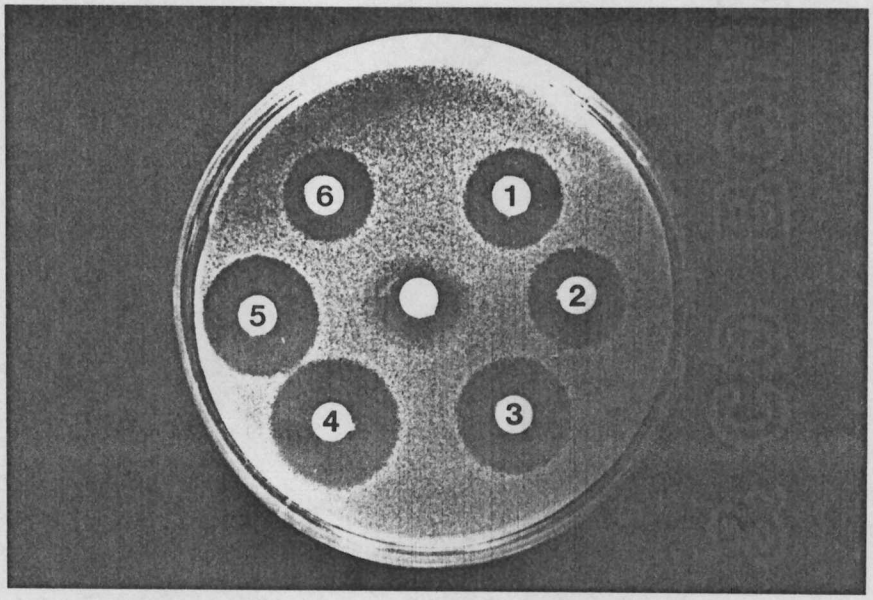

Figure 12. Halo assay for growth arrest.

Disk 1. 0.1 μg DHP^{8} DHP^{11} Nle^{12} Tridecapeptide
2. 0.25 μg DHP^{8} DHP^{11} Nle^{12} Tridecapeptide
3. 0.5 μg DHP^{8} DHP^{11} Nle^{12} Tridecapeptide
4. 1 μg DHP^{8} DHP^{11} Nle^{12} Tridecapeptide
5. 1 μg alpha-factor
6. 0.1 μg alpha-factor

Center disk. Approximately 0.1 μg ^{3}H-α-factor. The top agar contains 1×10^{6} 4202-15-3 cells. The medium is minimal.

determined at each of the ratios indicated in figure 13. The points approximate a straight line which is expected if both the unlabelled and labelled alpha-factors interact with the receptor in an identical manner.

Biological Activities of Unlabelled Alpha-Factor and Its Analogues

Biological activities of the unlabelled alpha-factor and its analogues were determined using two assays. Growth arrest activity was assessed using the halo assay and the ability to induce shmoo formation was evaluated using the microtiter assay. The results for both assays are listed in table 1.

Values for growth arrest indicate activity relative to the tridecapeptide. For each peptide 0.5, 1, 5, 8, and 10 ug were spotted on disks which had been placed upon YM-1 plates with top agar containing 1×10^6 4202-15-3 cells. At 36 hours, the resulting halos were measured. These values were plotted against the log of the amount of peptide applied. The slopes of the resulting lines were compared to the slope of the line for the native tridecapeptide to obtain the values in table 1.

The ability to induce shmoos was evaluated using the microtiter assay. Serial dilutions of each peptide were tested for shmoo inducing affect. The endpoints contained in table 1 indicate the last well in which morphological effect of the peptide was seen microscopically. The values in both assays show the same ranking of activities with the exception of the desTrp^1 αDns-His^2 CHA^3 dodecapeptide.

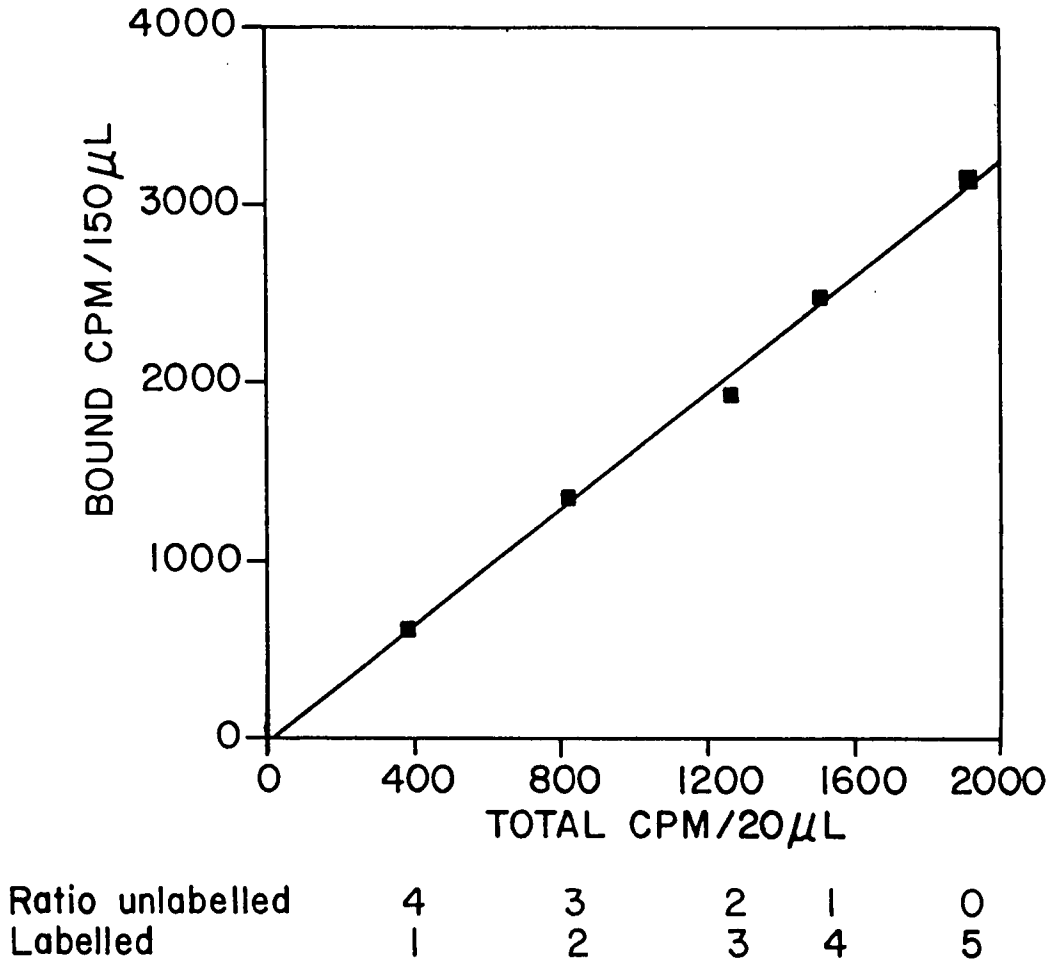

Figure 13. ^{3}H-α-factor interacts with the alpha-factor receptor in a way identical to its unlabelled homolog. The amount of ^{3}H-α-factor bound (cpm) is graphed vs. the total ^{3}H-α-factor present. The ratio of unlabelled α-factor to ^{3}H-α-factor for each point is indicated below the graph.

Table 1. Biological activity of α-factor and its analogues.

Peptide	Activity	
	Growth[a] Arrest	Shmoo[b]
Tridecapeptide	1	0.012
Asn^{5} Arg^{7} Tridecapeptide	1	0.012
NLe^{12} Tridecapeptide	1	0.012
DHP^{8} DHP^{11} NLe^{12} Tridecapeptide	1	0.012
Phe^{3} Tridecapeptide	0.92	0.024
des Trp^{1} Dodecapeptide	0.56	390
des Trp^{1} Ala^{3} Dodecapeptide	0	>25000
des Trp^{1} Phe^{3} Dodecapeptide	0	>25000
des Trp^{1} CHA^{3} Dodecapeptide	0.38	780
des Trp^{1} CHA^{3} D-Leu^{6} Dodecapeptide	0	>25000
des Trp^{1} CHA^{3} Lys^{7} (Acetyl) Dodecapeptide	<.20	1560
des Trp^{1} CHA^{3} Lys^{7} (Octanoyl) Dodecapeptide	0.28	780
des Trp^{1} CHA^{3} AIB^{8} Dodecapeptide	<.20	3130
des Trp^{1} CHA^{3} L-Ala^{9} Dodecapeptide	0	>25000
des Trp^{1} CHA^{3} D-Ala^{9} Dodecapeptide	0.33	780
des Trp^{1} αDns His^{2} CHA^{3} Dodecapeptide	0.37	97.6

[a]Growth arrest as measured by the halo assay. Halos of growth inhibition formed by different amounts of each of the mating factor peptides were measured on plates prepared as described in the methods section. The zone of growth inhibition determined by subtracting the disk diameter from the halo diameter was plotted as a function of the logarithm of the amount of α-factor applied to the disk. The values reflect the activity as represented by the slope of the line traced for each analogue relative to the tridecapeptide.

[b]Values represent activity endpoints in ng/ml for shmoo formation in the microtiter assay as described in the methods section.

Binding Assay Condition Optimization and Standardization

Cell growth. 4202-15-3 and 4202-1-2 cells were routinely grown to 1 X 10^7 cells/ml for use in the binding assay (0.4 absorbance units at 550nm). When harvested for assay at greater than 1 X 10^7 cells/ml the binding capacity of the cells was reduced(data not shown). Furthermore, use of an overgrown culture to restart a culture for use within 4 hours was unsuccessful. The best results were obtained when the cells were allowed to grow from an inoculum of 1 X 10^5 cells/ml as described in the methods section.

Wash procedure. In order to determine the best procedure for washing cells to remove unbound label, an experiment was done using methods previously found to maximize specific binding and minimize nonspecific binding (53). For the experiment, aliquots from a binding assay mixture of either a- or α-cells and 5.7 X 10^{-8} M ^{3}H-alpha-factor were taken and treated in one of the following ways:

1. Filtered directly, no wash.
2. Filtered directly, washed 1 time with YM-1+i.
3. Filtered directly, washed 2 times with YM-1+i.
4. Filtered directly, washed 3 times with YM-1+i.
5. Filtered directly, washed 4 times with YM-1+i.
6. Filtered directly, washed 5 times with YM-1+i.
7. Diluted into YM-1+i 10 times the volume of the aliquot and filtered.
8. Diluted into YM-1+i 10 times the volume of the aliquot and washed 3 times.

Treatment one was the least successful with the alpha cells showing nonspecific binding equal to 92%. Treatments 2-7 showed on the average 38±9% nonspecific binding. Treatment 8 was the most successful in that binding of ^{3}H-alpha-factor to alpha cells was reduced to 9% that of the a-cells. For this reason, procedure 8 was adopted for use in the binding assay.

Extinction Coefficients. An accurate determination of dissociation constants for unlabelled compounds in competitive displacement assays requires that the competitor concentrations are known precisely. So that comparisons between assays could be made if different stocks of the same unlabelled competitor were used, extinction coefficients for each of the three major peptide groups (peptides with two, one or no tryptophans) were determined. Table 2 shows the results from quantitative amino acid analyses on peptide solutions (at least one representative per group) for which absorbances at 220 nm and/or 280 nm had been read. Assuming 100% mole yield of the component amino acids in every case, the corresponding extinction coefficient was calculated according to the equation in note d of Table 2. Table 3 shows a summary of the extinction coefficients determined. As shown in table 3, the extinction coefficient determined for desTrp^{1} dodecapeptide at 280 nm is less than half of the extinction coefficient at 280 nm for the tridecapeptides containing two tryptophans. It is likely that the N-terminal tryptophan of the tridecapeptide contributes more to the absorbance at this wavelength than the position 3 tryptophan which participates in two peptide bonds.

Table 2. Quantitative amino acid analyses for extinction coefficient (ε) determination.

Peptide[a]	M.W.[f]	Absorbance[b] 220 nm	Absorbance[b] 280 nm	Actual[c] [M]	ε[d]	
Two Tryptophan-containing						
NLe^{12}	1666		0.136	1.04×10^{-5}	13077[e]	
One Tryptophan-containing						
des Trp^{1}	1498	1.114	0.148	2.73×10^{-5}	40806	5421[e]
Lacking Tryptophan						
des Trp^{1} Ala^{3}	1383	0.415		2.15×10^{-5}	19302	
des Trp^{1} CHA^{3} L-Leu^{9}	1521	0.368		1.95×10^{-5}	18872	
des Trp^{1} CHA^{3} D-Leu^{9}	1521	0.508		2.68×10^{-5}	18955	
des Trp^{1} CHA^{3} NLe^{12}	1447	0.334		1.78×10^{-5}	18764	

[a]All peptides listed are dodecapeptides except NLe^{12}.

[b]Solutions read were approximately 25 μg/ml.

[c]Values were obtained from quantitative amino acid analyses.

[d]Calculated as follows:

$$\frac{\text{Actual [M]}}{A_{220}} = \frac{1M}{\varepsilon}$$

[e]Calculated as in d however A_{280} was substituted for A_{220}.

[f]M.W. = molecular weight.

Table 3. Summary of extinction coefficients (ε).

Peptide	ε (M^{-1} x cm^{-1})[a]	
Tridecapeptides containing 2 tryptophans	13077 (280)	
des Trp^1 dodecapeptide Phe^3 tridecapeptide	40806 (220)	5421 (280)
des Trp^1 CHA^3 dodecapeptide derivatives des Trp^1 X^3 dodecapeptides (X ≠ Trp)	18973 (220)	

[a]Values in parentheses indicate wavelength for absorbance reading.

Similarly, the extinction coefficient determined for desTrp^1 dodecapeptide at 220 nm approximates twice the value of the 220 nm extinction coefficient for the desTrp^1 CHA^3 dodecapeptide derivatives and the desTrp^1 X^3 dodecapeptides. Examination of the traces of the 200-440 nm scans for the Nle^{12} tridecapeptide, desTrp^1 dodecapeptide and desTrp^1 CHA^3 dodecapeptide indicate a contributory absorbance around 220 nm which decreases from the Nle^{12} tridecapeptide to the desTrp^1 dodecapeptide and completely disappears in the scan of desTrp^1 CHA^3 dodecapeptide. The internal tryptophan therefore contributes to the absorbance read at 220 nm as well (for verification see 33). In order to standardize stocks of tridecapeptides containing two tryptophans, their absorbance was read at 280nm. Similarly, the concentrations of the desTrp^1 dodecapeptide and Phe^3 tridecapeptide group were determined by reading absorbances at both 220 and 280nm. desTrp^1 CHA^3 dodecapeptide derivatives and desTrp^1 X^3 dodecapeptides (where X $\neq$ Trp) solutions were standardized using absorbance readings at 220nm.

^{3}H-alpha-factor Degradation. MATa cells are known to contain a proteolytic activity responsible for cleaving the tridecapeptide between leucine 6 and lysine 7. To minimize pheromone hydrolysis, a protease inhibitor, TAME, was included along with other metabolic and energy inhibitors in the binding assay reaction and the cells used produce minimal amounts of the proteolytic activity due to a lesion in the BAR1 gene. However, since any change in the ^{3}H-alpha-factor concentration throughout the binding assay incubation would make impossible an accurate estimation of the binding parameters, an experiment was done to

assess ^{3}H-alpha-factor degradation in our system. a-Cells (1 X 10^{9} cells/ml) were incubated with 4 X 10^{-8} M ^{3}H-alpha-factor. Over the time course of 30 minutes, 50 ul aliquots were withdrawn, spun in a microfuge and 10 ul of the supernate was spotted on TLC plates for development in the solvent system described in the methods section. The autoradiograph of the plates is shown in figure 14. Plates A and B show that no degradation of the alpha-factor occurs during the binding assay incubation. Plate C shows a control in which alpha-cells were incubated with 4 X 10^{-8} M ^{3}H-alpha-factor and aliquots from 0 and 30 minutes were spotted. Although some streaking of the label occurred on this plate, no degradation is detected since comparison to the labelled stock without α-cells shows the same pattern.

Dependence of Binding on Cell Concentration

At equilibrium, the amount of ^{3}H-alpha-factor bound to a-cells was dependent on the cell concentration. This is represented in panels A and B of figure 15. Panel A shows the results from an experiment in which the percent of total ^{3}H-alpha-factor bound was obtained by determining the amount of unbound ^{3}H-alpha-factor from binding reaction filtrates. Specifically, after a 35 minute incubation, triplicate 150 ul aliquots of the binding reaction for each cell concentration were filtered and washed 1 time with 1.5 ml YM-1+i. The filtrate was counted to determine the amount of unbound ^{3}H-alpha-factor. 20 ul aliquots of the reaction mixture were withdrawn before filtering to determine the total amount of ^{3}H-alpha-factor present in each incubation. The percent bound was calculated by subtracting the percent unbound from 100

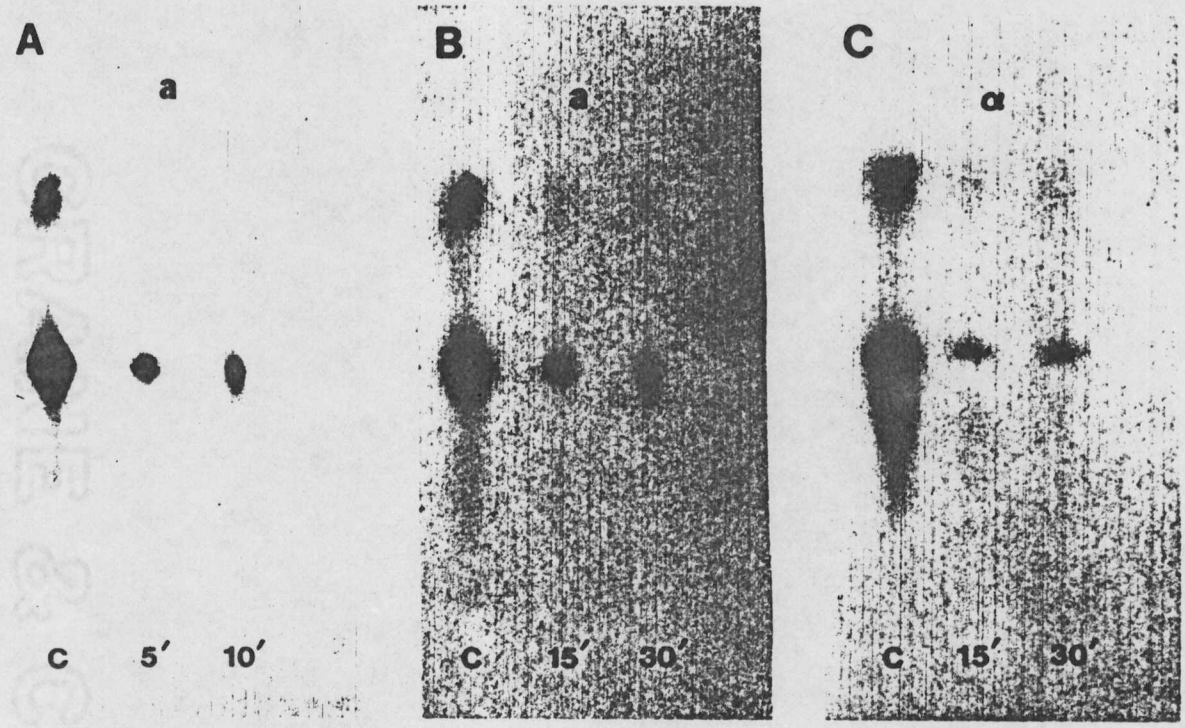

Figure 14. Assessment of ^{3}H-α-factor degradation during binding assay incubation.

Plate A. Lane 1 ^{3}H-α-factor
Lane 2 5' incubation with a-cells
Lane 3 10' incubation with a cells

Plate B. Lane 1 ^{3}H-α-factor
Lane 2 15' incubation with a-cells
Lane 3 30' incubation with a-cells

Plate C. Lane 1 ^{3}H-α-factor
Lane 2 15' incubation with α-cells
Lane 3 30' incubation with α-cells

3.4×10^{4} dpm of ^{3}H-α-factor were applied in control lanes (Lane 1, Plates A, B, C).

Figure 15. Effect of cell density on binding of ^{3}H-α-factor.

Panel A. Plot derived from counting aliquots of binding reaction filtrates.

Panel B. Plot derived from counting filter-retained cell-bound radioactivity.

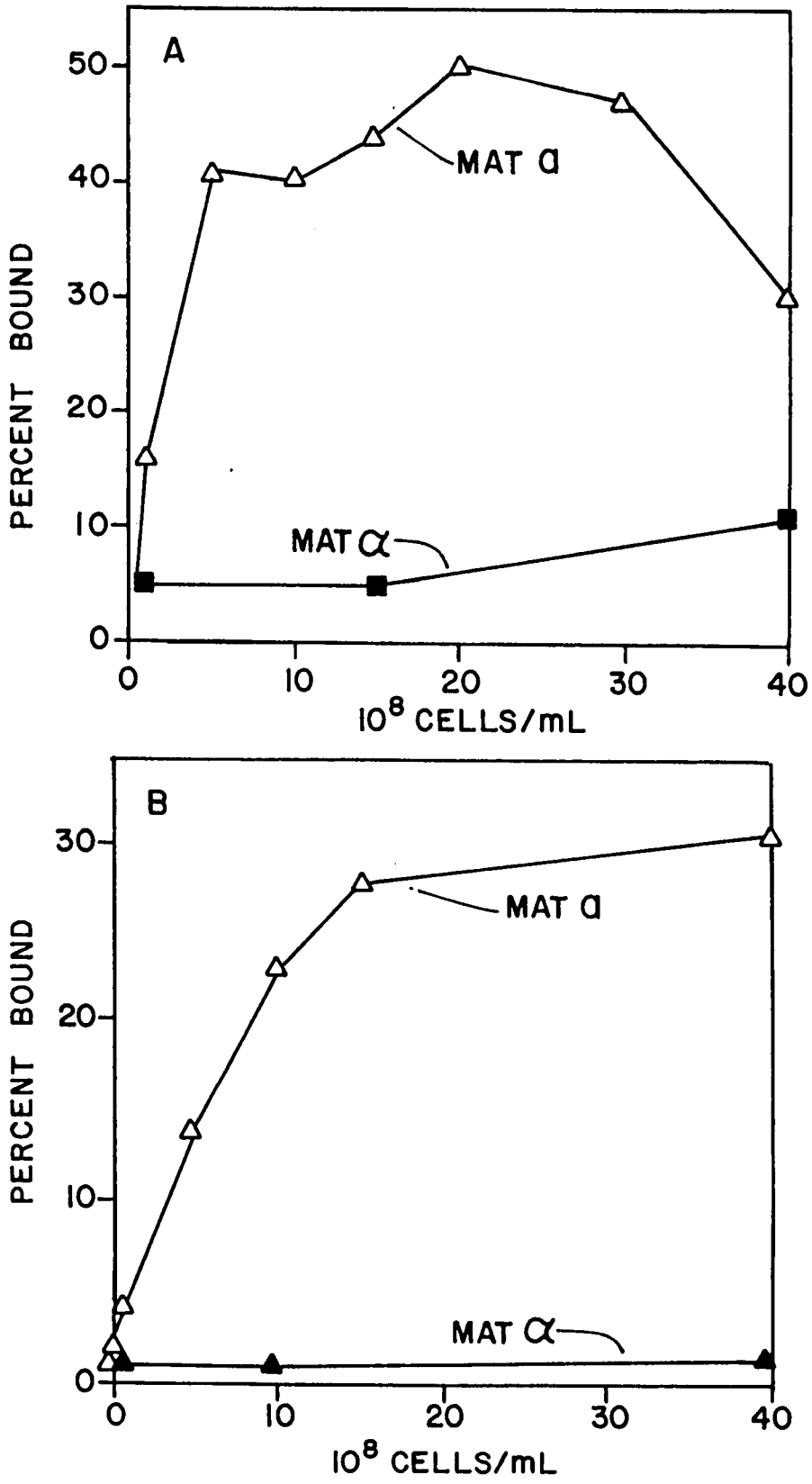
A
MAT a
MAT α
PERCENT BOUND
50
40
30
20
10
0
0
10
20
30
40
10^8 CELLS/mL
B
MAT a
MAT α
PERCENT BOUND
30
20
10
0
0
10
20
30
40
10^8 CELLS/mL

Figure 15.

(total). The amount of ^{3}H-alpha-factor removed from the binding reaction in this experiment by a-cells approached 50%.

In an identical experiment, the percent ^{3}H-alpha-factor bound was determined by counting the cell associated ^{3}H-alpha-factor retained after filtering and YM-1+i wash (see methods for details). These data are graphed in panel B of figure 15. The amount of ^{3}H-alpha-factor bound by a-cells in this experiment approached 30%. As previously determined, the filters quench associated-radioactivity by 23%. Therefore, both experiments suggest that between 50 and 55% of the ^{3}H-alpha-factor present can be removed by saturating cell concentrations.

Using an anti-alpha-factor antibody, a radioimmunoprecipitation was done to try to explain this failure to bind all the ^{3}H-alpha-factor present even at saturating cell concentrations. However, only 60% of the total amount of radioactivity in the form of ^{3}H-alpha-factor added could be precipitated (data not shown). In another experiment in which 4×10^{9} a-cells were exposed to α-factor (1×10^{-10} M; a 400-fold excess of binding sites to α-factor molecules), 75% of the ^{3}H-α-factor could be removed from the supernatant fluid with three successive exposures to fresh a-cells. Using the dissociation rate constants listed in table 4, it can be calculated that 6-12% of the ^{3}H-alpha-factor is dissociated from its receptor during the time involved in sample centrifugation and processing (2 min). Thus the percent of total ^{3}H-α-factor bound by a-cells in this experiment was 80%.

Table 4. Kinetically-derived rate constants for ^{3}H-α-factor association (k_1), dissociation (k_{-1}) and the equilibrium dissociation constant (K_D).

k_1 (M^{-1} min^{-1})	k_{-1} (min^{-1})	K_D (M)[a]
$3.99 \times 10^6 \pm 0.73$ (pseudo 1st order)[c]	$4.45 \times 10^{-2} \pm 0.22$ (1st order)[f]	$2.12 \times 10^{-8} \pm 0.62$
$2.03 \times 10^6 \pm 0.95$ (2nd order)[d]	$7.02 \times 10^{-2} \pm 0.79$ ($t_{\frac{1}{2}}$)[g]	
$2.74 \times 10^6 \pm 0.63$ ($t_{\frac{1}{2}}$)[e]		
N = 5[b]	N = 2[b]	N = 6[b]

[a]This value represents the average K_D calculated according to the equation in Appendix A and using all the possible combinations of k_1 and k_{-1} listed in the table.

[b]N equals the number of experimental determinations. Values listed include S.E.M.

[c]Calculated according to the pseudo 1st order rate equation, Appendix A.

[d]Calculated according to the 2nd order rate equation, Appendix A.

[e]Calculated according to the measured $t_{\frac{1}{2}}$, Appendix A.

[f]Calculated according to the 1st order rate equation, Appendix A.

[g]Calculated according to the measured $t_{\frac{1}{2}}$, Appendix A.

Failure to bind greater than 50-55% of the total label in figure 15, panels A and B, may be accounted for by (1) failure to completely solubilize the large number of filter-retained cells with scintillation cocktail aand subsequent lowering of counting efficiency and (2) greater dissociation of α-factor at very slow filtering rates due to high cell concentrations. Failure to remove greater than 60% of the total radioactivity by radioimmunoprecipitation is difficult to explain since use of the same antibody in an ELISA indicated the expected amount of ^{3}H-alpha-factor was present. Therefore because the data obtained from HPLC purification (figure 9), data from an isotopic dilution experiment (figure 13), ^{3}H-α-factor sequence determination and amino acid analysis (figures 10 and 11) indicate the ^{3}H-alpha-factor is pure and also because reactivity in the ELISA is at the level expected and successive exposure of 1 X 10^{-10} M ^{3}H-α-factor to fresh a-cells can remove greater than 80% of the radiolabel, subsequent calculations assumed 100% of the ^{3}H-α-factor was capable of binding a-cells.

Association of ^{3}H-Alpha-Factor with a-Cells

The time course for association of ^{3}H-alpha-factor with a-cells is shown in figure 16. Association is complete by 10 minutes at 25°C. Because less than 10% of the ^{3}H-alpha-factor was bound in these experiments the data in figure 16 can be plotted according to pseudo-first-order kinetics as in figure 17, panel A. The points yield a straight line crossing the X-axis near 0 with a

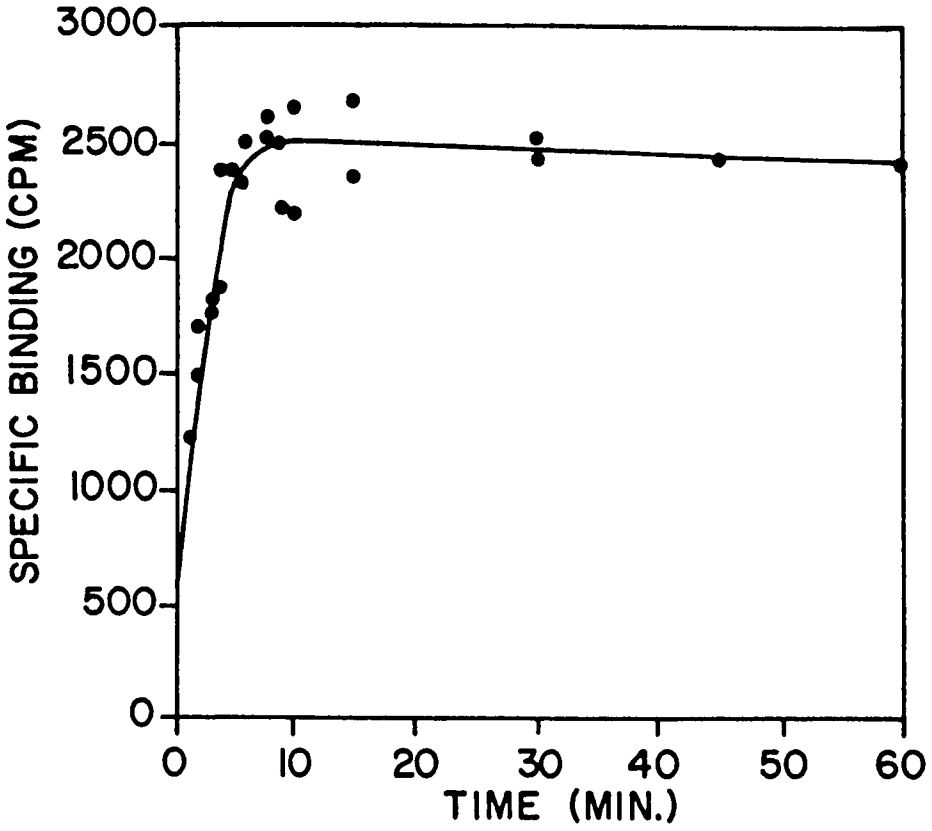

Figure 16. Time course for the association of ^{3}H-α-factor with a-cells. Specific binding equals the cpm bound to a-cells minus the cpm bound to α-cells.

Figure 17. Derivation of the rate constant for ^{3}H-α-factor association using the pseudo first order rate equation (Panel A) and the integrated 2nd order rate equation (Panel B). See appendix A for details.

Panel A. $k_1 = 3.52 \times 10^6\ M^{-1}\ min^{-1}$

Panel B. $k_1 = 4.17 \times 10^6\ M^{-1}\ min^{-1}$

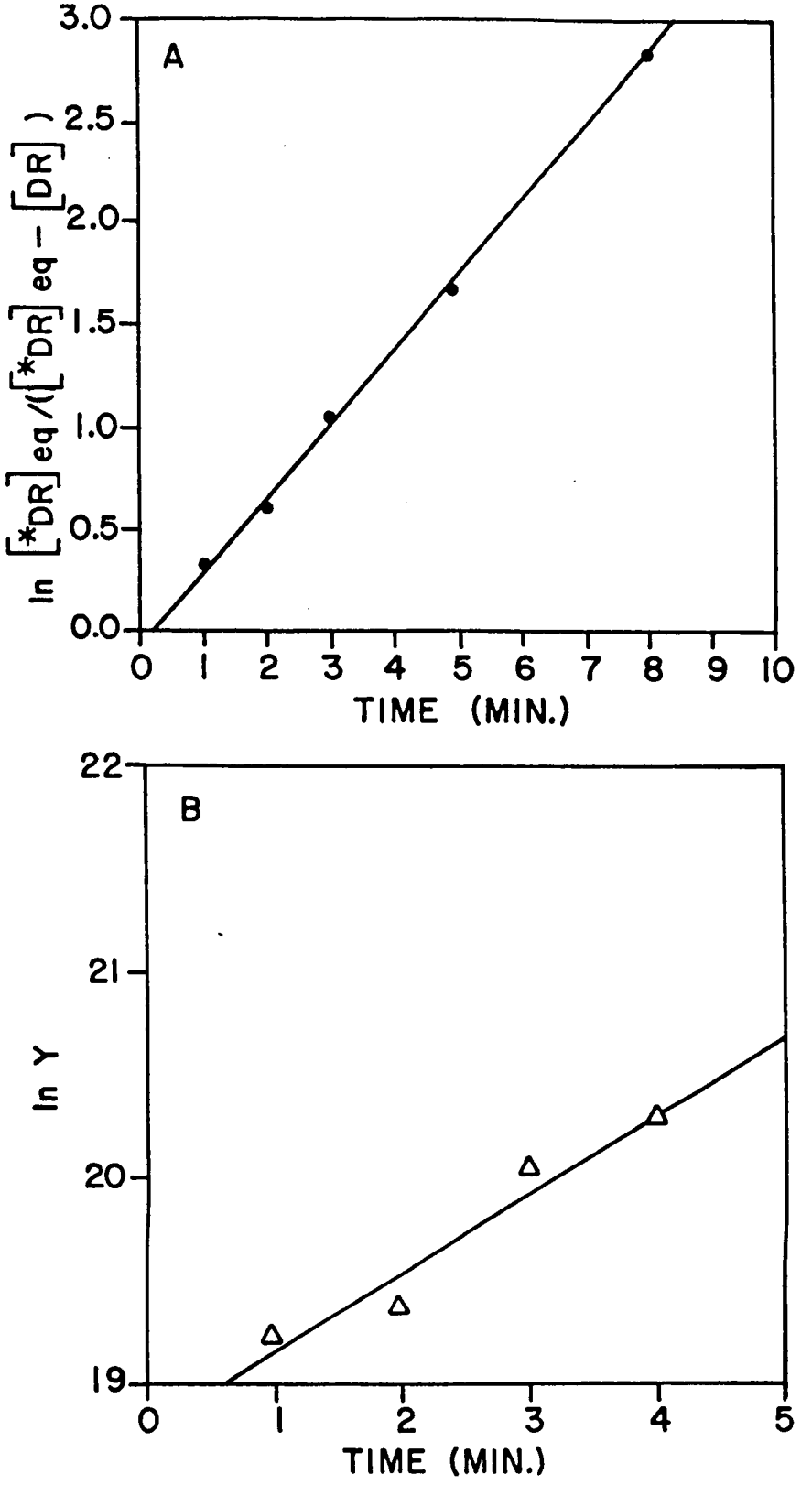
A
3.0
2.5
2.0
1.5
1.0
0.5
0.0
ln [*DR] eq /([*DR] eq − [DR])
0 1 2 3 4 5 6 7 8 9 10
TIME (MIN.)
B
22
21
20
19
ln Y
0 1 2 3 4 5
TIME (MIN.)

Figure 17.

$$\text{slope} = k_1\left[\frac{(L)_T(R)_T}{(LR)_e}\right]$$

(see appendix A). The k_1 determined from this plot = 3.52 X 10^6 M^{-1} min^{-1}.

Alternatively, if no assumptions are made concerning the relative concentration of ligand and binding sites, data can be plotted according to the integrated second order rate equation as in figure 17, panel B. From the

$$\text{slope} = k_1\left[\frac{(L)_T(R)_T}{(LR)_e} - (LR)_e\right]$$

(see appendix A) the k_1 derived from the integrated second order rate equation is calculated to be 4.17 X 10^6 M^{-1} min^{-1}.

Another method by which the rate constant for ^{3}H-alpha-factor association can be determined is through the measurement of the half-time for association ($t_{\frac{1}{2}}$). As long as binding has reached equilibrium, the $t_{\frac{1}{2}}$ can be estimated from a regression line of the initial association rate and substituted into the equation derived in appendix A. Estimating the $t_{\frac{1}{2}}$ from the data in figure 16, k_1 = 3.21 X 10^6 M^{-1} min^{-1} by this method.

The first column of table 4 lists the average association rate constants (k_1) calculated according to the three methods described above for five independent determinations (see appendix A for details). Averaging these three values, the rate constant for ^{3}H-alpha-factor association (k_1) is approximately 2.92 X 10^6 M^{-1} min^{-1}.

Time Course for the Dissociation of ^{3}H-Alpha-Factor from a-Cells

In order to determine dissociation rates, experimental conditions are fixed so that the reassociation of the ligand with the receptor is negligible. This can be accomplished by two methods: (1) Dilution of a binding reaction at equilibrium by 10 to 100 fold so that any rebinding of radioligand, once dissociated, is not detected or (2) Addition of unlabelled competing ligand to the dilution buffer so that any rebinding that occurs is likely to involve the unlabelled ligand. Figure 18 shows the results for a dissociation time course using the "infinite" dilution method (method 1). Figure 19 shows the time course for dissociation when excess unlabelled alpha-factor is present in the infinite dilution buffer (method 2). When the data in figure 19 is transformed and replotted as in the inset, virtually identical straight lines are traced. A straight line is expected if the dissociation is a first order reaction. The k_{-1} determined from this plot is 4.68×10^{-2} min^{-1}. Alternatively, if the half-time for dissociation is obtained from a linear regression of the initial dissociation rate in figure 18, a value of 7.81×10^{-2} min^{-1} is obtained. This value is a less precise estimate since the initial rate for dissociation is fast and this method relies on a regression line obtained using few points. The average rate constants for dissociation determined by these two methods for two different experiments are listed in column 2 of table 4. Equations for the calculations are found in appendix A.

The kinetics observed for association and dissociation are consistent with a model in which ^{3}H-alpha-factor/receptor complexes are

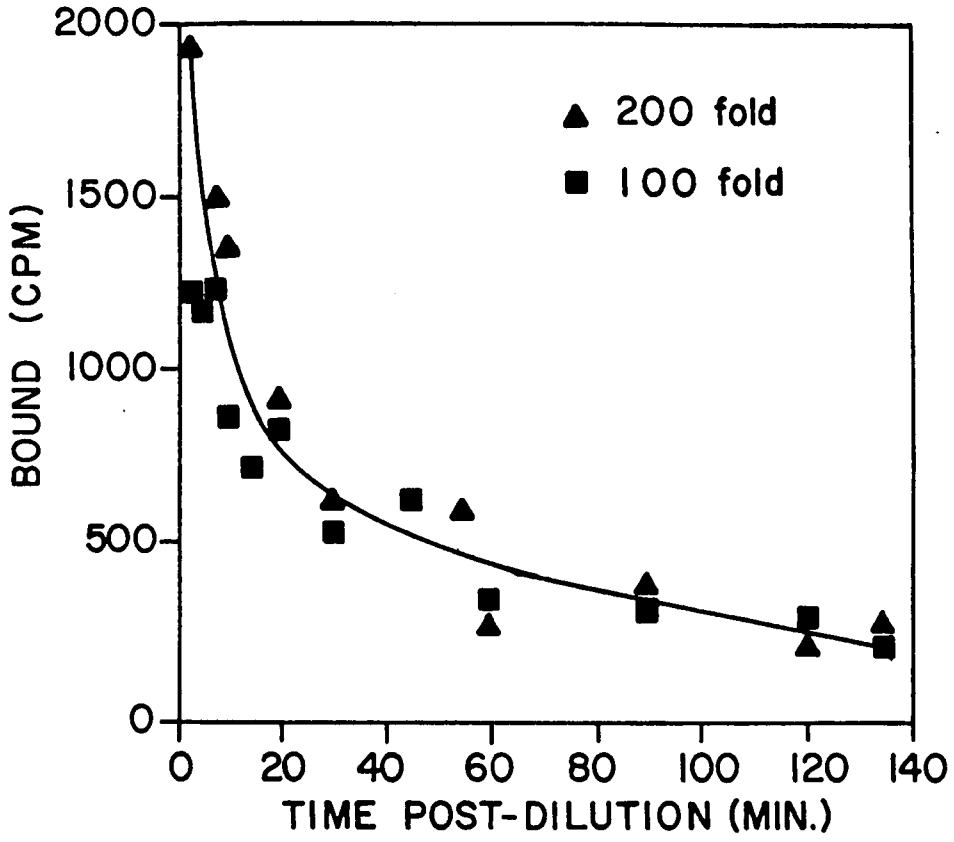

Figure 18. Time course for the dissociation of ^{3}H-α-factor from a-cells using the "infinite" dilution method.

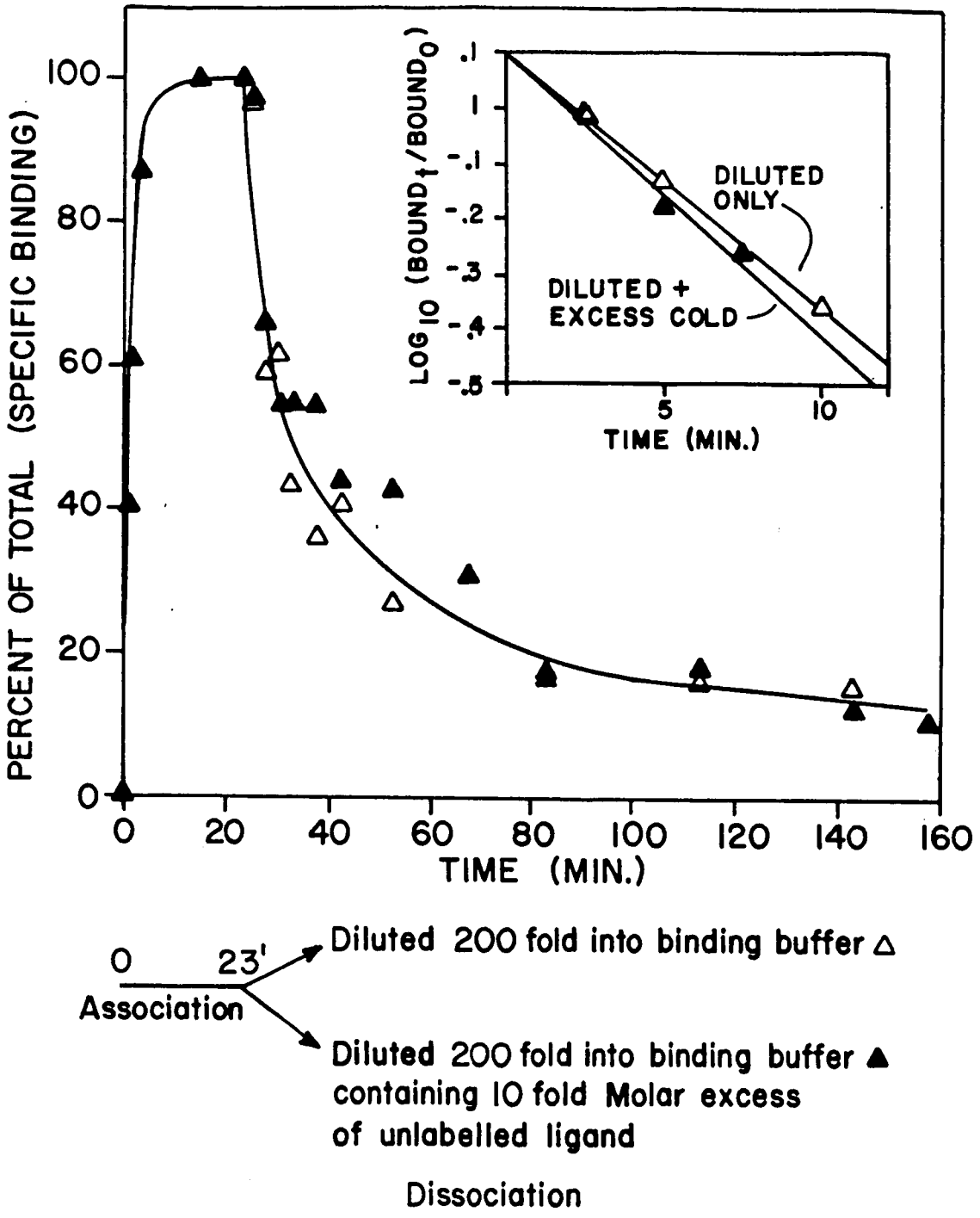

Figure 19. Time course for the dissociation of ^{3}H-α-factor from a-cells using both "infinite" dilution (Δ) and addition of excess unlabelled α-factor (▲). The experimental protocol is diagrammed below the figure. The inset shows the derivation of the rate constant for ^{3}H-α-factor dissociation using 1st order kinetics.

$k_{-1} = 4.68 \times 10^{-2}$ min^{-1}.

formed via a simple bimolecular reaction governed by the law of mass action. The equilibrium dissociation constant (K_D) therefore can be derived from the kinetically determined k_1 and k_{-1} using the equivalence

$$K_D = \frac{k_{-1}}{k_1} \quad .$$

The K_D (2.12×10^{-8} M) in table 4 is the average K_D calculated from all the combinations of k_1 and k_{-1} in columns 1 and 2 of the same table.

Steady State Saturation Binding

One of the features which identifies a physiologically relevant receptor is the characteristic of binding site saturability. Since a given number of cells is expected to possess a finite number of receptors, saturability can be assessed by examining binding as a function of increasing radioligand concentration. This was done and the data are graphed in figure 20. The inset of figure 20 shows a Scatchard plot derived from the saturation binding data. When a single ligand is interacting with a single population of receptors characterized by one dissociation constant for that ligand, the Scatchard plot shows a straight line. The resultant slope yields a K_D of 2.3×10^{-8} M and the x-intercept reveals a-cells contain approximately 13000 binding sites per cell.

A Hill plot of saturation data is represented in figure 21. The slope of this plot, the Hill coefficient (n_H), is 1.05. When n_H is equal to 1, the x-intercept of the Hill plot should equal the K_D of the

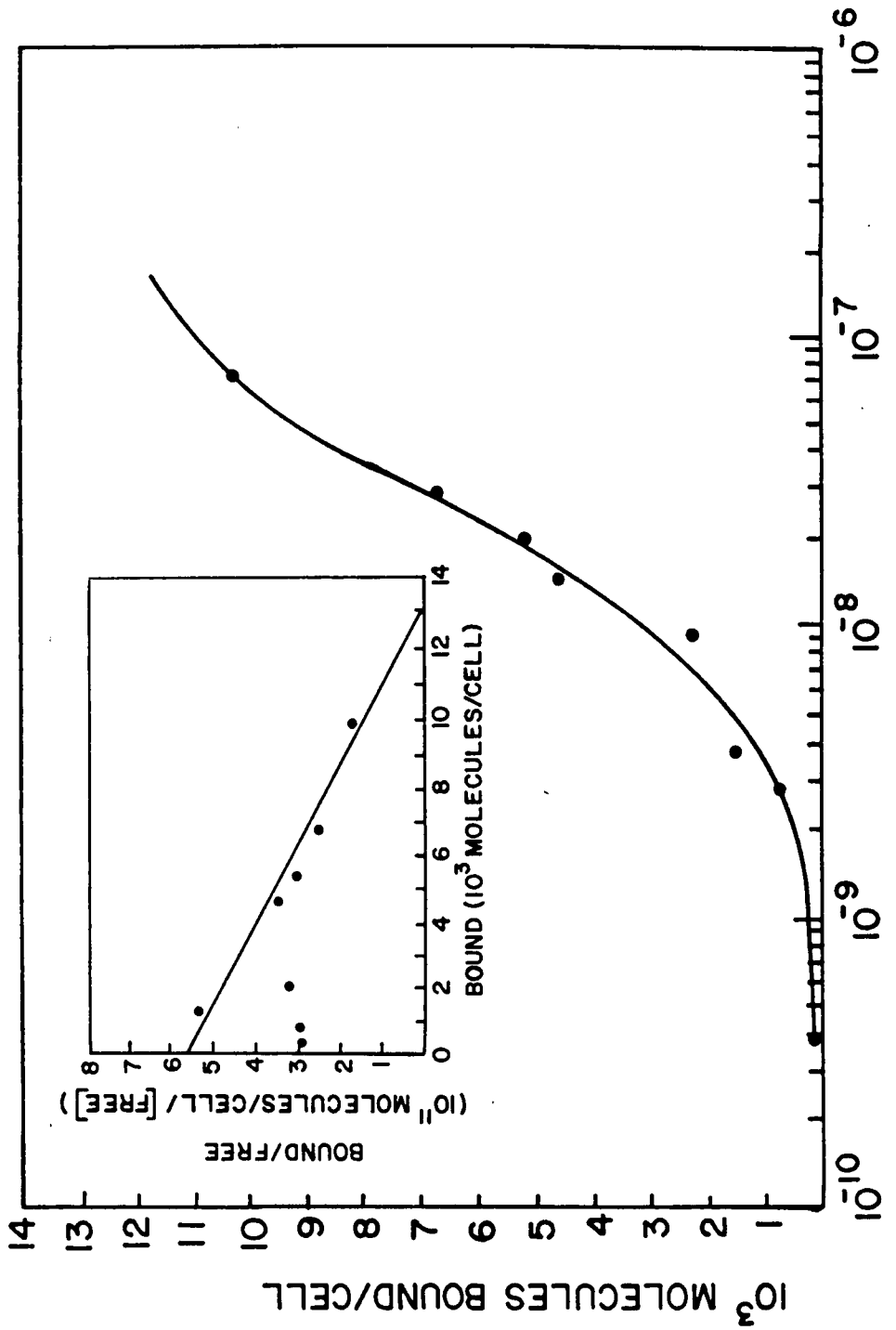

Figure 20. Saturation binding of ^{3}H-α-factor to a-cells. The inset represents a Scatchard plot of the binding data. $K_D = 2.32 \times 10^{-8}$ M; n = 13000 sites/cell.

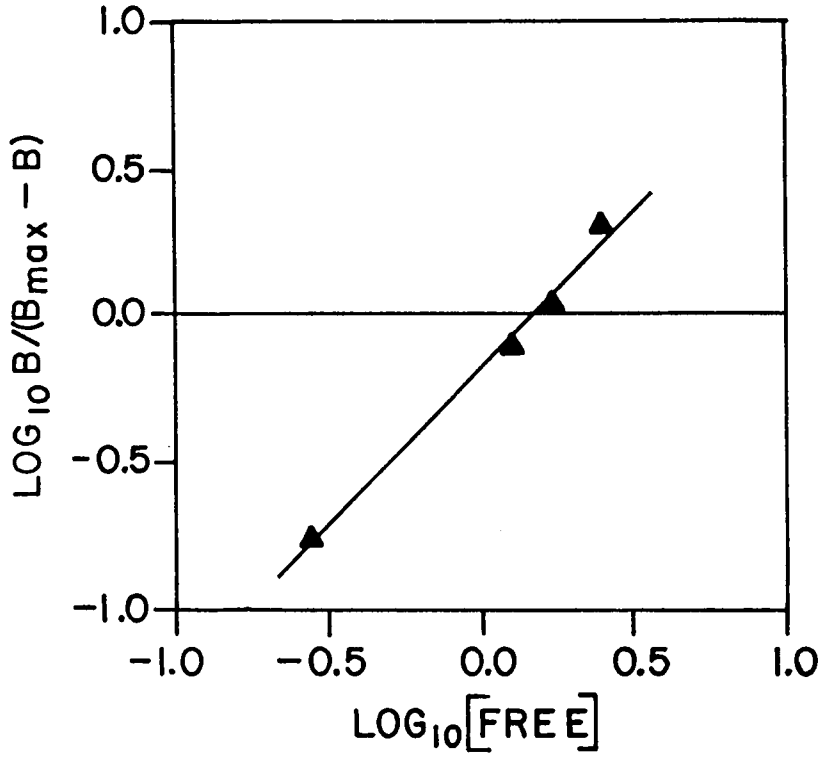

Figure 21. Hill plot derived from saturation binding data. n_H = 1.05; K_D = 1.51 x 10^{-8} M.

radioligand. The K_D derived from the Hill plot for binding of ^{3}H-alpha-factor to a-cells is 1.51 X 10^{-8} M.

Competition for Binding of ^{3}H-Alpha-Factor by Unlabelled Alpha-Factor and Its Analogues

The specificity of ^{3}H-alpha-factor binding was determined by incubating a-cells with a constant concentration of ^{3}H-alpha-factor (6 X 10^{-8} M) in the presence of increasing concentrations of unlabelled alpha-factor peptides. The competition profiles for a number of different peptides are shown in figures 22, 23, 24 and 25. The affinities of these competitors for the alpha-factor receptor are reflected in the IC_{50} values (the concentration of competitor which effectively competes for 50% of the specific ligand binding) and the K_D values listed in table 5 (for details of calculations, see appendix B). As the values listed in table 5 indicate, of those analogues tested only desTrp^1 CHA^3 D-ala^9 dodecapeptide, a biologically inactive analogue, did not compete effectively for binding to the alpha-factor receptor. All the other peptides tested, including the biologically inactive desTrp^1 Ala^3 desTrp^1 CHA^3 D-Leu^6 and desTrp^1 Phe^3 dodecapeptides competed to varying degrees (K_Ds from 1.34 X 10^{-8} M to 6.48 X 10^{-6} M). As expected, the natural sequence and several tridecapeptides showing biological activity equal to the natural sequence were the best competitors. All curves were found to be parallel and of normal steepness showing 10% to 90% competition over approximately an 81-fold range of competitor.

Once the equilibrium constants were determined, the Gibbs standard free energies were calculated using the equation found in appendix C

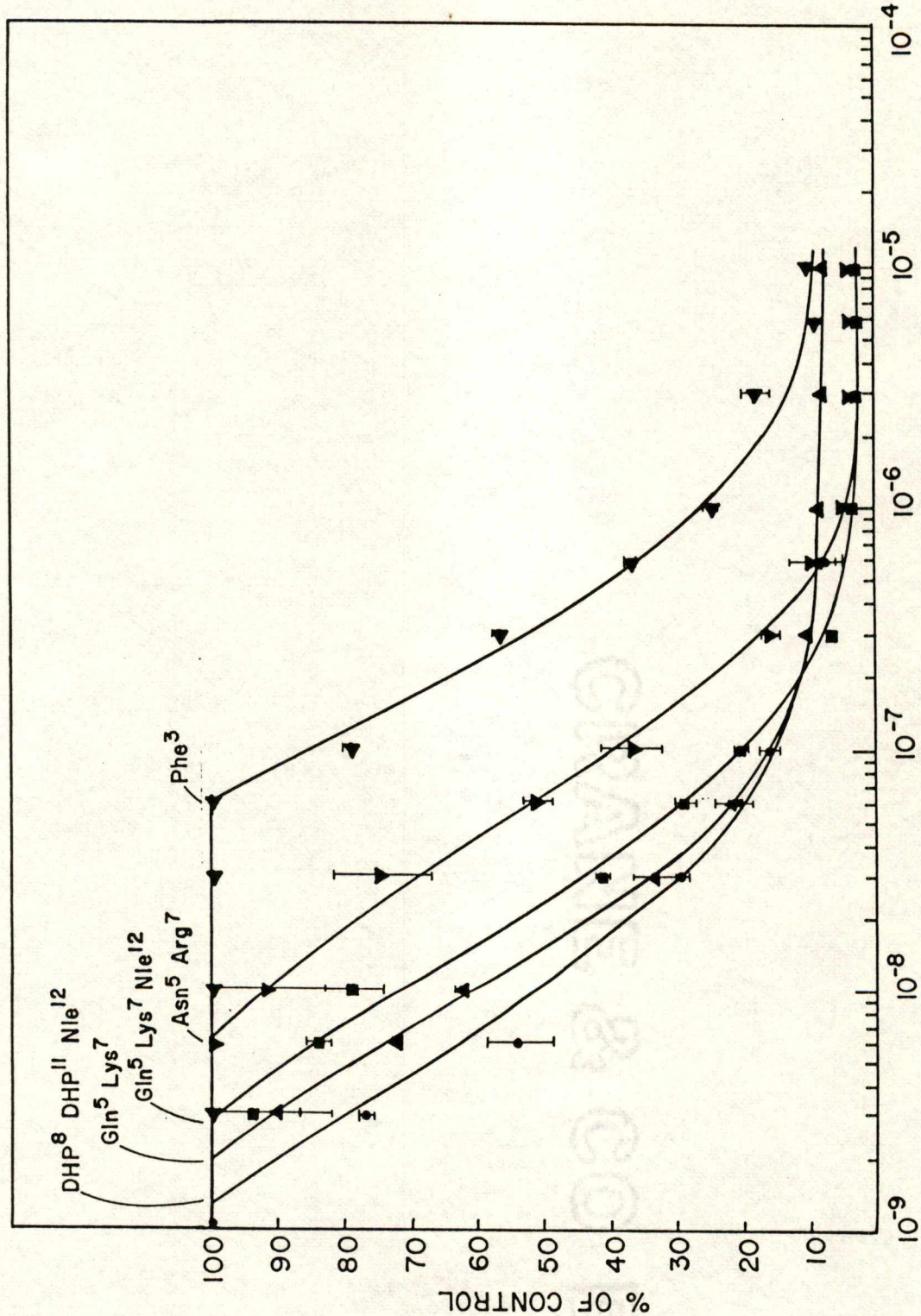

Figure 22. Competition for binding of ^{3}H-α-factor by unlabelled α-factor tridecapeptides. Bars indicate error.

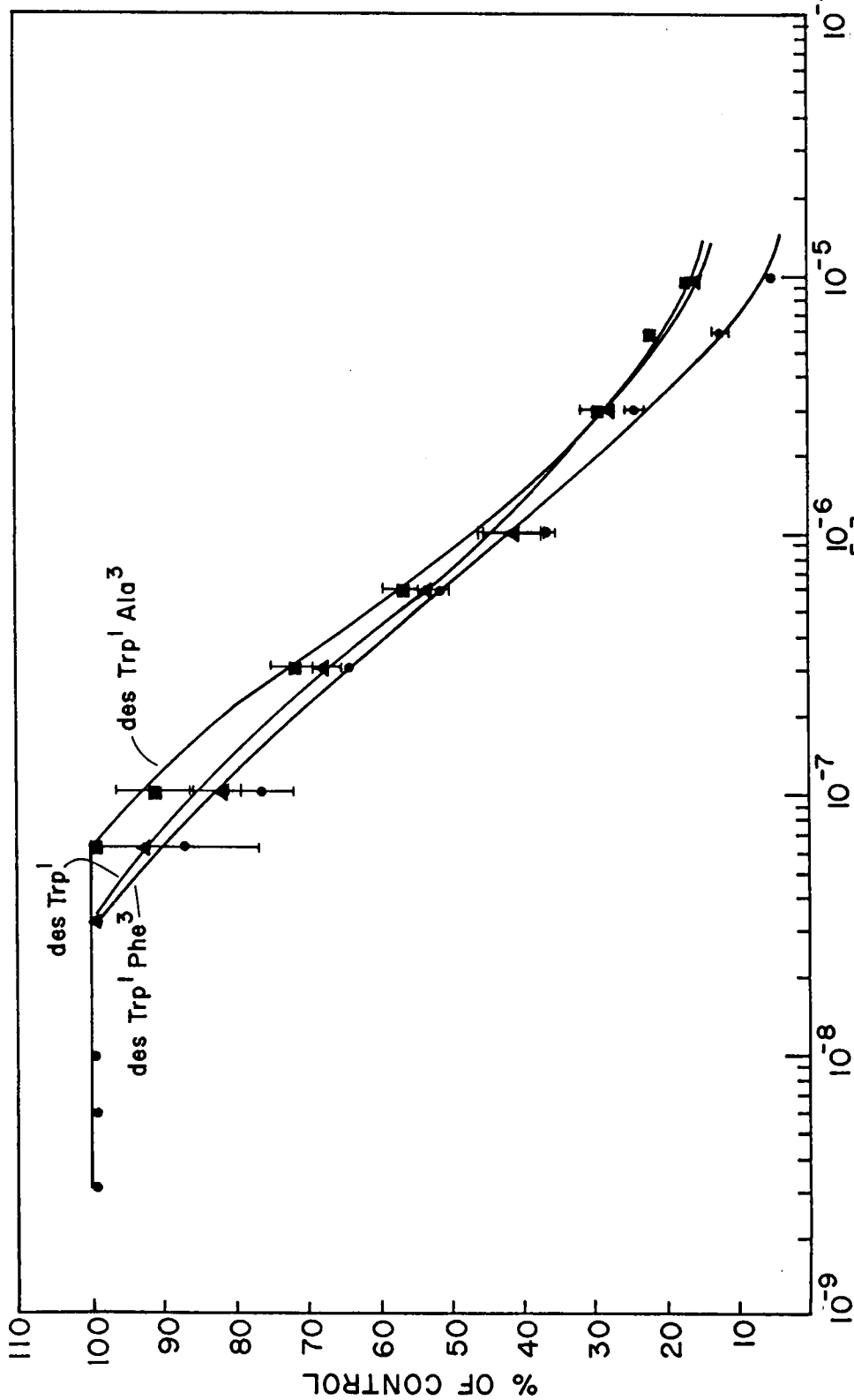

Figure 23. Competition for binding of ^{3}H-α-factor by unlabelled desTrp^{1} dodecapeptide and desTrp^{1} X^{3} dodecapeptide (X ≠ Trp). Bars indicate error.

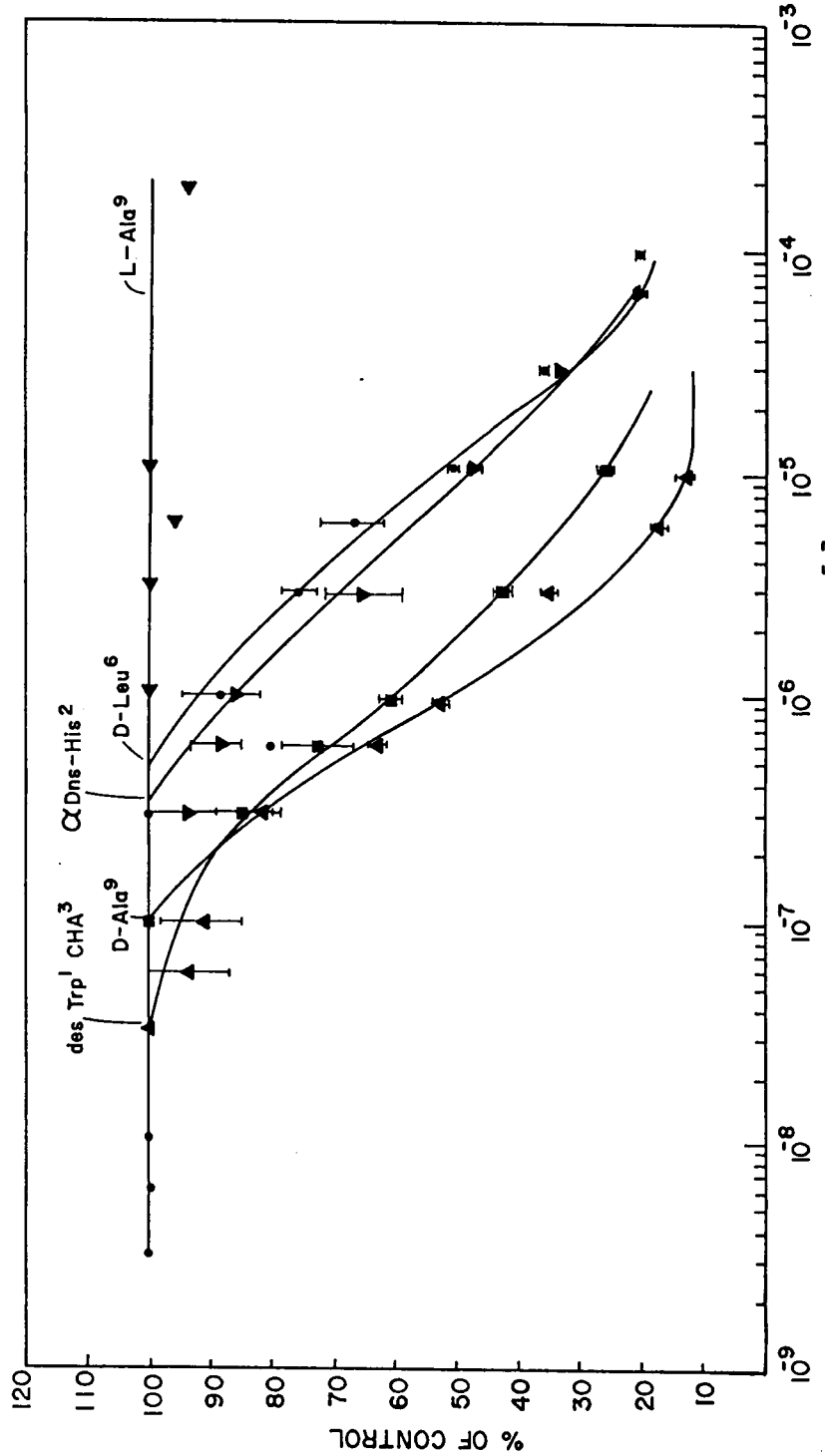

Figure 24. Competition for binding of ^{3}H-α-factor by unlabelled desTrp^{1} CHA^{3} dodecapeptides with intermediate K_Ds. One analogue desTrp^{1}CHA^{3} L-Ala^{9} dodecapeptide does not compete. Bars indicate error.

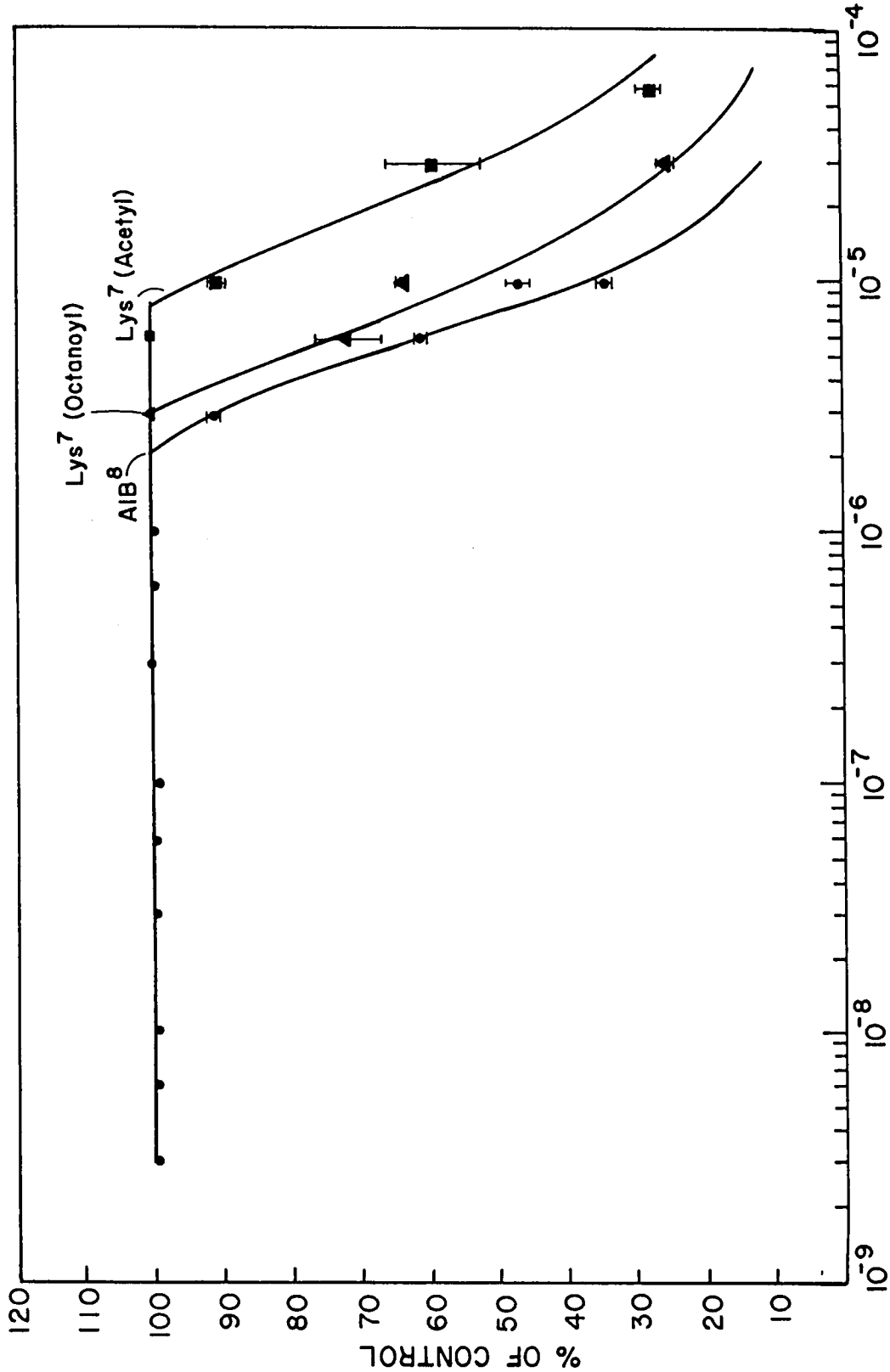

Figure 25. Competition for binding of ^{3}H-α-factor by unlabelled desTrp^{1} CHA^{3} dodecapeptides with the greatest K_Ds. Bars indicate error.

Table 5. Concentrations for 50% inhibition of binding (IC_{50}), binding dissociation constants (K_D) and Gibbs standard free energy changes (ΔG^o) for α-factor and its analogues.

Peptide	IC_{50} (M)[a]	K_D (M)[b]	ΔG^o (Kcal)[c]
Tridecapeptide	1.38×10^{-8}	1.34×10^{-8}[d]	-10.64
Asn^5 Arg^7 Tridecapeptide	6.51×10^{-8}	1.45×10^{-8}[d]	-10.60
NLe^{12} Tridecapeptide	2.3×10^{-8}	1.39×10^{-8}[d]	-10.62
		2.32×10^{-8}[e]	-10.32
		2.12×10^{-8}[f]	-10.37
DHP^8 DHP^{11} NLe^{12} Tridecapeptide	8.52×10^{-9}	1.88×10^{-8}[d]	-10.44
Phe^3 Tridecapeptide	3.08×10^{-7}	6.8×10^{-8}	-9.69
des Trp^1 Dodecapeptide	5.69×10^{-7}	1.28×10^{-7}	-9.32
des Trp^1 Ala^3 Dodecapeptide	5.51×10^{-7}	1.24×10^{-7}	-9.34
des Trp^1 Phe^3 Dodecapeptide	6.53×10^{-7}	1.47×10^{-7}	-9.24
des Trp^1 CHA^3 Dodecapeptide	1.48×10^{-6}	3.36×10^{-7}	-8.75
des Trp^1 CHA^3 D-leu^6 Dodecapeptide	7.5×10^{-6}	1.71×10^{-6}	-7.80
des Trp^1 CHA^3 Lys^7 (Acetyl) Dodecapeptide	2.83×10^{-5}	6.48×10^{-6}	-7.01
des Trp^1 CHA^3 Lys^7 (Octanoyl) Dodecapeptide	9.09×10^{-6}	2.08×10^{-6}	-7.68
des Trp^1 CHA^3 AIB^8 Dodecapeptide	6.82×10^{-6}	1.56×10^{-6}	-7.85
des Trp^1 CHA^3 L-Ala^9 Dodecapeptide	$>10^{-4}$	$>10^{-4}$	
des Trp^1 CHA^3 D-Ala^9 Dodecapeptide	8.23×10^{-7}	1.86×10^{-7}	-9.10
des Trp^1 αDns His^2 CHA^3 Dodecapeptide	7.08×10^{-6}	1.62×10^{-6}	-7.83

[a] IC_{50} = the concentration of competitor which inhibits binding of ^{3}H-α-factor by 50%. Values were calculated as the 50% point on a regression line incorporating the points of the appropriate competition curve from figures 22, 23, 24 and 25.

[b] $K_D = K_i$ calculated according to Linden (69). See equations in Appendix B.

[c] Gibbs standard free energy changes according to the equation in Appendix C.

[d] Binding dissociation constants (K_D) as determined by Scatchard analysis of the appropriate competition curves from figure 22.

[e] K_D as determined from Scatchard analysis of the ^{3}H-α-factor binding isotherm. See figure 19.

[f] K_D as determined from the measurement of k_{-1} and k_1 using ^{3}H-α-factor. See table 4.

(table 5). Comparison of the ΔG^{o} values mirror the trend in the K_Ds calculated for the analogues. Thus as expected, the ΔG^{o} which is reflective of the stability of receptor-ligand interaction is greatest (most negative) for the native tridecapeptide and closely related analogues.

Temperature Dependence of Alpha-Factor Binding

Changes in the Gibbs standard free energy are determined by changes in enthalpy (ΔH^{o}) and changes in entropy (ΔS^{o}). To determine whether the negative ΔG^{o}s associated with binding of alpha-factor results from a large positive entropy component or a large negative enthalpy component, competition assays were performed over a temperature range of 10^{o} to 40^{o}C using the tridecapeptide and desTrp^{1} Ala^{3} dodecapeptide. Figures 26 and 27 show the temperature dependence of tridecapeptide binding and desTrp^{1} Ala^{3} dodecapeptide binding, respectively. A greater shift in affinity is seen from 40^{o} to 10^{o}C for binding of the antagonist, desTrp^{1} Ala^{3} dodecapeptide (figure 27) than for binding of the agonist, tridecapeptide (figure 26). When the equilibrium dissociation constants derived from the competition curves at each temperature are used in Van't Hoff plots (figures 28 and 29), the individual parameters ΔH^{o} and ΔS^{o} can be determined (for details of the calculations see appendix C). Table 6 shows the enthalpy and entropy terms derived from the Van't Hoff plots in figures 28 and 29. These values indicate that binding of the agonist, tridecapeptide to a-cells is entropy-driven ($\Delta S^{o} > 0$), whereas binding of the antagonist, desTrp^{1} Ala^{3} dodecapeptide, to a-cells is enthalpy-driven ($\Delta H^{o} < 0$).

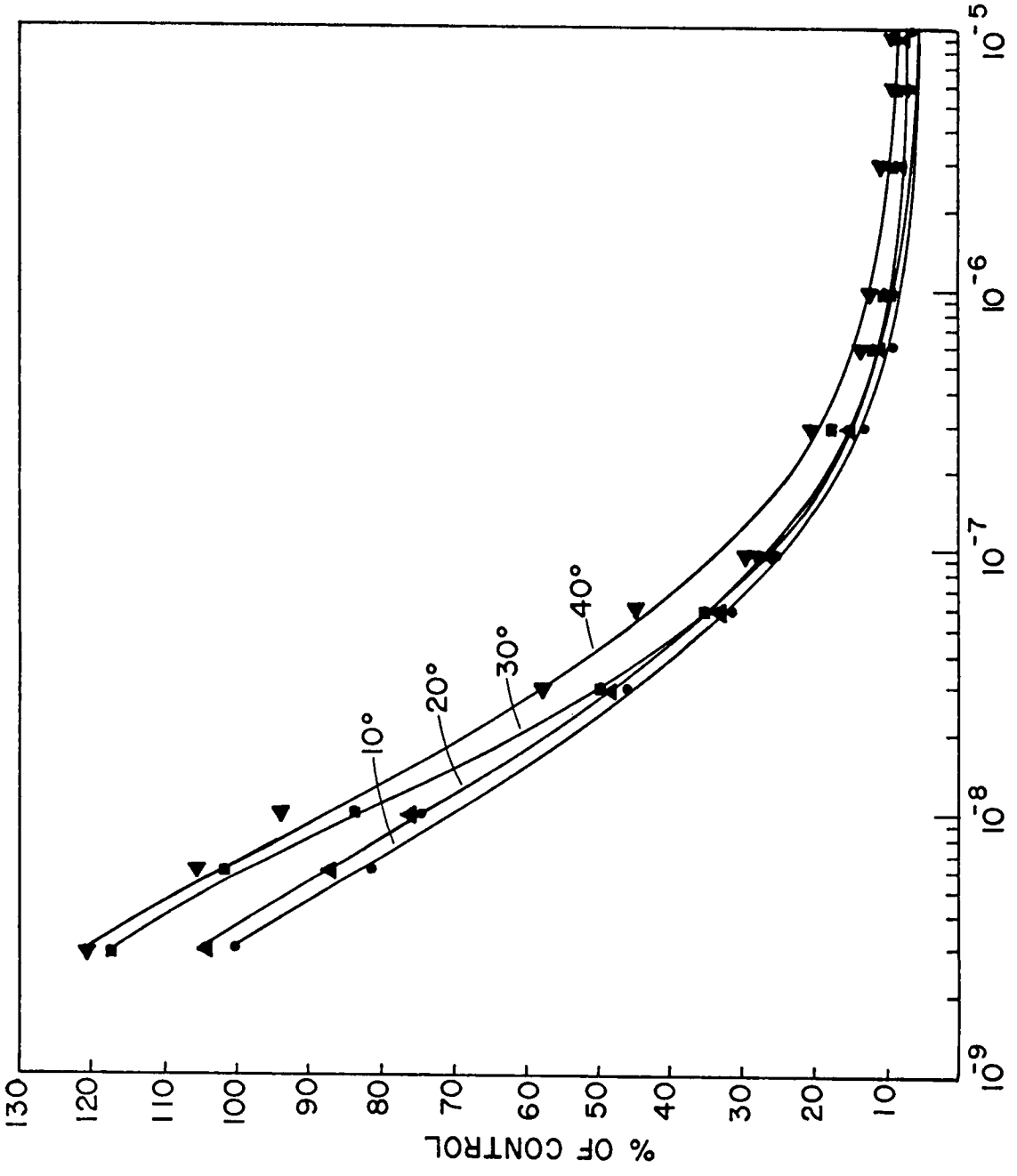

Figure 26. Competition for binding of ^{3}H-α-factor by Tridecapeptide from 10° to 40°C.

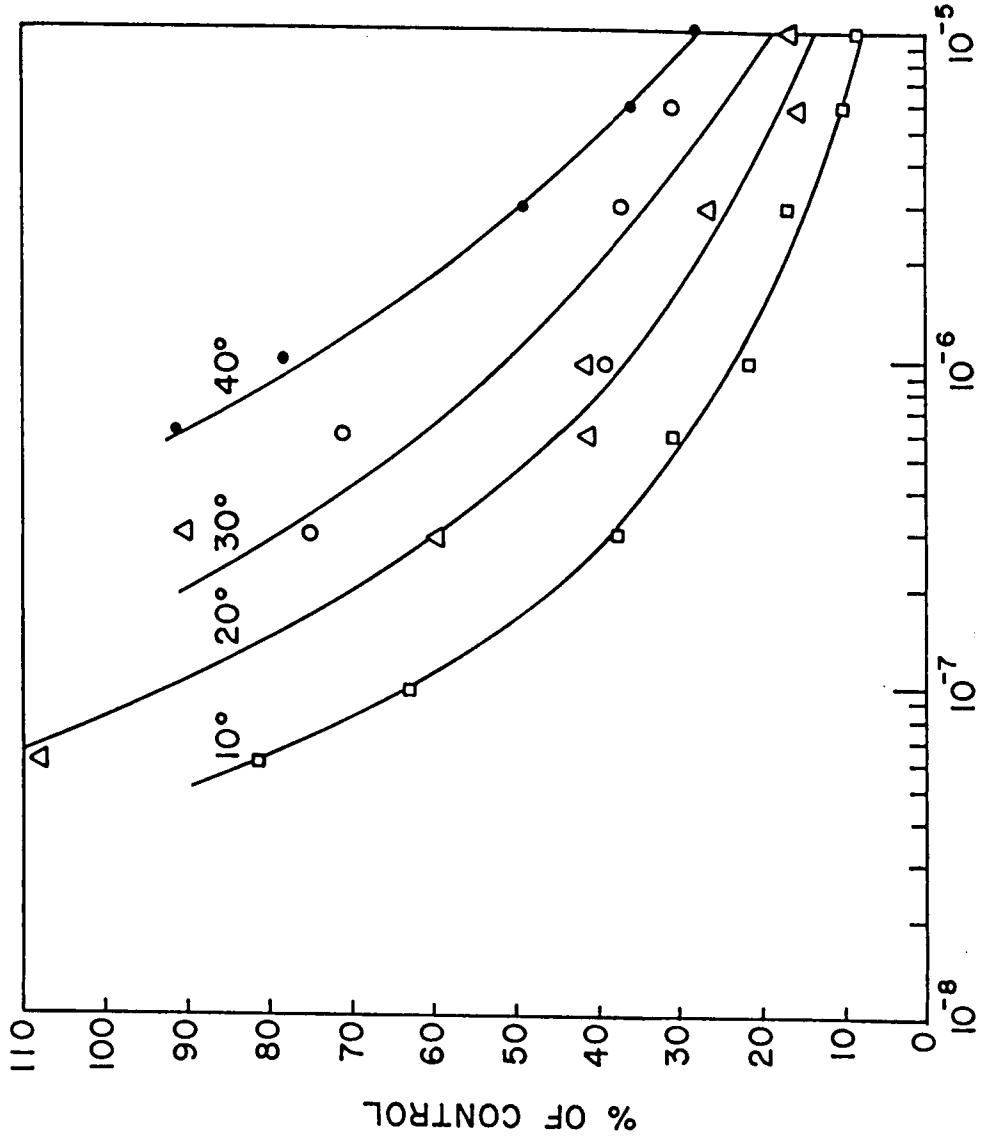

Figure 27. Competition for binding of ^{3}H-α-factor by desTrp^1 Ala^3 dodecapeptide from 10° to 40°C.

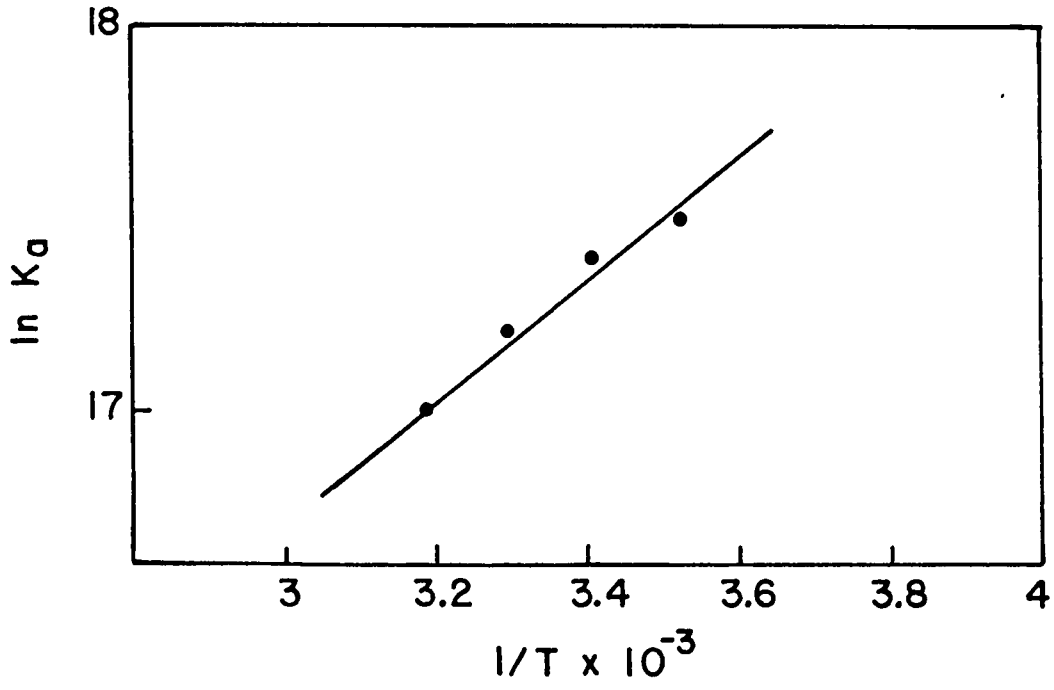

Figure 28. Van't Hoff plot for the tridecapeptide. See appendix C for details.

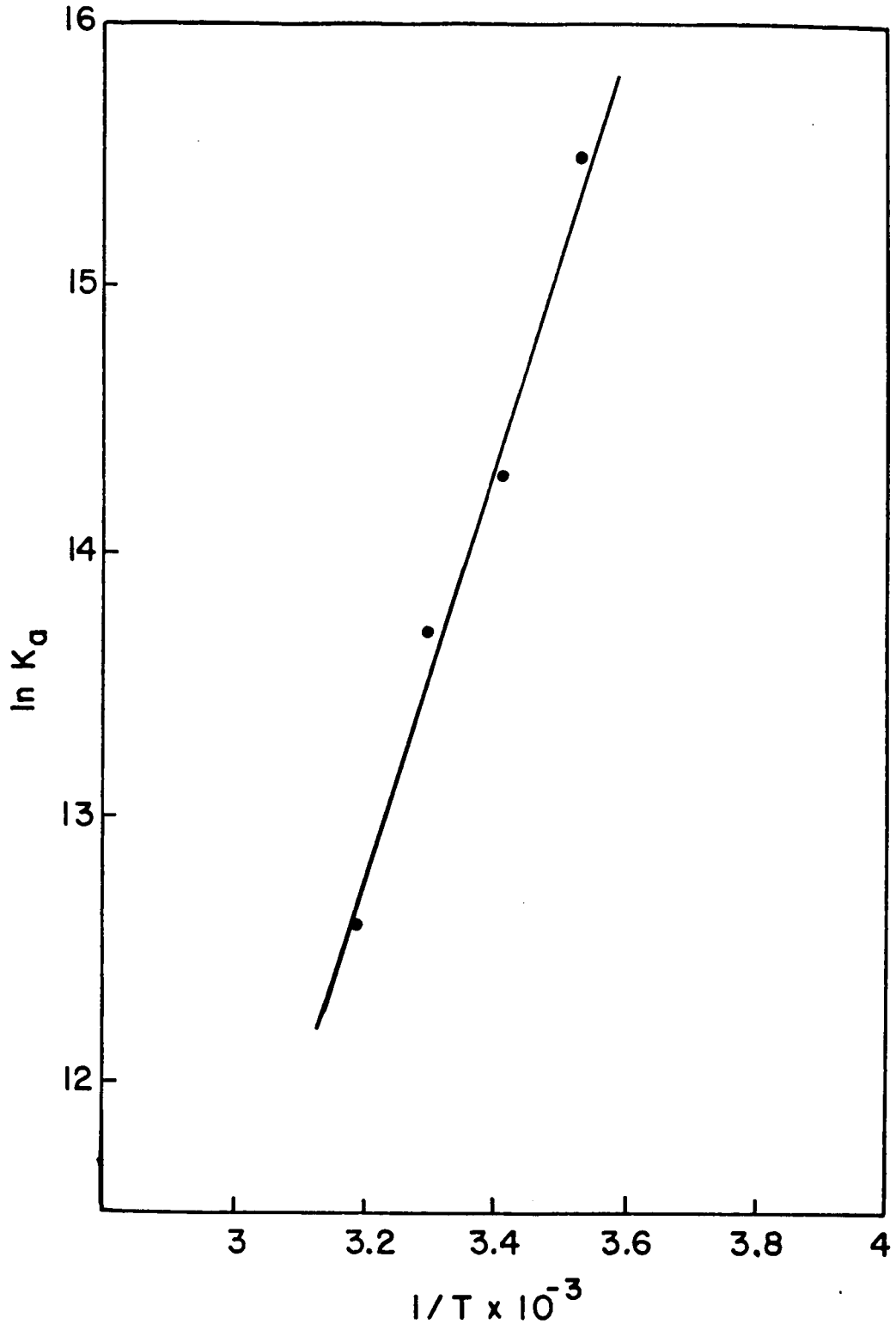

Figure 29. Van't Hoff plot for the desTrp^{1} Ala^{3} dodecapeptide. See appendix C for details.

Table 6. Thermodynamic parameters of ligand binding to the α-factor receptor.

Peptide	ΔG^{o} [a] (cal)	ΔH^{o} [b] (cal)	ΔS^{o} [c] (cal/deg)
Tridecapeptide	-10620	-2930	26.07
des Trp^{1} Ala^{3} dodecapeptide	-9340	-16352	-23.77

[a] Gibbs standard free energy changes according to the equation in Appendix C.

[b] Standard enthalpy change derived from Van't Hoff plots in figures 28 and 29.

[c] Standard entropy change derived from equations in Appendix C.

IV. DISCUSSION

The development of an assay for alpha-factor binding to a-cells was not an easy task. Problems encountered in early literature accounts of alpha-factor receptor binding included: (1) low specific activity of the labelled peptide, (2) metabolism and/or deactivation of the mating factor and (3) high levels of nonspecific binding to alpha-cells. Using biologically prepared ^{35}S-labelled alpha-factor, Jenness and coworkers (52) were the first to circumvent each of these problems and show specific binding of alpha-factor to a-cells. However, because the preparation of radiolabelled alpha-factor used in those studies was only partially pure, the binding parameters estimated by the authors were corrected in a second publication in which a commmercially synthesized ^{3}H-alpha-factor was used (53). The studies discussed here represent a complimentary effort to those previously published by Jenness et al. and further define the specificity of the alpha-factor/ receptor interaction by the use of unlabelled structural analogues of the alpha-factor pheromone.

Characterization of ^{3}H-Alpha-Factor

Past efforts to radioactively label alpha-factor have met with limited success. Several groups have reported the labelling of alpha-factor with ^{125}I (71, 37, 113, 70). Thorner et al. (113) tried to radiolabel alpha-factor with ^{125}I using the chloramine T method however, upon testing this label in a binding assay, the amount which bound to alpha-cells nonspecifically was unacceptably high. Lipke reported

similar findings (70). Attempts to label alpha-factor by less harsh chemical procedures using the Bolton-Hunter reagent were successful but no biological activity could be associated with the iodinated pheromone(this authors unpublished results). Although no biochemical characterization was performed on either iodinated peptide, it is likely that ^{125}I was incorporated into the tyrosine to a significant extent by both methods. Evidence from the laboratories of Naider (84) and Masui (75) suggest that large modifications to or loss of the carboxyterminal tyrosine result in pheromones with severely reduced biological activity.

Because ^{125}I has a short half life and incorporation into the tyrosine appears to reduce biological activity far below that of the native pheromone, alternative routes for the preparation of a radioactive alpha-factor were explored. As earlier stated the first successful binding assay developed for S. cerevisiae by Jenness et al. (52) used biologically produced ^{35}S-labelled alpha-factor. Although they were able to demonstrate specific binding of ^{35}S-alpha-factor to a-cells and not to α or a/α -cells, production of radiolabelled alpha-factor by this method has several disadvantages: (1) ^{35}S, like ^{125}I, has a relatively short half life (87.4 days), (2) Amounts of the labelled pheromone obtained by this method are small, usually between 75 and 750 pg (3-30ug/L; see 11) (3) Consistent incorporation of ^{35}S between batch preparations is difficult and (4) The label has to be purified from culture supernates.

In order to avoid the problems associated with biological preparation of an ^{35}S-labelled alpha-factor and not compromise the level

of specific activity needed for detection, tritium was incorporated into the alpha-factor pheromone. Tritium has a longer half life (12.43 years) than either ^{35}S or ^{125}I and can usually by incorporated into a peptide with no significant reduction in biological activity. Therefore through the catalytic reduction of a dehydroproline-containing alpha-factor in the presence of ^{3}H gas, a radiolabel of high specific activity, purity, biological activity and long shelf-life was prepared. Similar approaches have been successful for the incorporation of tritium into bradykinin (38), oxytocin (82), thyroliberin(TRH) (34) and angiotensin (39).

Examination of the crude ^{3}H-alpha-factor preparation from the catalytic exchange reaction revealed the presence of at least 9 radioactive species, only one of which comigrated with the unlabelled pheromone (see figure 7, p. 44). Significant errors and artifacts can bias the proper analysis of equilibrium binding data if impure labelled ligands are used (16). Because the validity of binding assays depends upon the correct assessment of [*L], the concentration of free radioligand at equilibrium and [*LR], the concentration of bound radioligand, the chemical and radiochemical impurities present were removed by further HPLC purification (see figures 8 and 9, p. 45 and 48).

The tritiated alpha-factor prepared had specific activity between 8 and 10 Ci/mmol. ^{3}H was found associated with both prolines in positions 8 and 11 of the pheromone (43% and 27% of the total radioactivity in the peptide, respectively) and to a significant extent (30%) in the histidine at position 2. Unexpected tritium incorporation at histidine

in a dehydroproline-containing derivative of GnRH has also been observed. In fact, tritiation of the native GnRH and angiotensin I molecules by catalytic exchange resulted in tritium incorporation into the histidines and subsequent specific activities of 7-9 and 5 Ci/mmol, respectively (61).

The biological activity of the tritiated alpha-factor equaled that observed for the native pheromone (see figure 12, p. 54). Furthermore, when the specific activity of tritiated alpha-factor was diluted stepwise, the reduction in specific binding to a constant amount of a-cells observed was linear (see figure 13, p. 56). Therefore the tritiated alpha-factor prepared for this study by catalytic reduction retains biological activity and interacts with the alpha-factor receptor in a way identical to the unlabelled native pheromone.

Kinetic and Equilibrium Parameters of the Alpha-Factor/Receptor Interaction

The simplest model of a ligand receptor interaction first developed by Clark (26) assumes a homogeneous univalent species of ligand and a single noninteracting population of binding sites. This situation can be described by the following second order reaction:

$$L + R \underset{k_{-1}}{\overset{k_1}{\rightleftharpoons}} LR$$

in which the interaction between the ligand and receptor is reversible, association is a bimolecular process and dissociation is a monomolecular one. At equilibrium, the law of mass action defines

$$K_A = \frac{k_1}{k_{-1}} = \frac{[LR]}{[L][R]} \qquad K_D = \frac{1}{K_A}$$

where K_D is the equilibrium dissociation constant, K_A is the equilibrium association constant, k_1 and k_{-1} are the kinetic rate constants for association and dissociation and [L], [R], and [LR] are the concentrations of free ligand, unbound receptor and ligand receptor complexes at equilibrium, respectively. The following section outlines studies involving ^{3}H-alpha-factor which describe the kinetic and equilibrium properties of the alpha-factor/alpha-factor receptor complex according to Clark's model. The results are discussed in light of the criteria necessary for demonstrating the involvement of a receptor in a physiological response.

The time course for association is an important indicator for demonstrating that a particular receptor is responsible for a physiological effect. The time course for binding should coincide with or precede the time course observed for the biological effect. When the time course for association of ^{3}H-alpha-factor with a-cells was examined, the k_1 or association rate constant was found to equal $2.9 \times 10^6\ M^{-1}\ min^{-1}$. Previous reports and this author's observations have indicated the chronological order of alpha-factor induced effects to be agglutination on the order of minutes, cell cycle arrest and morphological change on the order of hours. The k_1 calculated in this study shows that maximal binding precedes cell cycle arrest and morphological change. This data is consistent with one receptor

mediating these two effects. The time frame in which agglutination occurs, however, is shorter than the time required for maximal binding at the alpha-factor concentration and cell concentration used in this study. Although this may be indicative of a different receptor mediating this response and some evidence for two receptors has been previously published (4), the kinetics of association and the dose response curves for each effect suggest otherwise. Firstly, the association of ^{3}H-alpha-factor with the alpha-factor receptor appears to be a simple reversible bimolecular reaction. When association rate data are plotted according to pseudo-first-order kinetics (figure 16, p. 70) (correctly assumed since less than 10% of the ^{3}H-alpha-factor is bound in this experiment, i.e., [^{3}H-alpha-factor]>>[^{3}H-alpha-factor-receptor complexes]) a straight line results. Likewise, when these data are plotted according to the integrated second order rate equation (figure 16) which makes no assumptions concerning the relative concentration of ligand or binding sites, a straight line approximating the same value for k_1 results. Deviation from linearity in both plots would be expected if ^{3}H-alpha-factor were interacting with more than one population of receptors. Furthermore, linearity would not be expected if the different receptor populations possessed different affinities for ^{3}H-alpha-factor. Secondly, different dose response curves result when the three different biological effects (agglutination, growth arrest and shmoo) are examined. Agglutination can occur at alpha-factor concentrations of 10^{-11} M whereas growth arrest and shmoo formation require greater amounts of alpha-factor (10^{-10} M and 10^{-8} M,

respectively; 80). Given these observations and the kinetics which characterize ^{3}H-alpha-factor association, the three responses are mediated by the same receptor but probably occur at different levels of receptor occupancy, i.e., agglutination is induced at lower receptor occupancy than growth arrest and the shmoo morphology respectively. Additional evidence supporting this conclusion can be seen when the concentration at which half maximal induction of the three responses is compared with the concentration range over which receptor saturation for binding occurs (see 80 and figure 19, p. 76).

The kinetics for alpha-factor dissociation are also consistent with the interaction of a single receptor population possessing a fixed affinity for ^{3}H-alpha-factor. Dissociation kinetics are evaluated under conditions in which the reassociation of dissociated labelled ligand is unlikely. There are two methods by which this can be achieved: (1) dilution of a binding reaction at equilibrium by 10 to 100 fold so that any rebinding of radioligand, once dissociated, is not detected or (2) addition of unlabelled competing ligand to the dilution buffer so that any rebinding that occurs is likely to involve the unlabelled ligand. It is useful to examine and compare the dissociation which results from using both methods. As the data in figure 17, p. 71, indicate, when the infinite dilution method is used the dissociation profile observed is consistent with a first order process. The experiment shown in figure 18, p. 75, used both methods to determine the time course for dissociation. As indicated, the dissociation kinetics do not change when excess unlabelled alpha-factor is present. The inset

in figure 18, p. 75, represents a plot of the initial rate of dissociation for determination of the k_{-1}. Both conditions approximate $k_{-1} = 4.7 \times 10^{-2}$ min. The data trace essentially identical straight lines which are expected for a reaction that is fully reversible and consistent with a first order process. If dissociation had occurred more rapidly under conditions in which competitive displacement was allowed, negative cooperativity for binding would have been the interpretation. On the other hand, if more rapid dissociation had occurred by infinite dilution than competitive displacement, positive cooperativity in binding would have been implied.

From the association and dissociation rate data, a kinetic K_D can be determined according to the equivalence

$$K_D = \frac{k_{-1}}{k_1} \quad .$$

The values for a number of experimental determinations of k_1 and k_{-1} are found in table 4, p. 68. Using all the permutations of these values, an average kinetic K_D is calculated = 2.12×10^{-8} M.

Another important characteristic of a receptor-mediated process is that the binding sites are saturable since a finite number of sites are expected to exist per cell. Figure 19, p. 76, shows this characteristic for the alpha-factor receptor. Fundamental to the interpretation of this data is the accurate definition of nonspecific binding. Because there are two haploid mating types in S. cerevisiae which seem to be different only in their mating-type specific expression of a few genes

required for conjugation, the amount of specific ^{3}H-alpha-factor binding to a-cells can be determined in light of the nonspecific amount of ^{3}H-alpha-factor binding which occurs to alpha-cells. With this in mind, the specific binding of ^{3}H-alpha-factor to a-cells is plotted as a function of the $\log_{10}$ [^{3}H-alpha-factor] in the saturation isotherm of figure 19, p. 76.

Realistically, one can rarely saturate receptors with a radioligand due to radioligand expense or technical impractibility. For this reason, linear transformations have been developed allowing the estimation of the affinity of the receptor-ligand interaction (K_D) and the receptor density (R_{max}) from saturation isotherms. One of the most frequently used methods was developed by Scatchard in 1949 (98). By plotting the saturation data in figure 19 in the form of a Scatchard plot (inset, figure 19), a linear trace is obtained, the slope of which allows the estimation of the K_D (2.32×10^{-8} M) and the x-intercept which estimates the number of binding sites per cell(13000 sites/cell).

The proper use of the Scatchard plot has been at the center of much controversy since its inception (62, 90, 20, 123, 88, 100, 83). As pointed out by Klotz, many investigators are tempted to linearize data when in fact more complex phenomema are occurring (62). Furthermore, truncated isotherms obtained from the examination of binding over too small a range of radioligand concentration are commonplace. In many cases binding data beyond the inflection point of a [*LR] vs $\log_{10}$ [*L] curve is never acquired. When this is the situation, transformation of

the saturation data to the Scatchard plot can yield erroneous estimates for K_D and R_{max}.

A useful exercise according to Klotz is to replot the line derived from a Scatchard transformation onto a [*LR] vs $\log_{10}$ [*L] plot (62). If the curve obtained this way mirrors the curve obtained experimentally, then the values derived for K_D and R_{max} are likely accurate. Furthermore, binding measurements beyond the inflection point of the binding isotherm must be included. When the regression line of the Scatchard plot in the inset of figure 19, p. 76, was replotted as suggested above, a curve identical to the experimentally obtained saturation isotherm was traced. Furthermore the last point, 6×10^{-7} M free alpha-factor, is at 77% saturation according to the estimate of 13000 sites per cell.

Another transformation commonly applied to saturation binding data is the Hill plot. Developed originally to describe the positive cooperativity associated with binding of O_2 to hemoglobin (51), this plot yields the Hill coefficient (n_H) which is an indicator of whether complex interactions and/or degrees of cooperativity exist in ligand binding. As expected from the Scatchard plot discussed above, plotting saturation data according to the Hill equation yields a slope of 1.05 (see figure 20, p. 78). When n_H is equal to 1, the ligand is binding to a single species of receptor via a simple, reversible bimolecular reaction which obeys the law of mass action (68). Furthermore, when n_H approximates 1.0, the x-intercept of the Hill plot approximates the K_D for the radioligand. The x-intercept in figure 20 yields a K_D =

1.51×10^{-8} M. This value is equivalent within experimental error to the value of 2.32×10^{-8} M derived from the Scatchard plot.

When binding of a radioligand to a receptor represents binding to a single class of receptors in a reversible fashion with fixed affinity, the equilibrium dissociation constant determined from steady state saturation binding data should be equivalent to the K_D determined from kinetic data. This holds true for the data presented here (K_D from steady state saturation binding = 2.32×10^{-8} M; Kinetic K_D = 2.12×10^{-8} M).

Specificity of ^{3}H-Alpha-Factor Binding

Studies using unlabelled analogues provide useful information concerning structure-function relationships. The order of potency of unlabelled agonists in competing with ^{3}H-alpha-factor for binding should parallel the order of efficiency with which these agonists cause their biological effects if all the compounds are interacting with the same receptor. To quantitate the potency of the unlabelled alpha-factor analogues in competing for ^{3}H-alpha-factor binding, the IC_{50} (the concentration of competitor which effectively inhibits binding of ^{3}H-alpha-factor by 50%) was determined from the competition binding curves in figures 22, 23, 24 and 25, pp. 81-84. Table 5, p. 85, lists the IC_{50} and subsequent K_D values for each competitor. The results from bioactivity assays (growth arrest and shmoo induction) are listed in table 1, p. 57. When the analogues are ranked from the most potent (1) to the least potent (8) according to growth arrest, shmoo induction and

binding competition data, the lines of identity seen in figures 30 and 31 are obtained. Therefore as expected for biological effects mediated via a specific receptor, the binding affinities of the alpha-factor analogues parallel the degree to which they mediate physiological response.

All of the competition curves proceed from 10 to 90% competition over an 81-fold concentration range of competitor. Statistical analyses using pairwise t-tests revealed that the lines traced between 10 and 90% for all the competitors tested were parallel ($p=0.01$). This is important because curves of this nature are said to be of normal steepness and characteristic of ligand-receptor interactions which are bimolecular, reversible and obey the law of mass action (68). Thus data from the competition studies support the kinetic and saturation binding data discussed earlier that indicate the existence of only one receptor population, exhibiting one affinity, for the alpha-factor pheromone.

Three antagonists were identified in the competition studies, desTrp^1 Ala^3 dodecapeptide, desTrp^1 Phe^3 dodecapeptide and desTrp^1 CHA^3 D-Leu^6 dodecapeptide. The desTrp^1 Ala^3 and desTrp^1 Phe^3 dodecapeptides show binding affinities equal to the desTrp^1 dodecapeptide, however the desTrp^1 CHA^3 D-Leu^6 dodecapeptide exhibits a K_D 5-fold less than its parent compound, desTrp^1 CHA^3 dodecapeptide. None of these analogues show biological activity when tested in the halo or shmoo assays (see table 1, p. 57). It appears, therefore, that changes at these positions definitely influence receptor-mediated biological effects but have varied effects on binding affinity.

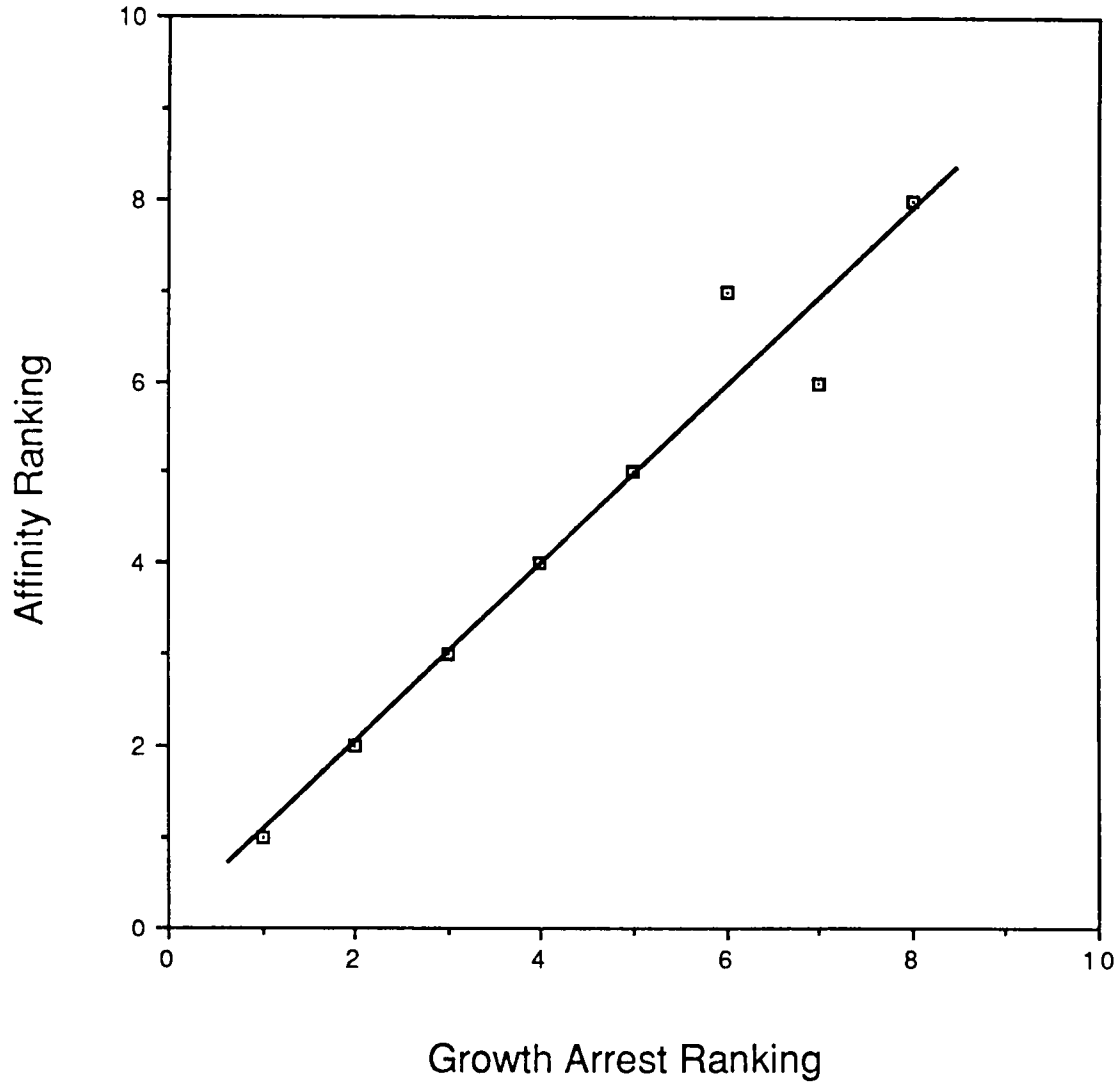

Figure 30. Identity plot correlating growth arrest activity and binding activity of the α-factor analogues. Points signify more than one analogue in some cases.

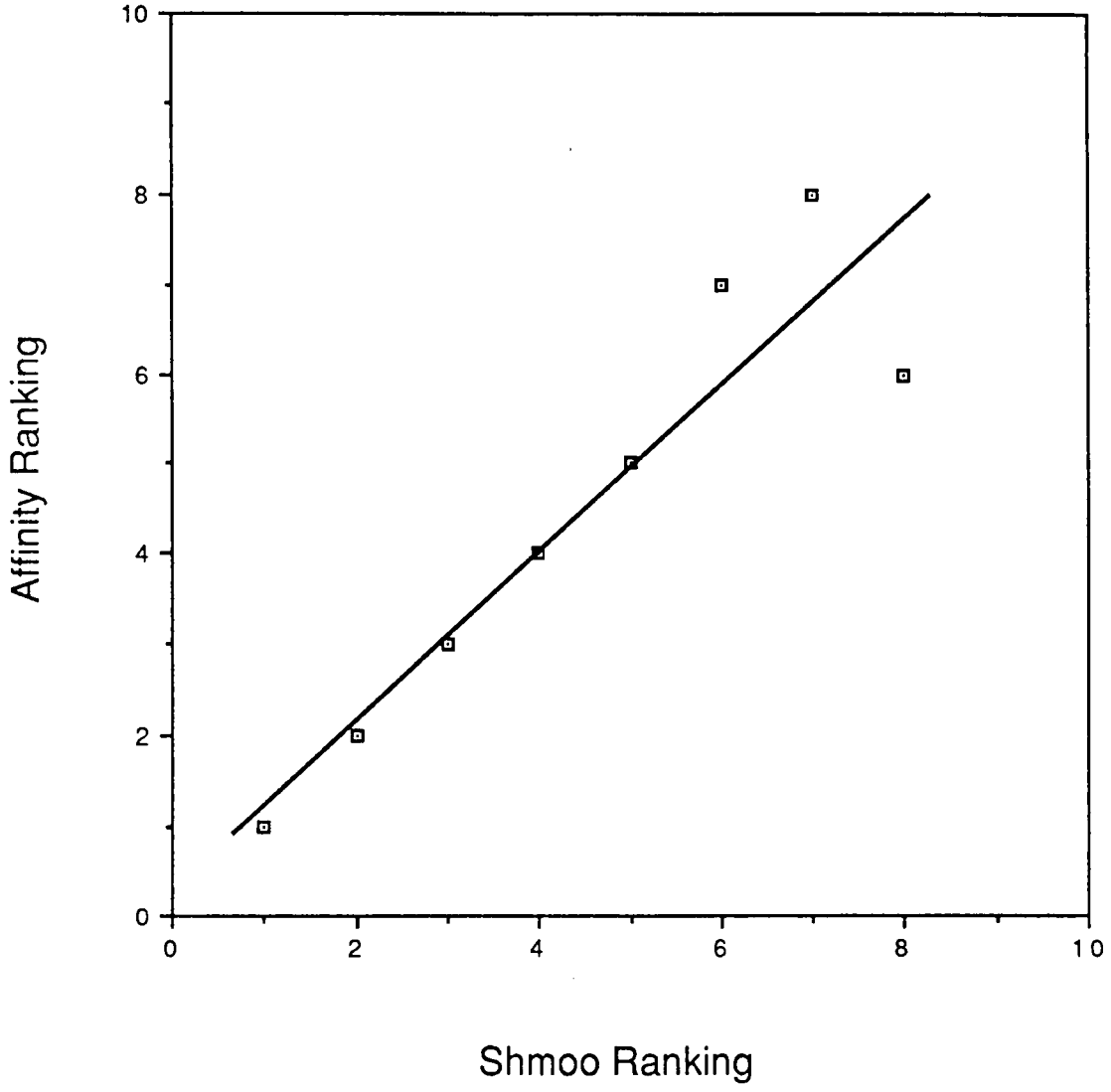

Figure 31. Identity plot correlating shmoo-inducing activity and binding activity of the α-factor analogues. Points signify more than one analogue in some cases.

Unlike the position 3 dodecapeptide analogues, substitutions at position 3 in the tridecapeptide do not result in loss of activity. When phenylalanine is substituted for tryptophan at position 3 in the tridecapeptide, the stability of the receptor/alpha-factor interaction, as represented by a ΔG^{o} = -9.69 Kcal, is less than the stability of the complex involving the native 13-mer (ΔG^{o} = -10.64 Kcal),but greater than that observed for any of the desTrp^{1} derivatives (ΔG^{o} s < -9.35 Kcal). With regard to biological activity, this suggests that changes in position three can be tolerated in the presence of the N-terminal tryptophan especially since substitutions at this position do not appreciably alter receptor-ligand stability.

Previous studies by Baffi et al. have shown that the ε amine of lysine is not necessary for biological activity (4). The pattern of competition for binding shown by desTrp^{1} CHA^{3} Lys^{7} (acetyl)- and desTrp^{1} CHA^{3} Lys^{7} (octanoyl)-dodecapeptides supports this notion. The more hydrophobic Lys^{7} (octanoyl) analogue binds better than the Lys^{7} (acetyl) analogue; the trend most likely responsible for their greater and lesser biological activities.

One inactive analogue, desTrp^{1} CHA^{3} L-Ala^{9} dodecapeptide did not compete for binding of ^{3}H-labelled alpha-factor. A similar analogue, desTrp^{1} CHA^{3} D-Ala^{9} dodecapeptide, competed effectively for binding of ^{3}H-alpha-factor and approximated a K_D slightly lower than the desTrp^{1} CHA^{3} dodecapeptide parent sequence. When aminoisobutyric acid (AIB or 2-methlyalanine) was substituted at position 8 in place of proline, a corresponding 5-fold increase in K_D was observed. Pro-Gly sequences

have been implicated in type IIβ bends (22, 41). Furthermore, type IIβ turns will tolerate D-residues but not L-residues (119). Substitution of AIB at position 8 should destroy the tendancy for a β bend in this region (Pro-Gly) of the alpha-factor if it does occur. In fact, the binding K_D increase observed for this analogue (desTrp^1 CHA^3 AIB^8 dodecapeptide) is probably due to that structural dissolution. On the other hand, the insertion of D-Alanine at position 9 should stabilize the βturn. The ΔG^o value for the interaction of desTrp^1 CHA^3 D-Ala^9 dodecapeptide with the alpha-factor receptor indicates that this stabilizing effect does occur. It is interesting to note that the stability of the interaction of the desTrp^1 CHA^3 D-Ala^9 dodecapeptide with the alpha-factor receptor is greater than the stability exhibited for the parent compound, desTrp^1 CHA^3 dodecapeptide. These observations lend additional support to evidence previously published by Naider et al. implicating a type IIβ bend as important for biological recognition and binding (84).

At least -1Kcal separates the ΔG^o values for all the desTrp^1 alpha-factor derivatives from the tridecapeptides analyzed in this study. A change of slightly over -1 Kcal in ΔG^o increases the corresponding equilibrium constant K by a factor of 10. Because the binding affinities for the dodecapeptides and most tridecapeptides tested are separated by a tenfold difference at least, it appears that the N-terminal tryptophan contributes significantly to the stability of the receptor-ligand complex.

The tridecapeptide analogues tested in this study exhibited less variation in their binding affinities. Conservative changes at positions 5 and 7 in the tridecapeptide result in no change in binding affinity or biological activity when compared to the native pheromone. The replacement of methionine 12 with norleucine in the biologically active NLe^{12} tridecapeptide also shows no difference in binding affinity when compared to the native 13-mer. Similarly, substitution at positions 8 and 11 decrease the stability of the alpha-factor/receptor interaction by only 180 calories; a very small difference to be shared by changes at 2 residues. These results, in addition to the ΔG^{o} differences between the $desTrp^{1}$ dodecapeptides and the tridecapeptides discussed above, may suggest that the complex formed by tridecapeptides with the alpha-factor receptor can tolerate a number of changes before binding affinity and consequently biological activity is affected.

Thermodynamic Analysis of the Temperature Dependence of Binding

Changes in the standard Gibbs free energy (ΔG^{o}) reflect changes in enthalpy as well as changes in entropy as indicated in the equation $\Delta G^{o} = \Delta H^{o} - T\Delta S^{o}$. Examining the binding of agonists and antagonists over a range of temperature enables the ΔH^{o} parameter to be determined from the slope of a Van't Hoff plot as described in appendix C. The temperature dependence of tridecapeptide and $desTrp^{1}$ Ala^{3} dodecapeptide binding are shown in figures 26 and 27, pp. 88, 88. Use of the data in these figures for the Van't Hoff plots in figures 28 and 29, pp. 89, 90, gives rise to the thermodynamic parameters listed in table 6, p. 91 (see appendix C for details of the calculations). Because these data conform

to straight lines, the enthalpy changes for both interactions are independent of temperature. Therefore it is unlikely that the ΔH^{o} values reflect a change in the heat capacities of the ligand or ligand-receptor complex or a change in ligand or receptor interaction as a result of a phase change in membrane lipids surrounding the receptor (68).

Binding reactions in general have a large entropy component. Positive entropy changes are favored thermodynamically since they contribute to large negative changes in free energy. As indicated in table 6, p. 91, binding of the agonist, tridecapeptide, is accompanied by a large positive entropy component whereas binding of desTrp^{1} Ala^{3} dodecapeptide, an antagonist, is characterized by a large enthalpy component. These results challenge the generalization made by Weiland et al. that receptor-agonist interactions are enthalpy-driven ($\Delta H^{o} < 0$) and receptor-antagonist interactions are entropy-driven ($\Delta S^{o} > 0$) (122).

The reaction of an antagonist with a receptor has been likened to other simple protein binding reactions in which information transfer is not involved. Interactions of this nature tend to yield positive entropy terms and slightly negative enthalpy terms. On the other hand, agonist-receptor interactions which result in activation of distal events for physiological response have been associated with large negative enthalpy terms (122). This is thought to be a consequence of the net negative entropy term caused by agonist induced conformational changes.

In light of these justifications, it is difficult to interpret the thermodynamic parameters found in this study associated with agonist and

antagonist binding to the alpha-factor receptor. Perhaps the binding of alpha-factor to its membrane-bound receptor involves interactions with the cell wall of S. cerevisiae. Perhaps both alpha-factor agonists and antagonists induce conformational changes but the larger net decrease in enthalpy associated with antagonist binding reflects a lower enthalpy of the conformational state induced by the antagonist. Clearly a straightforward interpretation is not forthcoming from the preliminary data presented here. Additional experiments testing whether the association or dissociation kinetics of either ligand change over the temperature range tested may better define the phenomena responsible for these observations.

Summary

The results discussed show that alpha-factor interacts with its receptor via a simple, reversible process which obeys the law of mass action. Association and dissociation kinetics predict values of 2.92×10^{6} M^{-1} min^{-1} for k_1 and between 4 and 7×10^{-2} min for k_{-1}. Saturation binding studies reveal an equilibrium dissociation constant equal to 2.32×10^{-8} M which approximates the kinetically derived K_D of 2.12×10^{-8} M. Scatchard and Hill analysis as well as dissociation behavior in the presence of excess unlabelled ligand indicate alpha-factor interacts with a homogeneous population of binding sites (13000 sites/cell) which do not interact and exhibit one affinity for the alpha-factor pheromone. Studies using unlabelled competitors reveal the specificity expected for a receptor-mediated process, i.e., binding affinities of alpha-factor analogues parallel their efficiency at

inducing biological activities. These competition results strengthen the structure function relationships already published. All of the alpha-factor competitors tested interact with the same homogeneous population of receptors. Preliminary evidence obtained from the thermodynamic analysis of the temperature dependence of alpha-factor and desTrp^{1} Ala^{3} dodecapeptide binding suggests that agonist binding is entropy driven and antagonist binding is enthalpy driven.

REFERENCES

REFERENCES

1. Achstetter, T. and H. D. Wolf. 1985. Hormone processing and membrane bound proteinases in yeast. EMBO J. 4:173-177.

2. Alberts, B., D. Dray, J. Lewis, M. Raff, K. Roberts, and J. D. Watson, 1983. Molecular Biology of the Cell. Garland Publishing, Inc., New York.

3. Baffi, R., J. M. Becker, P. A. Lipke and F. Naider. 1985. Structure-activity relationships in the dodecapeptide α-factor of Saccharomyces cerevisiae. Position 6 analogues are poor inducers of agglutinability. Biochemistry 24:3332-3337.

4. Baffi, R. A., P. Shenbagamurthi, K. Terrance, J. M. Becker, F. Naider and P. N. Lipke. 1984. Different structure-function relationships for α-factor-induced morphogenesis and agglutination in Saccharomyces cerevisiae. J. Bacteriol. 158:1152-1156.

5. Beck, J. S. and H. J. Goren. 1983. Simulation of association curves and Scatchard plots of binding reactions where ligand and receptor are degraded or internalized. J. of Receptor Res. 3:561-577.

6. Becker, J. M., S. Marcus, B. Kundu, P. Shenbagamurti and F. Naider. 1987. Towards the determination of the structure of the S. cerevisiae a-factor: an acylated pentapeptide blocks a-factor activity. Mol. Cellular Biol., in press.

7. Bender, A. and G. F. Sprague. 1986. Yeast peptide pheromones, a-factor and α-factor, activate a common response mechanism in their target cells. Cell 47:929-937.

8. Betz, R. and W. Duntze. 1979. Purification and partial characterization of a-factor: a mating hormone produced by mating-type a-cells from Saccharomyces cerevisiae. Eur. J. Biochem. 95:469-475.

9. Betz, R. and W. Duntze. 1987. Structure of a-factor from S. cerevisiae. Yeast (ed. H. J. Phaff). International Commission on Yeasts and Yeast-like Microorganisms of the International Union of Microbiological Societies.

10. Betz, R., V. L. MacKay and W. Duntze. 1981. a-Factor from Saccharomyces cerevisiae: partial characterization of a mating hormone produced by cells of mating type a. J. Bacteriol. 132:462-472.

11. Betz, R., T. R. Manney and W. Duntze. 1981. Hormonal control of gametogenesis in the yeast Saccharomyces cerevisiae. Gamete Res. 4:571-584.

12. Blumer, K. J., J. E. Reneke and J. Thorner. 1987. Biochemical studies of the α-factor receptor of Saccharomyces cerevisiae. Abstracts for the Yeast Genetics and Molecular Biology Meetings, San Francisco, CA, June 16-21.

13. Boeynaems, J. M. and J. E. Dumont. 1980. Outlines of receptor theory. Elsevier, New York.

14. Brake, A. J., C. Brenner, R. Najarian, P. Laybourne, and J. Merryweather. 1985. Structure of genes encoding precursors of the yeast peptide mating pheromone a-factor. Protein Transport and Secretion (ed. Gething, M. J.), Cold Spring Harbor Laboratory Press, Cold Spring Harbor, New York.

15. Brown, A. S., J. E. Mole, A. Weissinger and J. C. Bennett. 1978. Methanol solvent system for rapid analysis of phenylthiohydantoin amino acids by high pressure liquid chromatography. J. Chromat. 148:532-535.

16. Builder, S. E. and I. H. Segel. 1978. Equilibrium ligand binding assays using labeled substrates: nature of the errors introduced by radiochemical impurities. Analyt. Biochem. 85:413-424.

17. Burkholder, A. C. and L. H. Hartwell. 1985. The yeast α-factor receptor: structural properties deduced from the sequence of the STE2 gene. Nucleic Acids Res. 13:8463-8475.

18. Casperson, G. F., N. Walker, A. R. Brasier and H. R. Bourne. 1983. A guanine nucleotide-sensitive adenylate cyclase in the yeast Saccharomyces cerevisiae. J. Biol. Chem. 258:7911-7914.

19. Catt, K. J., J. P. Harwood, G. Aguilera and M. L. Dufau. 1979. Hormonal regulation of peptide receptors and target cell responses. Nature (London) 280:109-116.

20. Chamness, G. C., W. L. McGuire. 1975. Scatchard plots: common errors in correction and interpretation. Steroids 26:538-542.

21. Chan, R. K. and C. A. Otte. 1982. Isolation and genetic analysis of Saccharomyces cerevisiae mutants supersensitive to G1 arrest by a-factor and α-factor pheromones. Mol. Cell. Biol. 2:11-20.

22. Chou, P. Y. and G. D. Fasman. 1974. Conformational parameters for amino acids in helical β-sheet and random coil regions calculated from proteins. Biochemistry 13:211-245.

23. Chou, P. Y. and G. D. Fasman. 1978. Empirical predictions of protein conformation. Annu. Rev. Biochem. 47:251-276.

24. Chvatchko, Y., I. Howald and H. Riezman. 1986. Two yeast mutants defective in endocytosis are defective in pheromone response. Cell 46:355-364.

25. Ciejek, E. and J. Thorner. 1979. Recovery of S. cerevisiae a cells from G1 arrest by α-factor pheromone requires endopeptidase action. Cell 18:623-635.

26. Clark, A. J. 1933. The mode of action of drugs on cells. E. Arnold and Co., London.

27. Clark, A. J. L., S. Ishii, N. Richert, G. T. Merlino, and I. Pastan. 1985. Epidermal growth factor regulates the expression of its own receptor. Proc. Natl. Acad. Sci. 82:8374-8378.

28. Davis, T. N., M. S. Urdea, F. R. Masiarz and J. Thorner. 1986. Isolation of the yeast calmodulin gene: calmodulin is an essential protein. Cell 47:423-431.

29. Dmochowska, A., D. Dignard, D. Henning, D. Y. Thomas and H. Bussey. 1987. Yeast KEX1 gene encodes a putative protease with a carboxy peptidase B-like function involved in killer toxin and α-factor precursor processing. Cell 50:573-584.

30. Duntze, W., V. MacKay and T. B. Manney. 1970. Saccharomyces cerevisiae: a diffusable sex factor. Science 168:1472-1473.

31. Duntze, W., D. Stotzler, E. Bücking-Throm and S. Kalbitzer. 1973. Purification and partial characterization of alpha-factor, a mating type specific inhibitor of cell reproduction from Saccharomyces cerevisiae. Eur. J. Biochem. 35:357-365.

32. Emter, O., B. Mechler, T. Achstetter, H. Muller and D. H. Wolf. 1983. Yeast pheromone α-factor is synthesized as a high molecular weight precursor. Biochem. Biophys. Res. Commun. 116:822-829.

33. Fasman, G. 1965. The alpha amino acids. Dekker Press, New York.

34. Felix, A. M., C. T. Wang, A. A. Liebman, Ch. M. Delaney, T. Mowles, B. A. Burghard, A. M. Charnecki and J. Meienhofer. 1977. Synthesis, biological activity and tritiation of L-3,4-dehydroproline-containing peptides. Int. J. Peptide Protein Res. 10:299-310.

35. Fields, S. and I. Herskowitz. 1985. The yeast STE12 product is required for expression of two sets of cell-type-specific genes. Cell 42:923-930.

36. Finkelstein, D. B. and L. McAlister. 1981. α-Factor-mediated modification of a ^{35}P-labelled protein by MATa cells of Saccharomyces cerevisiae. J. Biol. Chem. 256:2561-2566.

37. Finkelstein, D. B. and S. Strausberg. 1979. Metabolism of α-factor by a-mating type cells of Saccharomyces cerevisiae. J. Biol. Chem. 254:796-803.

38. Fisher, G. H., D. I. Marlborough, J. W. Ryan and A. M. Felix. 1978. L-3,4-dehydroproline analogs of bradykinin. Archs. Biochem. Biophys. 189:81-85.

39. Fisher, G. H. and J. W. Ryan. 1979. Superactive inhibitors of angiotensin converting enzyme. FEBS LeH. 107:273-276.

40. Fujimura, H. and N. Yanagishima. 1984. Purification and genetic control of α-pheromone-inactivating glycoproteins in the yeast Saccharomyces cerevisiae. Curr. Genetics 9:39-45.

41. Gierasch, L. M., C. M. Deber, V. Madison, C. Niu, and E. P. Blout. 1981. Conformations of $(X\text{-}L\text{-}Pro\text{-}Y)_2$ cyclic hexapeptides. Preferred β-turn conformers and implications for β-turns in proteins. Biochem. 20:4730-4738.

42. Gottesman, M. M. 1980. Genetic approaches to cyclic AMP effects in cultured mammalian cells. Cell 22:329-330.

43. Hagen, D., G. McCaffrey, and G. F. Sprague. 1986. Evidence the yeast STE3 gene encodes a receptor for the peptide pheromone a factor: gene sequence and implications for the structure of the presumed receptor. Proc. National Acad. Sci. 83:1418-1422.

44. Hagen, D. C. and G. F. Sprague. 1984. Induction of the yeast α-specific STE3 gene by the peptide pheromone a-factor. J. Mol. Biol. 178:835-852.

45. Hartig, A., J. Holly, G. Saari and V. L. MacKay. 1986. Multiple regulation of STE2, a mating-type-specific gene of Saccharomyces cerevisiae. Mol. Cellular Biol. 6:2106-2114.

46. Hartwell, L. H. 1967. Macromolecular synthesis in temperature sensitive mutants of yeast. J. Bacteriol. 93:1662-1670.

47. Hartwell, L. H. 1980. Mutants of Saccharomyces cerevisiae responsive to cell division are controlled by a polypeptide mating hormone. J. Cell Biol. 85:811-822.

48. Hartwell, L. H. 1986. Conjugation in Saccharomyces cerevisiae: Role of the alpha factor receptor. Ann. Mtg. Am. Soc. Microbiology. Washington, DC, March 23-38.

49. Herskowitz, I. 1987. A master regulatory locus that determines cell specialization in yeast. The Harvey Lectures 81:67-92.

50. Hicks, J. B. and I. Herskowitz. 1976. Evidence for a new diffusable element of mating pheromones in yeast. Nature (London) 260:246-248.

51. Hill, A. V. 1913. The combinations of hemoglobin with oxygen and with carbon monoxide. I. Biochem. J. 7:471-480.

52. Jenness, D. D., A. C. Burkholder, and L. H. Hartwell. 1983. Binding of α-factor pheromone to yeast a cells: chemical and genetic evidence for an α-factor receptor. Cell 35:521-529.

53. Jenness, D. D., A. C. Burkholder and L. H. Hartwell. 1986. Binding of α-factor pheromone to Saccharomyces cerevisiae a-cells: Dissociation constant and number of binding sites. Mol. Cell. Biol. 6:318-320.

54. Jenness, D., B. S. Goldman and L. H. Hartwell. 1987. Saccharomyces cerevisiae mutants unresponsive to α-factor pheromone: α-factor binding and extragenic suppression. Mol. Cellular Biology 7:1311-1319.

55. Jenness, D. D. and P. Spatrick. 1986. Down regulation of the α-factor pheromone receptor in S. cerevisiae. Cell 46:345-353.

56. Johnson, A. D. and I. Herskowitz. 1985. A repressor (MATα2 product) and its operator control expression of a set of cell-type specific genes in yeast. Cell 42:237-247.

57. Julius, D., L. Blair, A. Brake, G. Sprague and J. Thorner. 1983. Yeast α-factor is processed from a larger precursor polypeptide: the essential role of a membrane-bound dipeptidyl aminopeptidase. Cell 32:829-852.

58. Julius, D., A. Brake, L. N. Blair, R. Kunisawa, and J. Thorner. 1984. Isolation of a putative structural gene for the lysine-arginine-cleaving endopeptidase required for processing of yeast prepro-α-factor. Cell 37:1075-1089.

59. Kamiya, Y., A. Sakarai, S. Tamura, N. Takahashi, T. Tsuchiya, K. Abe and S. Fukui. 1979. Structure of Rhodotorucine A, a peptidyl factor, inducing mating tube formation in Rhodosporidium toruloides. Agric. Biol. Chem. 43:363-369.

60. Katz, M. E., J. Ferguson and S. I. Reed. 1987. Temperature-sensitive lethal pseudorevertants of ste mutations in Saccharomyces cerevisiae. Genetics 115:627-636.

61. Klanschenz, E., M. Bienert, H. Egler, U. Pleiss, H. Niedrich, and K. Nikolics. 1981. Tritium labeling of gonadotropin releasing hormone in its proline and histidine residues. Peptides 2:445-452.

62. Klotz, I. 1982. Numbers of receptor sites from Scatchard graphs: facts and fantasies. Science 217:1247-1249.

63. Konopka, J. and L. Hartwell. 1986. The role of STE2 in mating. Abstracts of 13th Int. Conf. on yeast genetics and molecular biology, Aug. 31-Sept. 5, Banff, Alberta, Canada.

64. Kostriken, R., J. N. Strathern, A. J. S. Klar, J. B. Hicks and F. Heffron. 1983. A site-specific endonuclease essential for mating-type switching in Saccharomyces cerevisiae. Cell 35:167-174.

65. Kurjan, J. and I. Herskowitz. 1982. Structure of a yeast pheromone gene (MFα): a putative α-factor precursor contains four tandem copies of mature α-factor. Cell 30:933-943.

66. Lewin, B. 1983. Genes. John Wiley & Sons, NY.

67. Liao, H. and J. Thorner. 1980. Yeast mating pheromone α-factor inhibits adenylate cyclase. Proc. Natl. Acad. Sci. U.S.A. 77:1898-1902.

68. Limbird, L. E. 1986. Cell surface receptors: A short course on theory and methods. Martinus Nijhoff Publishing, Boston, MA.

69. Linden, J. 1982. Calculating the dissociation constant of an unlabeled compound from the concentration required to displace radiolabel binding by 50%. J. Cycl. Nucl. Res. 8:163-172.

70. Lipke, P. N. 1976. Morphogenetic effects of α-factor on S. cerevisiae a-cells. Ph.D. thesis, University of California, Berkeley.

71. Manness, P. F. and G. M. Edelmann. 1978. Inactivation and chemical alteration of mating factor α by cells and spheroplasts of yeast. Proc. Natl. Acad. Sci. U.S.A. 75:1304-1308.

72. Manney, T. R. 1983. Expression of the BAR1 gene in Saccharomyces cerevisiae: Induction by α mating pheromone of an activity associated with a secreted protein. J. Bacteriol. 155:291-301.

73. Manney, T. R., W. Duntze and R. Betz. 1981. Sexual Interactions in Eucaryotic Microbes (ed. O'Day, D. H. and Horgan, P. A.). Academic Press, NY.

74. Manni, A., M. J. Chambers and O. H. Pearson. 1978. Prolactin induces its own receptors in rat liver. Endocrinology 103:2168-2175.

75. Masui, Y., N. Chino, S. Sakakibara, T. Tanaka, T. Murakami and H. Kita. 1977. Synthesis of the mating factor of Saccharomyces cerevisiae and its truncated peptides: the structure-activity relationship. Biochem. Biophys. Res. Commun. 78:534-538.

76. Masui, Y., T. Tanaka, N. Chino, H. Kita and S. Sakakibara. 1979. Amino acid substitution of mating factor of Saccharomyces cerevisiae: structure-activity relationship. Biochem. Biophys. Res. Commun. 86:982-987.

77. Matsumoto, K., I. Uno, Y. Oshima, T. Ishikawa. 1982. Isolation and characterization of yeast mutants deficient in adenylate cyclase and cAMP-dependent protein kinase. Proc. Natl. Acad. Sci. U.S.A. 79:2355-2359.

78. Miller, A. M., V. L. MacKay and K. A. Nasmyth. 1985. Identification and comparison of two sequence elements that confer cell-type specific transcription in yeast. Nature (London) 314:598-603.

79. Miyakawa, T., T. Tachikawa, Y. K. Jeong, E. Tsuchiya, and S. Fukui. 1985. Transient increase of Ca^{2+} uptake as a signal for mating pheromone-induced differentiation in the Heterobasidiomycetous yeast Rhodosporidium toruloides. J. Bacteriol. 162:1304-1306.

80. Moore, S. A. 1983. Comparison of dose-response curves for α-factor-induced cell division arrest, agglutination and projection formation of yeast cells. J. Biol. Chem. 258:13849-13856.

81. Moore, S. A. 1984. Yeast cells recover from mating pheromone alpha factor induced division arrest by desensitization in the absence of alpha factor destruction. J. Biol. Chem. 259:1004-1010.

82. Moore, S., A. M. Felix and J. Meienhofer. 1977. Pharmacological effects of introducing a double bond into a binding site of oxytocin. Analogues with L-3,4-dehydroproline in position 7. J. Med. Chem. 20:495-500.

83. Munson, P. J. and D. Rodbard. 1983. Number of receptor sites from Scatchard and Klotz graphs: a constructive critique. Science 220:979-981.

84. Naider, F. and J. M. Becker. 1986. Structure-activity relationships of the yeast α-factor. CRC Critical Reviews in Biochemistry 21:225-249.

85. Nakayama, A. Miyajima and K. Arai. 1985. Nucleotide sequences of STE2 and STE3, cell type-specific sterile genes from Saccharomyces cerevisiae. EMBO J. 4:2643-2648.

86. Nakfuku, M., H. Itoh, S. Nakamura, and Y. Kaziro. 1987. Occurrence in Saccharomyces cerevisiae of a gene homologous to the cDNA coding for the α subunit of mammalian G proteins. Proc. Natl. Acad. Sci. 84:2140-2144.

87. Nasmyth, K. A. 1983. Molecular analysis of a cell lineage. Nature (London) 302:670-676.

88. Norby, J. G., P. Ottolenghi and J. Jensen. 1980. Scatchard plot: common misinterpretation of binding experiments. Analytical Biochem. 102:318-320.

89. Ohsumi, Y. and Y. Anraku. 1985. Specific induction of Ca^{2+} transport activity in MATa cells of Saccharomyces cerevisiae by a mating pheromone, α-factor. J. Biol. Chem. 260:10482-10486.

90. Paul, S. M., R. L. Hanger, B. A. Hulihan-Giblin, and P. Skolnick. 1984. Analyzing nonlinear Scatchard plots. Science 223:76-78.

91. Powers, S., S. Michaelis, D. Broek, S. Santa Anna, J. Field, I. Herskowitz and M. Wigler. 1986. RAM, a gene of yeast required for a functional modification of RAS proteins and for production of mating pheromone a-factor. Cell 47:413-422.

92. Raths, S. P. Shenbagamurthi, F. Naider and J. M. Becker. 1986. Biological activity of the Asn^5, Arg^7 tridecapeptide encoded by MFα2 of Saccharomyces cerevisiae. J. Bacteriol. 168:1468-1471.

93. Reem, G. H. and N. H. Yeh. 1984. Interleukin 2 regulates expression of its receptor and synthesis of gamma interferon by human T lymphocytes. Science 225:429-430.

94. Riezman, H. 1985. Endocytosis in yeast: several of the yeast secretory mutants are defective in endocytosis. Cell 40:1001-1009.

95. Ruiz, T. and L. Rodriguez. 1986. Effect of anticalmodulin drugs on the action of yeast α-factor pheromone. Arch. Microbiol. 145:104-106.

96. Sakagami, Y., M. Yoshida, A. Isogai, and A. Suzuki. 1981. Peptidal sex hormones inducing conjugation tube formation in compatible mating-type cells of Tremella mesenterica. Science 212:1525-1527.

97. Samokhin, G. P., L. V. Lizlova, J. D. Bespalova, M. I. Titov and V. N. Smirnov. 1979. Substitution of Lys^7 by Arg does not affect biological activity of α-factor, a yeast mating pheromone. FEMS. Microbiol. Lett. 5:434-438.

98. Scatchard, G. 1949. The attractions of proteins for small molecules and ions. Ann. N.Y. Acad. Sci. 51:660-672.

99. Shenbagamurthi, P., R. Baffi, S. A. Khan, P. Lipke, C. Pousman, J. M. Becker and F. Naider. 1983. Structure activity relationships in the dodecapeptide α-factor of Saccharomyces cerevisiae. Biochemistry 22:1298-1304.

100. Siiteri, P. K. 1984. Receptor binding studies. Science 223:191-193.

101. Singh, A., E. Y. Chen, J. M. Lugoroy, C. N. Chang, R. A. Hitzeman and P. H. Seeburg. 1983. Saccharomyces cerevisiae contains two discrete genes coding for the α-factor pheromone. Nucleic Acids Res. 11:4049-4063.

102. Smith, R. A., M. J. Duncan and D. T. Moir. 1985. Heterologous protein secretion from yeast. Science 229:1219-1224.

103. Sprague, G. F., L. C. Blair and J. Thorner. 1983. Cell interactions and regulation of cell type in the yeast Saccharomyces cerevisiae. Ann. Rev. Microbiology 37:623-642.

104. Sprague, G. F., R. Jensen and I. Herskowitz. 1983. Control of yeast cell type by the mating type locus: Positive regulation of the α-specific STE3 gene by the MATα1 product. Cell 32:409-415.

105. Sterne, R. E. and J. Thorner. 1986. Processing and secretion of a yeast peptide hormone by a novel pathway, p. 189. Abstracts for the Ann. Mtg. Amer. Soc. Cell Biol., Washington, D.C.

106. Stotzler, D., H. Klitz and W. Duntze. 1976. Primary structure of α-factor peptides from Saccharomyces cerevisiae. Eur. J. Biochem. 69:397-400.

107. Strathern, J., J. Hicks and I. Herskowitz. 1981. Control of cell type by the mating type locus: The α1-α2 hypothesis. J. Mol. Biol. 147:357-372.

108. Tachikawa, T., T. Miyakawa, E. Tsuchiya, and S. Fukui. 1987. A rapid and transient increase of cellular Ca^{2+} in response to mating pheromone in Saccharomyces cerevisiae. Agr. Biol. Chem. 51:1209-1210.

109. Tallon, M. A., P. Shenbagamurthi, S. Marcus, J. M. Becker and F. Naider. 1987. Synthesis and biological activity of amino terminus extended analogues of the alpha mating factor of Saccharomyces cerevisiae. Biochemistry, in press.

110. Tanaka, T. and H. Kita. 1978. Site of action of mating factor in a-mating type cells of Saccharomyces cerevisiae. Biochem. Biophys. Res. Commun. 83:1319-1324.

111. Tanaka, T., H. Kita and K. Narita. 1977. Purification and its structure-activity relationship of mating factor of Saccharomyces cerevisiae. Proc. Jpn. Acad. 53:67-70.

112. Tanaka, T., H. Kita, T. Murakami, and K. Narita. 1977. Purification and amino acid sequence of mating factor from Saccharomyces cerevisiae. J. Biochem. 82:1681-1687.

113. Thorner, J. 1980. in The Molecular Genetics of Development (ed. Leighton, T.). Academic Press, NY.

114. Thorner, J. 1981. Molecular Biology of the Yeast S. cerevisiae (ed. Strathern, J. N., Jones, E. W. and Broach, J. R.). Cold Spring Harbor Laboratory, NY.

115. Throm, E. and W. Duntze. 1970. Mating-type-dependent inhibition of deoxyribonucleic acid synthesis in Saccharomyces cerevisiae. J. Bacteriol. 104:1388-1390.

116. Toda, T., I. Uno, T. Ishikawa, S. Powers, T. Kataoka, D. Broek, S. Cameron, J. Broach, K. Matsunoto, M. Wigler. 1985. In yeast, RAS proteins are controlling elements of adenylate cyclase. Cell 40:27-36.

117. Tripp, M. L., R. Pinon, J. Meisenhelder and T. Hunter. 1986. Identification of phosphoproteins correlated with proliferation and cell cycle arrest in Saccharomyces cerevisiae: Positive and negative regulation by cAMP-dependent protein kinase. Proc. Natl. Acad. Sci. U.S.A. 83:5973-5977.

118. Veigl, M. L., T. C. Vanaman and W. D. Sedwick. 1984. Calcium and calmodulin in cell growth and transformation. Bioch. et Biophys. Acta 738:21-48.

119. Venkatachalam, C. M. 1968. Stereochemical criteria for polypeptides and proteins. V. Conformation of a system of three linked peptide units. Biopolymers 6:1425-1436.

120. Waldmann, T. A., C. K. Goldman, R. J. Robb, J. M. Depper, W. J. Leonard, S. O. Sharrow, K. F. Bongiovanni, S. J. Korsmeyer and W. C. Greene. 1984. Expression of Interleukin 2 receptors on activated human B cells. J. Exp. Med. 160:1450-1466.

121. Weast, R. C. 1984. CRC Handbook of chemistry and physics. CRC Press, Inc. Boca Raton, Fla.

122. Weiland, G. A., K. P. Minneman and P. B. Molinoff. 1979. Fundamental difference between the molecular interactions of agonists and antagonists with the β-adrenergic receptor. Nature 281:114-117.

123. Weisiger, R. A., J. L. Grollan, and R. K. Ockner. 1982. Scatchard plots. Science 215:312-131.

124. Wilson, K. L. and I. Herskowitz. 1984. Negative regulation of STE6 gene expresssion by the α2 product of Saccharomyces cerevisiae. Mol. Cellular Biology 4:2420-2427.

125. Wolcott, J. A., C. Wust and A. Brown. 1984. Identification of immunologically cross-reactive proteins of Sinbis virus: Evidence for unique conformation of E1 glycoprotein from infected cells. J. Virol. 49:379-385.

126. Yanagishima, N. 1984. Encyclopedia of Plant Physiology, New Series, Volume 17: Cellular Interactions (ed. Linskens, H. F. and Heslop-Harrison, J.). Springer-Verlag, NY.

APPENDICES

APPENDIX A

RATE EQUATIONS FOR THE ASSOCIATION AND DISSOCIATION OF LIGAND-RECEPTOR COMPLEXES

For the reaction

$$L + R \underset{k_{-1}}{\overset{k_1}{\rightleftharpoons}} LR$$

L = ligand

R = receptor

k_1 = rate constant for association

k_{-1} = rate constant for dissociation

I. k_1 Determination (68)

A. Pseudo-1st Order Rate Equation

$$\ln\left[\frac{(LR)_e}{(LR)_e - (LR)}\right] = k_1 t \cdot \frac{(L)_T(R)_T}{(LR)_e}$$

Plot $\ln\left[\frac{(LR)_e}{(LR)_e - (LR)}\right]$ vs time Slope $= k_1\left[\frac{(L)_T(R)_T}{(LR)_e}\right]$

$(L)_T$ = total ligand concentration

$(R)_T$ = total concentration of binding sites

$(LR)_e$ = concentration of ligand-receptor complexes at equilibrium

(LR) = concentration of ligand-receptor complexes at time, t.

B. Second Order Rate Equation (68)

$$\ln \left[\frac{(LR)_e[(L)_T - (LR)(LR)_e/(R)_T]}{(L)_T[(LR)_E - (LR)]}\right] = k_1 t \left[\frac{(L)_T(R)_T}{(LR)_e} - (LR)_e\right]$$

$$\text{Plot } \ln \left[\frac{(LR)_e[(L)_T - (LR)(LR)_e/(R)_T]}{(L)_T[(LR)_e - (LR)]}\right] \text{ vs time}$$

$$\text{Slope} = k_1 \left[\frac{(L)_T(R)_T}{(LR)_e} - (LR)_e\right]$$

C. $t_{\frac{1}{2}}$ Measurement

$$k_1 = \frac{0.693}{t_{\frac{1}{2}}} \times \frac{1}{(L)} \times \frac{(RL)}{(RL) + (R)} \qquad (13)$$

$t_{\frac{1}{2}}$ = time at which binding is one half equilibrium binding (association)

(L) = concentration of free ligand at equilibrium

(R) = concentration of free receptor at equilibrium

(RL) = concentration of receptor ligand complexes at equilibrium.

II. k_{-1} Determination

A. $t_{\frac{1}{2}}$ Measurement

$$k_{-1} = \frac{0.693}{t_{\frac{1}{2}}} \qquad (68)$$

$t_{\frac{1}{2}}$ = time at which one half binding at time 0 is dissociated.

B. First Order Rate Equation (68)

$$\ln\left[\frac{(LR)_t}{(LR)_0}\right] = k_{-1}t$$

$(LR)_t$ = receptor ligand complexes at time, t

$(LR)_o$ = receptor ligand complexes at initiation of dissociation (time zero)

$$\text{Plot } \ln \frac{(LR)_t}{(LR)_0} \text{ vs time} \qquad \text{Slope} = -k_{-1}$$

III. Equilibrium Dissociation Constant (K_D)

$$K_D = \frac{k_{-1}}{k_1} \tag{68}$$

APPENDIX B

EQUATIONS FOR CALCULATING IC_{50} and K_D OF UNLABELLED COMPETITORS FROM COMPETITION PROFILES

I. IC_{50} Determination

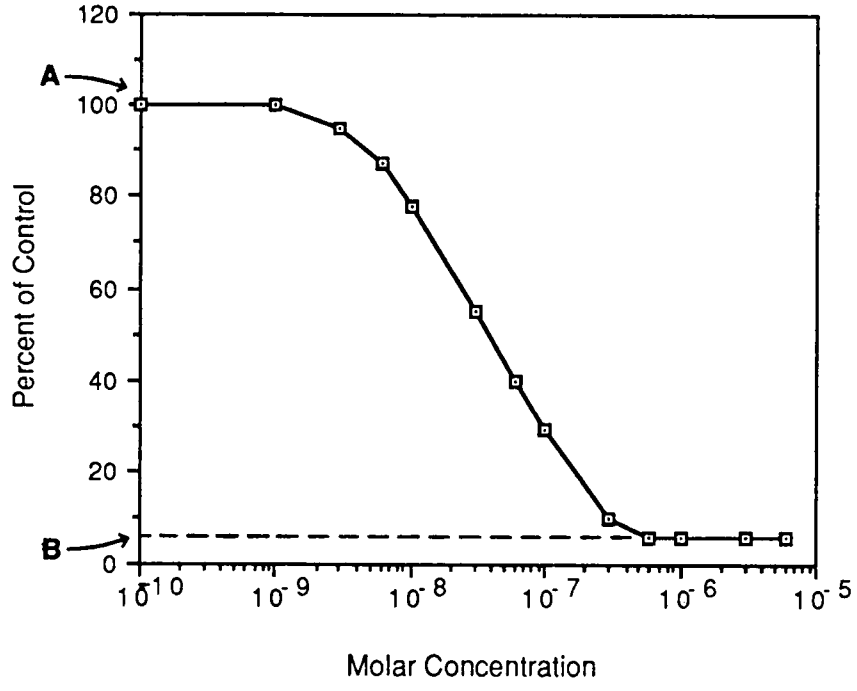

Figure B-1. Log competitor concentration vs binding (% of control).

Determine:

$$\frac{A-B}{2} = X$$

A = % binding at no competition

B = that percentage of radioligand binding which cannot be removed by increasing concentrations of competitor (= nonspecific binding)

X = percent at which one half the binding of radioligand was prevented

Given the above calculation:

IC_{50} = concentration of competitor at which X% binding of ^{3}H-α-factor was obtained.

This concentration (IC_{50}) was determined from a linear regression of points defining the binding inhibition range for a particular competitor.

II. K_D Determination (= K_I)

$$[I]_{free} = IC_{50} - R_{TOT} + \frac{R_{TOT}}{2}\left[\frac{[*L]}{K_D + [*L]} + \frac{K_D}{K_D + [*L] + R_{TOT}/2}\right]$$

Then

$$K_I = \frac{[I]}{1 + \frac{[*L]}{K_D} + \frac{R_{TOT}}{K_D}\left[\frac{K_D + [*L]/2}{K_D + [*L]}\right]} \qquad (69)$$

R_{TOT} = total receptor binding site concentration

[I] = concentration of competitor, I, free in the incubation at equilibrium in the absence of inhibitor, I.

[*L] = concentration of radioligand, *L, free in the incubation at equilibrium.

K_D = K_D value for the radioligand, *L.

K_I = K_D value for the competitor, I

IC_{50} = IC_{50} of the inhibitor, I.

APPENDIX C

EQUATIONS FOR CALCULATING THERMODYNAMIC PARAMETERS OF RECEPTOR-LIGAND INTERACTIONS

I. Gibbs standard free energy change, ΔG^{o} (68)

At constant temperature and pressure

$$\Delta G^{o} = -RT \ln K_{A} \qquad (1)$$

R = gas constant, 1.99 cal/mol·deg

T = temperature, in degrees Kelvin (Kelvin = $^{o}C + 273^{o}$)

K_{A} = equilibrium association constant, M^{-1}

II. Entropy (S) and Enthalpy (H) (68)

At constant temperature and pressure

$$\Delta G^{o} = \Delta H^{o} - T\Delta S^{o} \qquad (2)$$

ΔH^{o} = enthalpy difference between reactants and products

ΔS^{o} = entropy difference between reactants and products

T = temperature, in degrees Kelvin (Kelvin = $^{o}C + 273^{o}$)

To determine the individual parameters ΔH^{o} and ΔS^{o}:

Plot $\ln K_{A}$ vs $1/T$ (^{o}K) "Van't Hoff plot" (68)

$$\text{Slope} = \frac{-\Delta H^{o}}{R}$$

R = gas constant, 1.99 cal/mol·deg

ΔS^{o} can be calculated from equation (2)

VITA

Susan Kay Raths was born in Memphis, Tennessee on November 23, 1959. She attended Georgian Hills Elementary and Junior High School and graduated from Memphis Catholic High School in 1977. The following September she entered The University of Tennessee at Knoxville where she graduated as a Phi Beta Kappa in June, 1981 with a B.A. in microbiology. After working as a research technician in the Department of Microbiology, Susan decided to enter the graduate program in Microbiology in September of 1982.

Susan is married to Scott Hooper formerly of Detroit Lakes, Minnesota. She has accepted a postdoctoral position with Dr. Howard Riezman at The Swiss Institute for Experimental Cancer Research (ISREC) in Epalinges, Switzerland.